Czech Technical University in Prague

Faculty of Electrical Engineering

Department of Electromagnetic Field

Principles of Applicators Design for Microwave Hyperthermia and Physiotherapy

Doctoral Thesis

Barbora Vrbová

Prague, July 2013

Ph.D. Programme: Electrical Engineering and Information Technology

Branch of study: Radioelectronics

Supervisor: ***Prof. Ing. Jan Vrba Ph.D.***

Supervisor-Specialist: ***Ing. Ladislav Oppl Ph.D.***

Abstract

The main aim of this doctoral thesis is to bring new scientific contributions to the topics of medical applications of EM field, especially to microwave thermotherapy.

Therefore it deals with the study of 3D SAR simulations done firstly for homogeneous planar resp. cylindrical agar phantoms, because this gives us basic information about the true behavior of the EM wave irradiated from our proposed applicators, i.e. tools (resp. antennae) for irradiation of EM wave into biological tissue or its phantom in order to create EM field exposure for high quality treatment of patients. Our work focused on the study of superposition effects by using a matrix of hyperthermia applicators.

The logical continuation was then to study the 3D SAR distribution in true anatomical model of human body, again focusing on the study of superposition effects by using a matrix of hyperthermia applicators. On the other hand array applicators can be used for treatment of diseases on bigger areas for clinical purposes.

Another important topic of this doctoral thesis is an initial study and optimization of applicators for intracavitary treatment. As an original contribution of this doctoral thesis we consider a feasible study of the combination of external and interstitial applicator.

Last but not least, this doctoral thesis describes analytical and numerical study of surface waves and methods how to eliminate them, because they may cause so called hot-spots problem.

Based on these results this doctoral thesis brings a proposal of applicators suitable for medical applications and for biological experiments (including numerical simulations of their SAR distribution and measurements of temperature distribution in agar phantom).

Keywords: EM field in medicine, thermotherapy, hyperthermia, cancer treatment, regional treatment, local treatment, microwave applicator, intracavitary applicator, SAR distribution, surface wave, agar phantom, anatomical model.

Abstrakt

Hlavným cielom disertačnej práce je priniesť nové vedecké príspevky k témam lekárskych aplikácií v EM oblasti, predovšetkým v mikrovlnnej termoterapii. Preto sa zaoberá štúdiom 3D simulácií SARu, jednak pre prípad homogénneho rovinného resp. valcového agarového fantómu, pretože to nám môže dať základné informácie o skutočnom správaní EM vlny vyžiarenej z nami navrhnutých aplikátorov, tj. zariadení (resp. antén) pre vyžarovanie EM vlny do biologického tkaniva alebo jeho fantómu za účelom vytvorenia EM expozície pre vysokú kvalitu liečby pacientov. Práca bola zameraná na štúdium superpozičných účinkov pomocou matice hypertermických aplikátorov.

Logickým pokračovaním bolo štúdium 3D SAR distribúcie v anatomickom modeli ľudského tela, opäť so zameraním na štúdium účinkov superpozície pomocou matice aplikátorov. Na druhú stranu matica aplikátorov môže byť použitá na liečbu ochorení u väčších plôch pre klinické účely.

Ďalšou dôležitou témou tejto dizertačnej práce je pôvodná štúdia a optimalizácia aplikátorov pre intrakavitárnu liečbu. Ako veľmi originálny prínos tejto dizertačnej práce považujeme štúdiu uskutočniteľnosti kombinácie externého a intersticiálneho aplikátoru.

V neposlednom rade táto dizertačná práca popisuje analytické a numerické štúdie povrchových vĺn a metód ako ich odstrániť, pretože môžu spôsobiť tzv. hot-spot problém.

Na základe týchto výsledkov dizertačná práca prináša návrh aplikátorov vhodných na lekárske aplikácie a pre biologické experimenty (vrátane numerických simulácií ich SAR distribúcie a meranie rozloženia teplôt v agarom fantóme).

Kľúčové slová: EM pole v medicíne, termoterapia, hypertermia, regionálna liečba, lokálna liečba, mikrovlnný aplikátor, intrakavitárny aplikátor, SAR distribúcia, povrchová vlna, agarový fantóm, anatomický model.

Acknowledgments

First of all I would like to thank to my supervisors, Prof. Ing. Jan Vrba, Ph.D. and Ing. Ladislav Oppl, Ph.D, for their valuable advices, suggestions, and consultations during my Ph.D. studies. They supported me significantly during all my doctoral studies, taught me the basics of scientific work, helped me to improve my knowledge of the electromagnetic field, especially in the field of microwaves. In this way they helped me to achieve the results presented in this doctoral thesis.

My gratitude is also extended to a management of the Department of EM field, especially to its head, Prof. Ing. Miloš Mazánek, PhD., and to all colleagues from this department for the opportunity to spend my doctoral studies in a very nice working environment.

I give my most special gratitude to my family, because it gives me so much love and support and it believes I do a great job. Finally, I would like to thank to my friends, who always stand by me and on whom I can always rely.

Notation and constants

Overview of notations and constants most commonly used in the text of this doctoral thesis is given in the following table. Note that the same symbols may be used for different quantities. The meaning of the notation is therefore always explained in the text again.

α	(-)	attenuation constant
β	(rad^{-1})	phase constant
B	(T)	phasor of vector of magnetic field flux
c_0	($m\ s^{-1}$)	velocity of ligth
δ	(m)	penetration depth
D	($C\ m^{-2}$)	phasor of vector of electric field flux
E	($V\ m^{-1}$)	phasor of vector of electric field strength
ε	(-)	complex permittivity
ε_0	($F\ m^{-1}$)	permittivity of vacuum
ε_r	(-)	relative permittivity
ε'	(-)	real part of complex permittivity
ε''	(-)	imaginary part of complex permittivity
ε_∞	(-)	optic permittivity
ε_s	(-)	static permittivity
f	(Hz)	frequency
f_c	(Hz)	cut-off frequency
f_r	(Hz)	working frequency
H	($V\ m^{-1}$)	phasor of vector of magnetic field strength
H	(-)	function of homogeneity
$H_0^{(2)}$	(-)	Hankel function of zero order and second kind
J	($A\ m^{-2}$)	phasor of vector of current density
J_0	(-)	Bessel function
j	(-)	imaginary unit
k_c	(m^{-1})	cross-section constant in waveguide
l_s	(m)	length of centre circle of water bolus
λ_0	(m)	wavelength
λ_v	(m)	wavelength of the transmission line
μ	(-)	magnetic permeability
μ_c	(-)	complex permeability
μ_0	($H\ m^{-1}$)	permeability of vacuum
μ_r	(-)	relative permeability
r_s	(m)	radius of centre circle of water bolus
R	(-)	reflection coefficient
ρ	(C)	charge
ρ_t	($g\ cm^{-1}$)	density of biological tissue
s_{ij}	(-)	s-parameter,

s_{11}	(-)	s-parameter, input reflection coefficient
σ	(S m^{-1})	electric conductivity
t	(s)	time
T	(°C)	temperature
tan δ	(-)	loss factor
V	($mWcm^{-1}$)	blood flow
Z_0	(Ω)	impedance in vacuum
Z_v	(Ω)	wave impedance

List of Figures

List of Tables

Contents

1. Introduction

Electromagnetic fields (EMFs) - one of the fundamental forces in nature plays an important role in modern physics, due to their influence on atomic and molecular behaviour. As a result their influence on physical and chemical processes can have important effects on basic biological processes, with consequent knock-on effects on biological systems and their physiology. The area of EMFs positive or negative effect on human and animal health, therefore, has been continuously increasing in importance. Electromagnetic forces have existed since the "Big Bang" at the very beginning of the universe, and have played an important role in the development of the universe ever since. It took approximately 5 billion years, before scientists began to discover the basics of EMFs, with James Clark Maxwell, the first to formulate a set of equations describing the EMF (1861-62) that united previously unrelated observations, experiments and equations.

More recently, there has been an explosion in anthropogenically produced EMFs. Especially high frequency EMFs, with radio and microwave frequencies from sources such as radars, radio transmitters and especially cellular (mobile) phones becoming a common part of our environment over the last 20 years . Reflecting its possible harmful effects (the term "EM smog" has often been used for this situation). Of growing importance among the many sources of this EM smog is the rapidly increasing number of mobile phones being used and their associated base stations. What is of concern is that the source of radiation during a phone call is very close to the head of the caller, which raises the important question of possible negative effects of high frequency EMFs on the human body, and especially on the brain [1 - 3]. High frequency EMFs are capable of influencing tissues through both thermal and non-thermal effects. While both are frequently discussed at scientific meetings, non-thermal effects in particular remain poorly understood due to the difficulty of distinguishing them from thermal effects. Quite often current scientific reports tend to be too imprecise to obtain a comprehensive conclusion on the safety of high frequency EMFs and therefore it is one of the objectives of. However, the discovery of biogenic magnetite is present not only in lower living organisms (like bacteria) but also in higher organisms like insects, fish, and small mammals. Even human beings (e.g. evidenced in the brain tissue – [4]) have to be taken in account in the light of new technologies and an increase of "EM smog" for addressing a revaluation of potential effects on all organism, nervous system and behaviour. Another important biological mechanism that is the calcium ion network, fundamental for many cell functions and also for the immunological response of cells of the innate immunity expressing Ca++-dependant lectin-like receptors are demonstrated to be affected by EMFs. Once again, the present conditions of EM pollution address a reconsideration of some cell functions in relation to the different and most frequent kind of EM emissions can be a constant hazard in our current day life [5].

For some time now, the effects of EMF exposure on biological systems have been a topic of deep interest for both scientists and the general public, with high expectations regarding information on possible EMF hazards or possible uses for EMFs as regards new treatments in medicine. As a result, a lot of new research has taken place on this subject. It is increasingly important that researchers take an interdisciplinary viewpoint in order to effectively organise such research activities. In particular, there is a need for doctors and biologists on the one hand and EMF experts (e.g. physicists) on the other.

Many international activities are now focused on studies of the influence of EMFs on humans, the importance of their effect according to their intensity, time and modality of exposition, and especially on the possible harmful influence of mobile phones on the brain of their users (such studies often involving the tracking of several thousands of people but with the risk of bias due to the difficulties in collecting complete and certain data about the effective modalities of exposition to the mobile phone EMF). Other studies, however, include the influence of EMFs on control of pain [6], on the possible speeding-up of recovery time following injury, bone fracture or surgical operation [7], on cancer development (procarcinogenic effect, [8]; not carcinogenic effect, [9]; anticarcinogenic effect, [10]) and on their immunological effects [11]. About cancer we need to remember the importance of heat shock proteins (HSPs), a category of proteins discovered as chaperons for protecting functional molecules in the cell during thermal stress. They are present in the cells ready to avoid the denaturation of proteins or to remove from the cellular metabolism damaged proteins when temperature is increasing over the physiological threshold. According to the stress duration they can be also induced accumulating with antiapoptotic effects. In cancer they can have a double and even opposite role: on one hand, HSPs can protect the cancer cell from local stresses (e.g. prolonged exposure to thermal and not-thermal effects of EMFs) and from the toxic activity therapeutic of therapeutics, producing resistance to treatment and cell survival. On the other hand, they can be used for their chaperoning of tumour proteins when a quite rapid necrosis is induced by therapeutic hyperthermia (e.g. MW induced hyperthermia) helping the uptake and presentation of tumour antigens by immune cells with enhanced anticancer immune response [12]. They represent a chapter of renewed interest both for cancer diagnosis, monitoring and treatment with close relation to the evolution of understanding, evaluation and application of EMF effects.

In a different domain of EMF study and application, high frequency of EMFs also show great promise as bactericidal agents [13], especially as regards changes to water structure and DNA. Changes in water molecule structure, for example, may lead to an increase in hydration in cellular proteins and other compounds; while conformational changes in DNA can result in damage to genetic information [14]. Bacteria, under EMF treatment, can become more sensitive to chemicals, including antibiotics [15]. It is important, therefore, that such mechanisms are clearly identified in order to better understand the effects of altered metabolic pathways in bacteria and effects on their antibiotic resistance.

According to the progressive developments in the studies on EMFs, the therapeutic effects of interaction between EMFs and biological systems have been utilised in the

fields of oncology, physiotherapy and urology since the late 1970s. Nowadays, microwave thermotherapy is a common cancer therapeutic tool in many countries, including the EU, the USA, Japan and China. Thanks to clinical research undertaken at the Medical Faculty of Charles University, in combination with dissertation research undertaken at the Department of EMF at the Czech Technical University (CTU), microwave thermotherapy was already use in the former Czechoslovakia in 1981, with more than 1000 cancer patients have been successfully treated at Bulovka Hospital in Prague using the process since then.

2. State of the Art in the field of Microwave Thermotherapy

State of the Art consists of five main points. The first point describes general introduction into medical applications of microwaves inspired above all by ref. [16, 17]. The next point gives information about microwave hyperthermia in clinical applications, third point deals with clinical applications of physiotherapy. The fourth point introduces new principles of optimized design of applicators used in microwave thermotherapy, and the fifth point gives a description of hyperthermia treatment planning.

2.1 General introduction into medical applications of microwaves

Through the centuries there have been many recorded references to the treatment of human diseases, including cancer with increased temperature. An already famous aphorism of Hippocrates from 400 BC ends with words:

Those diseases which medicines do not cure, iron (the knife) cures;
those which iron cannot cure, fire cures;
and those which fire cannot cure, are to be reckoned wholly incurable.

Some reports in the 19^{th} and early 20^{th} century are describing remission of a variety of tumours using both localized and systemic means of inducing hyperthermia, but these used methods were mostly uncontrollable providing unpredictable results [18]. Thanks to the rapid development of technology and especially medical technology in the early eighties we can talk about microwave thermotherapy, which is being used in medicine for the cancer treatment and for treatment of some other diseases.

We can divide medical applications of microwaves into two major groups, namely on clinical and medical results and trends. Medical applications of microwaves are divided into the three basic groups according to purpose:

- treatment of patient (with the use of thermal or non-thermal effects of microwaves),
- diagnostics of diseases (e.g. permittivity measurement, microwave tomography, etc.),
- part of a treatment or diagnostic system (e.g. linear accelerator, etc.).

Microwave thermotherapy, which is used in medical applications, is based on thermal effect. Temperatures up to 41^{o}C are used for applications in physiotherapy and this method is called microwave diathermia. Microwave hyperthermia uses the temperature interval between 41^{o}C and 45^{o}C for cancer treatment. Microwave ablation (destruction of cells) occurs, when the temperature is more than 45^{o}C. Such microwave thermo ablation can be used in cardiology (for heart stimulations, treatments of heart arrhythmias, fibrillations, microwave angioplastics), and in urology (for treatment of Benign Prostatic Hyperplasia – BPH treatment).

Microwave thermotherapy is often used in combination with other medical therapeutical methods, like e.g. immunotherapy, chemotherapy, radiotherapy or chirurgical treatment, for cancer treatment.

In the Czech Republic local microwave hyperthermia and thermo ablations in cancer treatment, thermo ablations in cardiology and BPH thermotherapy are the most significant medical applications up to now [17].

2.2 Hyperthermia

Basic clinical methods used for cancer treatment are radiotherapy and chemotherapy. These therapeutic methods have many undesirable effects, such as e.g. effects of ionizing radiation, etc.. Another method used for treatment of oncology diseases is hyperthermia, which is one of cancer treatment methods based on local thermotherapy.

From clinical and biological point of view microwave hyperthermia is based on differences in the behaviour of healthy tissue and tumour tissue under enhanced temperatures. This method is based on the principle of destruction of malignant cells by artificially increasing the temperature above 41^{o}C, while healthy tissue survives temperatures of 45^{o}C [19]. In such case self-protective mechanism of malignant cells fails, they turn to apoptosis. Temperature in the area to be treated grows up in biological tissue due to absorption of power of electromagnetic waves, because biological tissue represents a lossy dielectric environment Absorbed energy of electromagnetic wave is thus changed into a thermal energy, which means a increase of temperature. The blood flow in tumour cells decreases with increasing temperature, and so the temperature in tumour cells increases even more rapidly. In temperature interval between 41^{o}C and 45^{o}C tumour tissue is destroyed (an apoptosis of tumour cells is being induced) [20].

Disadvantage of hyperthermia (potential risk) could be creation of hot spots in the treated area - this can be eliminated by use of a water bolus. This bolus should be inserted between surface of biological tissue and applicator aperture. Water bolus can improve transition of electromagnetic waves into treated area and it can help to optimize the temperature profile in the treated area.

The duration of a single hyperthermia treatment typically does not exceed 50 minutes. The level of the hyperthermic dose depends on temperature and time.

A standard hyperthermia system consists mainly from a high power rf. or microwave generator, set of thermal sensors, and especially, a set of different types and different aperture shapes and dimensions applicators.

2.3 Physiotherapy

Physiotherapy helps to improve movement and physiological functions. One of the methods used for physiotherapy is microwave diathermia [17], which is based on the principle of heating of treated part of human body, but to much lower temperature level than in hyperthermia, usually in the temperature range between 37^{o}C and 40^{o}C. Important effect in microwave diathermia is hyperaemia, which brings a strong analgesic effect/ consequence.

Microwave diathermia is used for the treatment of rheumatic diseases, improves tissue healing, reduces chronic pain, has a relaxing effect on skeletal muscles and relieves spasms. Applicators used for physiotherapy (diathermia) can be very similar to those used in local hyperthermia.

2.4 Applicators used in microwave thermotherapy

In hyperthermia applications there are treated areas, which are situated on the surface or near to the surface of human body. In such case for treatment of malignant cells local or superficial applicators should be used (most often waveguide applicators [21,22] or applicators formed by section of transmission line [23]).

A variety of microwave technologies used for microwave applicators is also increased by category of applicators based on the principle of evanescent mode waveguide, which can be applied for deep local thermotherapy treatment [24].

A special group of applicators is being represented by intracavitary applicators, which are inserted direct inside the body cavity, and therefore these applicators have cylindrical or plane shape. The basic type of intracavitary applicator is a monopole, which is excited by coaxial feed [25]. To improve focusation of EM energy into tissue helical coil structure can be added to monopole. The main usage of intracavitary applicators is above all firstly to coagulate malignant cells in prostate for BPH treatment in urology [26-28] and secondly, by using microwave ablation to treat atrial fibrillation [29].

If the malignant cells cover large area of human body, e.g. on head, neck, back, stomach or on extremity of human body, applicators with bigger dimensions can be used or is created array of several applicators [30-33]. In this case we talk about regional hyperthermia treatment. A lot of kinds of applicators are described in journal of European Society of Hyperthermic Oncology (ESHO) [34].

2.5 Hyperthermia treatment planning

Hyperthermia treatment planning is firstly based on reconstruction of a 3D anatomical model of the area to be treated [35], secondly on selection of the right type of applicator for a particular type of hyperthermia treatment and last but not least – on evaluation of treatment. This procedure will then result in obtaining necessary information for optimal treatment. Treatment planning then allows prediction of 3D SAR in the treated area due to certain settings of hyperthermia system.

First step is the generation of a segmentation of 3D anatomically based biological model from set of 2D slides of computer tomography (CT) or magnetic resonance (MRI) by using a dedicated computer program [36,37]. Created model is imported into the program [38], which is used for treatment planning. Such this program must by good cooperation allow calculation of EM field and SAR distribution. For these calculations is usually utilized SEMCAD X, which calculates examples based on the FDTD method. This method is suited for simulations inhomogeneous models and can be efficiently implemented in hardware accelerations [39].

3. Main Aims of Doctoral Thesis

The main aim of my research and scientific activities leading to the goal create and submit my dissertation thesis is to design and evaluate applicators for clinical use of microwave thermotherapy for treatment of cancer and other diseases.

3.1. Main aims of doctoral thesis

It is important to identify main aims (so called "dissertable core") of my doctoral thesis. Therefore I describe here the main targets of my doctoral thesis, focusing on the objectives which have been already earned and introducing those of the future work:

a) New model of microwave hyperthermia system coupled to patient body, based on signal flow graph theory (see Chapter 5, please).
b) Proposal of a new definition for evaluation of the SAR homogeneity during the treatment (see Chapter 6, please).
c) Feasibility study of focusing possibilities for deep heating and for case of regional treatment, when EM power is either in the phantom or in the patient body irradiated from several apertures with possibility to set up different amplitudes and phases in each of these apertures (see Chapters 7 and 8, please).
d) Analytical and numerical study of excitations of surface waves, which in therapy can cause so called hot-spots(see Chapter 9, please).
e) Feasibility study of superposition of EM field irradiated both from external and from intracavitary applicators (see Chapter 10 and 11, please).

In this development - attention is particularly paid on the penetration depth of the treatment into the biological tissue, using numerical simulations of SAR distribution and temperature measurements on agar phantoms for its estimation. Further, temperature distribution simulations in complex biological tissue models considering the influence of non-linear blood perfusion and temperature diffusion will be made. Finally the possibility to export the results of the experiment in clinical practice, considering the possibility to build an array of applicators to treat bigger areas and to work at different ISM frequencies will be analyzed.

3.2. Contents of doctoral thesis

In this part I would like to describe in more detail the topics and the content of the main parts/chapters of my doctoral thesis.

The first chapter ("Introduction") specifies orientation of this doctoral thesis to topics of medical applications of EM field (especially microwave technologies) to microwave thermotherapy above all.

The second chapter ("State of the Art in the field of Microwave Thermotherapy") represents a general introduction into medical applications of microwaves, specifying definitions of the hyperthermia and physiotherapy. Then applicators which can be used for the treatment of patients by microwave thermotherapy and principles of hyperthermia treatment planning are described here.

The third chapter (“Main Aims of Doctoral Thesis”) identifies the main goals (i.e. main pillars - so called “disertable core”) of my doctoral thesis first of all. Then description of content of all chapters of this doctoral thesis is given here.

The fourth chapter (“Applicators for Microwave Hyperthermia and Physiotherapy”) touches topics such as the interaction of EM field with biological tissue and defining basic parameters of microwave applicators. Furthermore it deals with the description of applicators for local and deep local treatment, basic rules of design of TEM, intracavitary and regional applicators. An original model of studied situation, i.e. applicator coupled to biological tissue, based on oriented graphs theory is proposed here in this chapter. Importance of impedance matching is explained here. Definition of an effective treatment area with respect to SAR distribution and the effective treatment area with respect to temperature distribution is given here. Last but not least, the importance of assessment and testing of microwave applicator properties is justified here in this chapter.

In fifth chapter (“Design of Applicators for Microwave Thermotherapy”) I describe the design of the applicators used in my work for research activities. Furthermore in this chapter I have proposed a new microwave part for the hyperthermia system (i.e. applicator coupled from one side to power generator and from the other side to biological tissue to be treated) based on theory of oriented graphs. This model can be considered as one of my original contributions to the topics of microwave thermotherapy systems.

The sixth chapter (“Microwave Thermotherapy in cancer treatment: Evaluation of Homogeneity of SAR Distribution”) is based on following paper of mine [L1,L6]. In this chapter I have propose a new definition of the SAR homogeneity, which according to my opinion is a very important parameter for quality of treatment. Design of applicator and a series of simulations demonstrating usage of homogeneity definition are given here.

The seventh chapter (“Study of focusing principles for regional treatments by array of applicators in homogeneous phantom”) is based on following paper of mine [L4,L9,L16]. Setup of applicator used for series of simulations demonstrating homogeneity of SAR in case of dielectrically homogeneous model of area to be treated is given here in this chapter.

The eighth chapter (“Study of focusing principles for regional treatments by array of applicators in anatomical model”) is based on following paper of mine [L2,L3,L10,L11,L17]. Several setups of applicators used for series of simulations demonstrating homogeneity of SAR in case of anatomical model of area to be treated is given here in this chapter.

The ninth chapter (“Study of Hot-Spots Induced by Electromagnetic Surface Waves) is based on following paper of mine [L8,L18]. This chapter brings analytical and numerical simulations to explain and consequently to eliminate excitations of surface waves. In this case we eliminate surface waves by optimization of dimensions of water bolus.

The tenth chapter (“Intracavitary Helix Applicator to be used for BPH and for Prostate Cancer Treatment”) is based on following paper of mine [L5,L12]. This chapter deals

with new results in area of intracavitary microwave applicators which can be used e.g. for prostate cancer treatment and for Benign Prostatic Hyperplasia (BPH) treatment as well.

The eleventh chapter (“Feasibility of Treatment Based on Combination of External and Intracavitary Applicators”) brings analytical and numerical simulations to verify possibility to combine external and interstitial applicators for treatment by microwave thermotherapy.

The twelfth chapter (“Conclusions”) gives a summary of the original results obtained in the frame of this doctoral thesis and then some notes on possible continuation in future research in this field.

In LIST OF CANDIDATE’S WORKS RELATING TO THE DOCTORAL THESIS there is a list of my research and scientific activities – i.e. list of published papers, list of research projects which I have participated as a member of a research team, list of my memberships in congress organizing committees.

4. Applicators for Microwave Hyperthermia and Physiotherapy

In this chapter we would like to describe the basic principles which should be used for the design of microwave hyperthermia and physiotherapy applicators. These principles are mainly given by interaction of electromagnetic field with biological tissue studied from a of physics and technique point of view - i.e. from the point of view of propagation of EM in the biological tissue, which behaves like a lossy dielectric material

4.1. Basic description of the apparatus for microwave thermotherapy

Apparatus for rf. and/or microwave thermotherapy typically consists of following several very important parts:

- Microwave power generator (typically working at one of ISM frequencies like e.g. 27, 40, 434, 2450 MHz, sometimes at some other frequency, like e.g. 70 and 915 MHz). Output power of this generator must be proportional to the volume of area to be treated, typically it is in the range from 100 up to 2 000 W.
- Applicator (resp. antenna) irradiates EM power into area to be treated. As in this case we do not radiate EM power to big distances (everything important happens few centimeters out from applicator aperture, we prefer to speak about applicator and not about antenna.
- Coaxial feeder – i.e. coaxial cable bringing microwave power from generator into the applicator.
- Thermometer with probes for temperature measurement (e.g. termocouples, thermistors) is used to determine development of temperature during the treatment.

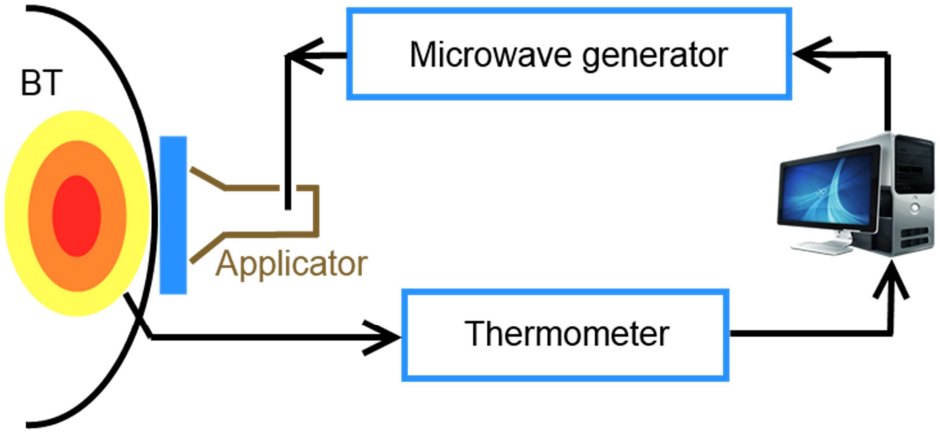

Fig. 4.1 Equivalent scheme of the apparatus for microwave thermotherapy.

- Water bolus is used for several purposes – it can stabilize the surface temperature of the treated area, it can improve impedance matching between applicator and treated biological tissue and it can reduce risk of hot spots.

- Control computer with implemented control software can control all the treatment procedure in order to achieve optimal treatment results.
- Treatment planning is then simulation of the treatment of selected patient. It is based on EM simulation of SAR distribution in the area to be treated at first and based on this result 3D temperature distribution can be calculated.

4.2. Interaction of electromagnetic field with biological tissue

To be able to study the interaction of EM field with biological tissue it is necessary to calculate and/or to measure the distribution of EM field in the area to be treated and subsequently to determine spatial distribution of EM energy absorbed in the biological area to be treated by microwave thermotherapy. For the calculation of EM field quantities values generally it is necessary to solve the Maxwell's equations.

$$rot\ \boldsymbol{H} = \frac{\partial \boldsymbol{D}}{\partial t} + \boldsymbol{J_v} \tag{4.2}$$

$$rot\ \boldsymbol{E} = -\frac{\partial \boldsymbol{B}}{\partial t} \tag{4.2}$$

Two additional Maxwell's equations are needed to be able to respect boundary and initial conditions:

$$div\ \boldsymbol{D} = \rho \tag{4.3}$$

$$div\ \boldsymbol{B} = 0 \tag{4.4}$$

If we have to solve the EM field in a matter (which is our case if we are interested to solve EM field in biological tissue area) then we have to take into account the three so called material equations for solution of Maxwell's equations in inhomogeneous environment:

$$\boldsymbol{D} = \varepsilon \boldsymbol{E} \tag{4.5}$$

$$\boldsymbol{B} = \mu \boldsymbol{H} \tag{4.6}$$

$$\boldsymbol{J_v} = \sigma \boldsymbol{E} \tag{4.7}$$

Interaction of EM field with biological tissue is influenced to a great extent by tissue permittivity ε. Tissue permeability μ is essentially the same as that of free space, therefore the magnetic losses are negligible. The biological tissue behaves as a lossy dielectric thus we have to consider the permittivity ε in complex form. Complex permittivity of loss material is generally dependent on frequency *f* and to certain extent on temperature *T* as well.

$$\varepsilon^* = \varepsilon' - j\varepsilon'' = \varepsilon'(1 - j\tan\delta) \tag{4.8}$$

$$\tan\delta = \frac{\omega\varepsilon' + \sigma}{\omega\varepsilon'} \tag{4.9}$$

Electric conductivity of considered tissue σ then can be expressed as:

$$\sigma = 2\pi f \varepsilon_0 \varepsilon' \tag{4.10}$$

In biological tissue the rf. and/or microwave EM field induces free movement of electrons and ions, polarization of atoms and molecules and rotation of molecules bound in dipoles. As a result of this effect on free or bound charges two types of current are induced:

a) Conductive current, whose density $\mathbf{J}_v$ is expressed as:

$$\boldsymbol{J_v} = \sigma E = 2\pi f \varepsilon_0 \varepsilon'' E \tag{4.11}$$

b) Displacement current, whose density $\mathbf{J}_0$ is expressed:

$$\boldsymbol{J_0} = \varepsilon_0 \varepsilon' \frac{\partial E}{\partial t} = 2\pi f \varepsilon_0 \varepsilon' E \tag{4.12}$$

Relation between density of conductive and the displacement current can be determined by tangent of loss angle δ.

$$\frac{J_v}{J_0} = \frac{2\pi f \varepsilon_0 \varepsilon'' E}{2\pi f \varepsilon_0 \varepsilon' E} = \frac{\varepsilon''}{\varepsilon'} = \tan\delta \tag{4.13}$$

where σ is the electric conductivity of biological tissue under consideration [S/m]. EM energy turns to heat particularly due to following mechanism: When the alternate field takes effect, vibrating electric particles lag behind the exciting intensity of the electric field; the current is not fully in phase with electric field intensity.
It is possible to describe mathematically this phase in that way that we virtually split up the movement of electrons into:

- Component that follows electric field intensity.
- Component that is in phase with difference of potentials on electrodes.

The first component mentioned above determines the real part of permittivity ε´, the other one is the cause of loss current heating up the dielectric and determining imaginary (conductive) part of permittivity ε´´. From this then follows that relative permittivity depends on the polarization charge value of dipole and alternate losses depend on the weight and volume of moving particle. The quality of dielectric is thus given by ratio of particle charge and particle mass [17].

When the electromagnetic energy goes through the biological tissue it is absorbed and turned into heat which results in temperature increase of biological tissue within the irradiated area. Spatial distribution of temperature induced the way mentioned above (resp. depth of EM wave penetration, resp. depth of efficient treatment) depends on various factors [16]. The most significant factors are mentioned below:

- Type of EM wave (planar, spherical, cylindrical, etc.).
- The frequency of EM wave.
- Spatial distribution of biological tissue within irradiated volume.
- Dielectric and thermal parameters of the tissues in area under consideration.

The discussed situation gets more complicated with a non-uniform system of blood vessels and their reactions to rising temperature caused by microwave heating. The organism tries to decrease the temperature by increasing the volume of blood flowing into the treated area. Figure 4.2 describes typical distribution of temperature T within homogenous tissue. The drop of temperature near the surface is caused either by cold circulating air or by cooling of the surface of the treated area by water bolus with thermo regulated water [17].

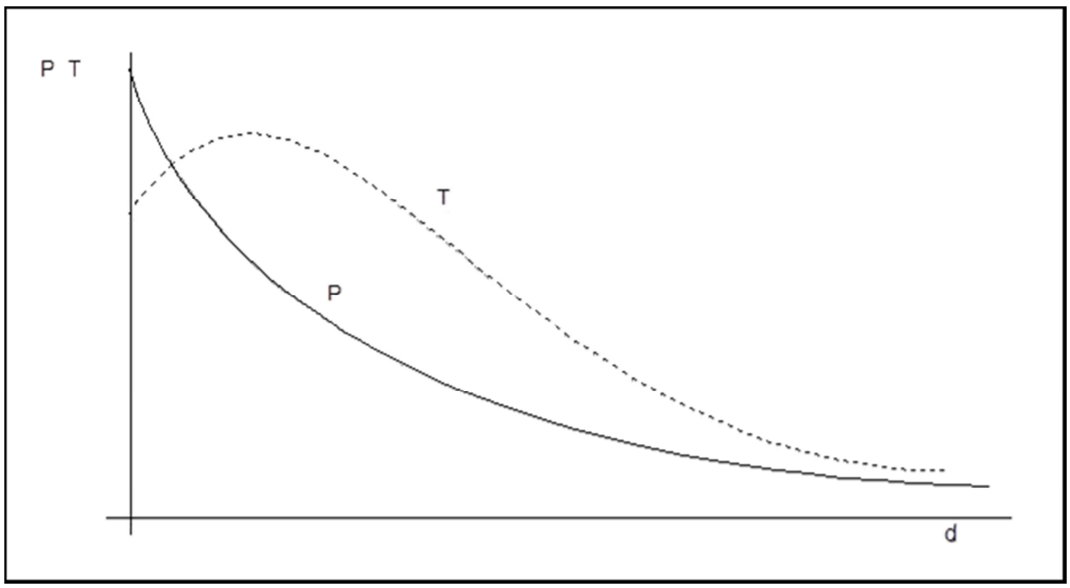

Fig. 4.2 Typical distribution of power P and temperature T at the depth d for the case of EM wave with propagating into biological tissue [17].

4.3. Basic parameters of EM applicators

The most important factor when determining a suitable working frequency of rf. and/or microwave applicators used in hyperthermia oncology is the penetration depth of the EM field into biological tissue [17]. The penetration depth is inversely proportional to the imaginary part of complex permittivity given by conductivity of given tissue and by frequency of the EM field.

$$d = \frac{1}{\sqrt{\pi\sigma\mu f}} \tag{4.14}$$

With respect to the usual operating frequencies of the applicators 27, 434, 915 MHz (all of them belong to ISM frequency bands reserved for industrial, scientific and medical applications), it can be concluded that the lower the frequency the deeper the penetration depth. The most common type of applicator would be a rectangular waveguide-based applicator with dominant TE_{10} mode. The surface area of the volume of the treated biological tissue limits the dimensions of applicator aperture. So a situation, where for given dimensions of the aperture the desired operating frequency *f* lies under the cut-off

frequency f_c of the waveguide dominant mode, can happen quite often. There are several ways how to solve this problem e.g. by modifying the cross-section of the used waveguide (using e.g. "H" or "π" waveguides), by filling the waveguide with high relative permittivity material (e.g. distilled water), but both these solutions introduces additional weight (limiting handling simplicity), realization complexity and costs. Alternatively a lumped capacitor can be inserted into a piece of waveguide operating under f_c which together with wave impedance of the waveguide (inductive for TE modes) forms a resonant circuit, which then can transmit EM high frequency energy into biological tissue.

4.4. Waveguide applicators for local and deep local treatment

Waveguide in general is a metal tube of any cross section (most often its cross section has rectangular or circular shape). Waveguide type applicator type consists of a waveguide section used for transmission of EM power from microwave power generator to the area to be treated. Discussed applicator is from one side closed with short-circuiting conductive wall and the other opened side is attached (bound) to biological tissue to be treated. Electromagnetic energy enters the applicator through coaxial structure whose purpose is to excite the desired mode in applicator. We have to differentiate two following cases:

- Applicator excited with a frequency higher than the cut-off frequency of the used waveguide.
- Applicator excited with a frequency lower than the cut-off frequency of the used waveguide, i.e. the case of evanescent mode applicator.

Waveguide based applicators

The waveguide applicators are appropriate for the treatment of both small and large tumours positioned near the surface of the tissue. In the central part of their aperture the distribution of electromagnetic field is very similar to planar wave thus it is possible to accomplish the deepest penetration depth for the particular frequency and aperture dimensions. Basic advantages of the waveguides are:

- The lowest level of losses of the EM energy to be transferred.
- Possibility to transfer the highest level of power.
- Very broad band with respect to frequencies to be transferred.
- Totally suppressed energy leakage of EM power.

The distribution of electromagnetic field in microwave waveguide is determined by solving the Maxwell's equations without sources by e.g. variable separation method. We are able to calculate EM field distribution with basic mathematical knowledge of rectangular waveguides. To study circular waveguides Bessel functions are used. Studying of electromagnetic field distribution in waveguides of other than rectangular or circular cross section leads to the use of either less usual functions or more often numerical methods. The energy is transferred when the waveguide is excited with a frequency higher than the cut-off frequency of the desired EM mode. Under this cut-off frequency the EM wave is exponentially damped along the waveguide and it is referred to as an evanescent mode.

Evanescent mode waveguide applicator

Evanescent mode waveguide type applicator is excited by a frequency lower than the cut-off frequency. The reason why the applicator is excited under its cut-off frequency is that the frequency of high-frequency medical devices is often determined by desired depth of electromagnetic wave penetration into biological tissue. This technique reduces the dimensions of waveguide circuitry, allows producing compact, low weight, easy to tune and handle devices operating on low frequency and thus ensuring desired penetration depth.

The theory of evanescent mode applicators proceeds from well-known waveguide theory. Waveguides are usually operated in a frequency band between cut-off frequency of dominant and that of the first higher-order mode. For frequencies in this region propagation constant β and wave impedance Z_0 are purely real numbers. However if a particular mode is exited under its cut-off frequency the propagation constant is purely imaginary.

$$\beta = \sqrt{k^2 - k_c^2} = -j\sqrt{k_c^2 - k^2} = -jk\sqrt{\frac{k_c^2}{k} - 1} = -jk\sqrt{\frac{f_c^2}{f} - 1} = -j|\beta|, \tag{4.15}$$

and wave impedance Z_{0TE} and Z_{0TM} of (rectangular waveguide) TE respective TM mode (e.g. [17] or [16]) is given by

$$Z_{0TE} = j\frac{k}{\sqrt{k_c^2 - k^2}}\sqrt{\frac{\mu}{\varepsilon}}, Z_{0TM} = -j\frac{\sqrt{k_c^2 - k^2}}{k}\sqrt{\frac{\mu}{\varepsilon}}. \tag{4.16}$$

It has been shown Eq. (4.16) that the rectangular waveguide has an inductive characteristic admittance Y0. At the same time, the biological tissue has a capacitive admittance Yb = Gb+jCb whose absolute value does not differ too much from that of Yc (1/Z0) in the frequency range of our interest. The different signs of the imaginary parts of these two admittances implies the principal possibility to implement a simple resonator, e.g. to insert a separate capacitance into the waveguide and consider the biological tissue just as a load of the resonator.

Connecting the lumped capacitance to the inductive element, a circuit with a desired resonance frequency can be obtained. The inductive element excites a number of TE and TM modes inside the waveguide but since the operating frequency lies under the cut-off frequency, these higher order modes are attenuated according to the attenuation constant described by the equation (4.15).

From eq. (4.15) follows that the distance of the inductive element from the biological tissue is a fundamental design parameter since, the proper choice of the distance allows to sufficiently attenuate the undesirable higher order modes. A modal filter can be also employed in order to suppress the unwanted modes and ensure the undisturbed field of the dominant mode at the aperture of the applicator.

4.5. TEM wave microwave applicators for local and deep local treatment

Construction of TEM wave applicator type is usually based on a section of rf. or microwave TEM wave uniform transmission line. Cut-off frequency in this case is equal to zero. One side of the discussed applicator is short-circuited with conductive wall and the other side with opened aperture is attached (bound) to biological tissue (BT) to be treated. To enlarge aperture of discussed applicator we can use a horn TEM transmission line. Very often between applicator and BT there is a water bolus (B). Electromagnetic energy usually enters

the applicator through coaxial structure whose purpose is to excite the desired mode in applicator.

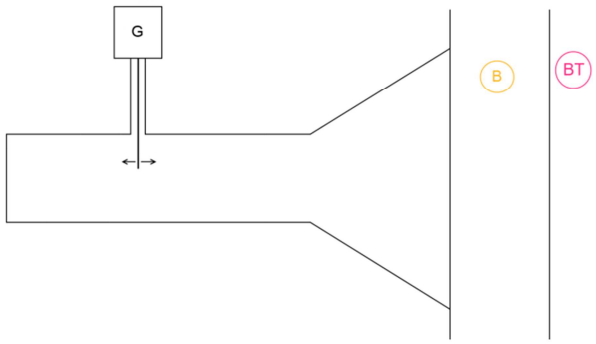

Fig. 4.3 Typical construction of a TEM applicator.

4.6. Intracavitary applicators

Sometimes tumours are situated in patient body areas, where it's very difficult or even impossible to deliver microwave energy to these areas in human body either by local external or regional applicators. In such cases so called intracavitary or interstitial applicator can be used. Intracavitary applicators thus have to have appropriate size to be possible to insert them into a cavity. These applicators are of cylindrical or very flat shape usually.

Coaxial intracavitary applicators

Coaxial transmission line technology based intracavitary applicators have appropriate the geometrical shape for intracavitary treatment and also the manufacturing process is simple and cheap. They are made in form of half wave length dipoles or quarter wave length monopoles so they are very suitable for rf. and microwave frequencies (e.g. f = 434 MHz or higher). Helical structure can be used for intracavitary treatment as well.

There aren't specific theories to implement this type of antenna; so it is necessary to assume some simplifying hypothesis and make a series of simulations to get the best antenna. The wavelength at working frequency is found by following equation:

$$f_r = \frac{c_0}{\lambda_0 \sqrt{\varepsilon_{eff}}} \tag{4.17}$$

It's possible to get the effective wavelength λ by the following relation:

$$\lambda = {\lambda_0}/{\sqrt{\varepsilon_{eff}}} \tag{4.18}$$

in which, ε_{eff} is the effective electric permittivity, function of relative permittivity of cable ε_{cable} and a relative permittivity of biological tissue ε_{bt} . As a first simplifying assumption usually we use following equation:

$$\varepsilon_{eff} \approx \frac{\varepsilon_{cable}+\varepsilon_{bt}}{2} \tag{4.19}$$

Planar intracavitary applicators

Planar intracavitary applicators are derived from microwave planar technology circuits and resonators. These applicators are usually formed by narrow strip of rectangular, circular or elliptical resonant structure separated by dielectric layer from grounded conductive plane. These applicators have flat shape appropriate for placement to mouth cavity.

4.7. Applicators for regional treatment

Applicators for regional treatment use converging cylindrical or elliptical wave or at least its part for heating of large human body areas. Such a wave propagates inward from body surface. Thus if we know the radius and dielectric properties of heated tissue we can choose frequency in such a way that the temperature in a tissue rises from surface to center. As a contraindication for patient undergoing thermotherapy treatment is the use of pacemakers and other metal implants. These implants might be heated by electromagnetic field so much that either the adjacent tissue or implanted device itself could be damaged.

4.8. Effective treatment area with respect to SAR distribution

In chapter 6 of this doctoral thesis we will describe and explain how our new definition of the homogeneity of SAR distribution. We will introduce a special function *H* describing this quantity and to determine, on which parameters will depend the value of this function. As a basic definition of such function describing SAR homogeneity we will propose to use following equation:

$$H = \mathrm{SAR}_{max}/\mathrm{SAR}_{min} \tag{4.20}$$

where SAR_{max} is a maximum value of SAR in the studied volume and SAR_{min} is a minimum SAR value in a studied volume. Such definition enables quantitative evaluation of SAR distribution homogeneity over the heated area. Its efficacy in appreciation of SAR patterns quality is demonstrated on idealized and real SAR distributions. The *H* parameter of applicators widely used in clinics can be calculated easily. *H* could be assumed as a useful parameter additional to the qualified effective field size in characterizing the applicator's properties.

From Eq. (4.20) it follows, that we will be able to specify three basic cases of homogeneity quality (and function *H* value):

1. *Perfect homogeneity of* SAR, when in all studied volume SAR_{min} is almost equal to SAR_{max} (i.e. function *H* is almost equal to 1).
2. *Very good homogeneity*, when in all studied volume $\mathrm{SAR}_{min} > \mathrm{SAR}_{max}/2$ (i.e. function *H* is in interval between 1 and 2).
3. *Poor homogeneity*, when in studied volume there is region in which $\mathrm{SAR}_{min} < \mathrm{SAR}_{max}/2$ (i.e. function *H* is bigger than 2).

It is evident, that for such a definition a critical value of SAR homogeneity is a case when $H = 2$. Critical value here means a boundary between acceptable (i.e. at least very

good SAR homogeneity) and/or not-acceptable (i.e. very poor SAR homogeneity) distribution of SAR for treatment of selected patient.

4.9. Effective treatment area with respect to temperature distribution

As mentioned for the homogeneity of SAR distribution in paragraph 4.8. can be in similar be applied to homogeneity of temperature distribution, because both these quantities are coupled between them by so called Penne's bioheat equation. Many investigators have studied blood flow and the temperature in biological bodies by using heat transfer analysis, which deals with transient and spatial heating inside bodies simultaneously [40-42]. To solve the temperature distribution for thermal therapy is widely used the Penne's bioheat transfer equation. This equation describes the exchange magnitude of heat transfer between tissue and blood occurs only in the capillaries without taking into account blood vessels [43].

$$\rho_t c_t \frac{\partial T}{\partial t} = q + \gamma_t \Delta T - V(T - T_b) \tag{4.21}$$

where

t is the time,
$q = q(x,y,z,t)$ is energy delivered by EM field, here q = SAR
$T = T(x,y,z,t)$ designates the temperature,
$T_b = T_b(x,y,z,t_o)$ is the temperature of blood.

Physical meaning and values of the here used constants for the case of high water contents tissue are:

ρ_t = 0,965 [g/cm^3] ... density of biological tissue (BT)
c_t = 3 586 [mJ/g/C] .. specific heat of BT
V = 5,45 [mW/cm^3/C] blood flow and temperature capacity of BT
γ_t = 5,84 [mW/cm/C] spec. temp. conductivity of BT.

The possibilities for analytical solution of this equation are limited to only a few cases - like e.g. "one dimensional" case of plane wave penetrating in homogeneous phantom. Therefore computers are to be used to solve this equation to obtain the temperature $T(x,y,z,t)$ time dependence and space distribution. For the treatment planning of microwave thermotherapy it is possible to use e.g. software product SEMCAD.

Even if this equation is widely used, it does not take into account some very important parameters, like e.g.:

a) It does not account for the directivity of blood flow,
b) It does not account for the discreteness of vessels,
c) It is based on the assumption of local equilibrium between blood and environmental temperature, which is true only for small capillaries,
d) It usually does not consider temperature dependence of tissue parameters.

4.10. Evaluation of applicators for microwave thermotherapy

Evaluation of hyperthermia applicators is very important to guarantee a high level of quality assurance for treatment of patients. Basically we have to evaluate four main parameters:

- Impedance matching of studied applicators.
- 3D SAR distribution created by studied applicators in the area to be treated.
- 3D temperature distribution created by studied applicators in the area to be treated.
- 3D distribution of microwave power spread around hyperthermia system.

Impedance matching of studied applicators will be in details discussed in Chapter 5 and 3D SAR distribution for case of different applicators resp. different arrays of applicators will be discussed in chapters 6 to 11 then.

Evaluation of SAR of hyperthermia applicators can be done by two following methods:

- by aid of IR camera,
- by aid of water phantom.

Evaluation of hyperthermia applicators by aid of IR camera can bring information about both SAR and temperature 3D distribution. For assessment of tested applicator it is useful to carry out measurement by heating the phantom. When we are testing the applicator by this way, it is necessary to measure the temperature very quickly (up to 1 minute) after the heating with as finest resolution of temperature distribution as possible in 3D phantom of biological tissue. Phantoms of biological tissue used for hyperthermia applicator testing should match the following properties of tissue such as:

- permittivity
- electrical conductivity
- heat conductivity
- specific heat
- effect of blood vessels (cooling of tissue by influent blood and taking into account biological system defense reaction – i.e. with rising temperature the volume of influent blood is rising as well)
- spatial distribution of biological tissue in treated area

For modelling of tissues with high water content (e.g. muscle tissue) agar gelatine can be used. This method of applicator evaluation enables to determine SAR (Specific Absorption Rate, [W/kg]) distribution that shows absorbed microwave power in 1 kg of tissue. By IR camera measured temperature distribution we can easily recalculate to SAR distribution by aid of following formula:

$$\mathrm{SAR} = c\,\frac{\Delta T}{\Delta t} \qquad \left[{}^{W}/_{kg}\right] \tag{4.22}$$

Evaluation of SAR of hyperthermia applicators in the water phantom means to measure the EM field power distribution in front of the aperture of this applicator. The E-field

distribution can be measured by the dipole antenna. The length of this antenna must be much smaller then $\lambda/4$ (λ is the wavelength of measured field in this media). The voltage induced in this antenna supply the LED. The optical signal from the LED is leaded by the optical fiber outside the phantom to the optical detector.

5. Design of Applicators for Microwave Thermotherapy

This chapter is based on manuscript of the paper: “Design of Applicators for Microwave Thermotherapy”. To be published.

Following on from Chapter 3 of this doctoral thesis, its main aims are to contribute to the theory and design methods of applicators for microwave thermotherapy. As mentioned before design of applicators for microwave thermotherapy should fulfill several important requirements:

1. Delivery of microwave power into the treated area
2. Optimization of SAR distribution in the treated area.
3. Optimization of temperature distribution in the treated area.
4. Minimization of EM field scattered around hyperthermia system.

The first of these requirements – optimized delivery of microwave power into the treated area - will be discussed in this chapter. The other three requirements will be studied in following chapters of this doctoral thesis.

5.1. Impedance matching of microwave thermotherapy applicators

If we want to deliver a major part of the microwave power into the biological tissue (i.e. area to be treated) we have to minimize the reflections of EM power in the microwave part of hyperthermia system. Microwave theory and techniques generally enables us to implement systems with very negligible levels of reflection.

Current literature usually only mentioned/discussed the reflections between applicator aperture and water bolus or the surface of biological tissue. In such a case we usually get a very simple frequency behavior of reflection coefficient – shape approaching to resonant peak.

In this chapter we would like to demonstrate, that in general situations this can be far more complicated. In order to do so in part 5.2 we will describe the typical topology of waveguide type resp. TEM transmission line type applicator and in part 5.3 we will create a model of such an applicator based on the theory of oriented graphs. From this graph more complicated response of reflection coefficient frequency behavior can arise.

5.2. Topology of applicators for microwave thermotherapy

According to comments on Fig. 4.3, the construction of a waveguide type or TEM wave applicator type is usually based on a section of waveguide or rf. resp. microwave TEM wave uniform transmission line (K). One side of the discussed applicator is short-circuited with a conductive wall and the other side with a opened aperture is attached (bound) to biological tissue (BT) to be treated. To enlarge aperture of discussed applicator we can use a waveguide horn or horn TEM transmission line (H). Very often between applicator and (BT) there is a water bolus (B).

EM energy, generated by microwave power generator (G), usually enters the applicator through coaxial transmission line (I) which enters into waveguide or TEM transmission line via capacitive probe (T) and thus it excites the desired mode in the applicator. As this capacitive probe excites EM power going in two directions: one wave goes in direction to (BT) and the other one in the opposite direction, we have that other one wave to return

back to (BT) by aid of shorting plate (Sh). Correct phase of returned wave can be adjusted by correct length of transmission line section (J).

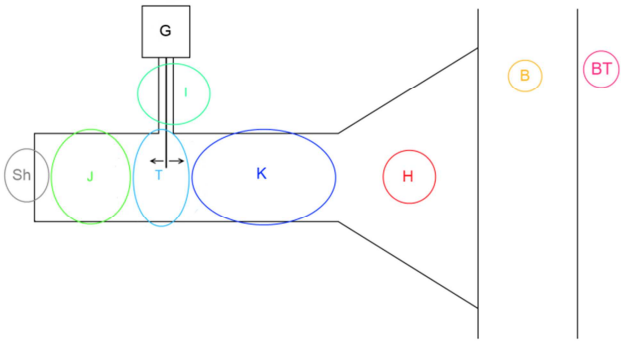

Fig. 5.1 Discussed applicator coupled to biological tissue.

5.3. Signal flow graph of applicator coupled to biological tissue

In this paragraph we would like to propose a description of the case described in previous paragraph by aid of a signal flow graphs. In literature we have found only a very simple model of this case [16], here we would like to propose much more sophisticated model displayed on Fig. 5.2. As it can be seen in this figure, each of parts mentioned in description to Fig. 5.1 (i.e. sections G, I, T, J, Sh, K, H, B and BT) are represented in this oriented graph by a number of corresponding one, two and three port elements.

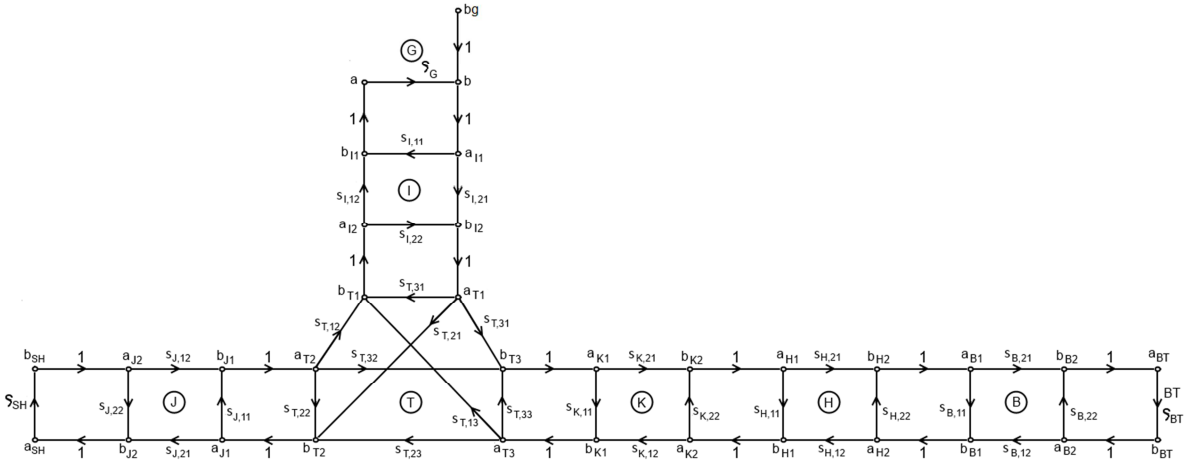

Fig. 5.2 Signal flow graph model of the applicator coupled to biological tissue.

To analyze behavior of studied case of microwave applicator coupled to biological tissue (described by previous figure) we have to determine scattering matrices of each part of discussed system, i.e. scattering matrices for sections G, I, T, J, Sh, K, H, B and BT:

$$s_G = \begin{bmatrix} s_{G,11} & s_{G,12} \\ s_{G,21} & s_{G,22} \end{bmatrix} \tag{5.1}$$

$$s_I = \begin{bmatrix} s_{I,11} & s_{I,12} \\ s_{I,21} & s_{I,22} \end{bmatrix} \tag{5.3}$$

$$s_T = \begin{bmatrix} s_{T,11} & s_{T,12} & s_{T,13} \\ s_{T,21} & s_{T,22} & s_{T,23} \\ s_{T,31} & s_{T,32} & s_{T,33} \end{bmatrix} \tag{5.4}$$

$$s_J = \begin{bmatrix} s_{J,11} & s_{J,12} \\ s_{J,21} & s_{J,22} \end{bmatrix} \tag{5.5}$$

$$s_{Sh} = \begin{bmatrix} s_{Sh,11} \end{bmatrix} \tag{5.6}$$

$$s_K = \begin{bmatrix} s_{K,11} & s_{K,12} \\ s_{K,21} & s_{K,22} \end{bmatrix} \tag{5.7}$$

$$s_H = \begin{bmatrix} s_{H,11} & s_{H,12} \\ s_{H,21} & s_{H,22} \end{bmatrix} \tag{5.8}$$

$$s_B = \begin{bmatrix} s_{B,11} & s_{B,12} \\ s_{B,21} & s_{B,22} \end{bmatrix} \tag{5.9}$$

$$s_{BT} = \begin{bmatrix} s_{BT,11} \end{bmatrix} \tag{5.10}$$

Scattering matrices for sections G, I, T, J, Sh, K, H and B is possible to determine either by analytical resp. numerical calculation or by measurement (i.e. experimental evaluation). Scattering matrix for section BT can be determined by aid of a signal flow graph calculated e.g. for different cases of 3D configurations of different tissues, described in paragraph 5.4 and displayed in Fig. 5.4.

Second step in the procedure is to analyze the behavior of the studied case of microwave applicator coupled to biological tissue we have to determine transfer functions *T* between selected nodes of this signal flow graph by aid of so called Mason rule. In our case the transfer function $T_{BT,G}$ (i.e. transfer function from node b_{g} to node a_{BT}) is for us the most important one:

$$T_{BT,G} = \frac{a_{BT}}{b_G} \tag{5.11}$$

where

a_{BT} is a generalized voltage wave incident on biological tissue surface,

b_G is a generalized voltage wave going out from microwave generator.

We have to take into account, that all generalized scattering parameters in the discussed signal flow graph are frequency dependent. So to be able to do an exact analysis of the studied case we have to know the frequency behavior of each mentioned element in the discussed signal flow graph.

Ideally when microwave power is delivered to biological tissue with a minimum of internal reflections inside applicator itself, its coaxial feeder, water bolus, etc. (in this way parasitic internal resonances will be strongly suppressed), values of mentioned scattering matrices should approach to following values:

$$s_G = \begin{bmatrix} 0 & 0 \\ 1 & 0 \end{bmatrix} \tag{5.12}$$

$$s_I = \begin{bmatrix} 0 & 1 \\ 1 & 0 \end{bmatrix} \tag{5.13}$$

$$s_T = \begin{bmatrix} 0 & s_{T,12} & s_{T,13} \\ s_{T,21} & 0 & s_{T,23} \\ s_{T,31} & s_{T,32} & 0 \end{bmatrix} \tag{5.14}$$

$$s_J = \begin{bmatrix} 0 & s_{J,12} \\ s_{J,21} & 0 \end{bmatrix} \tag{5.15}$$

$$s_{Sh} = [-1] \tag{5.16}$$

$$s_K = \begin{bmatrix} 0 & s_{K,12} \\ s_{K,21} & 0 \end{bmatrix} \tag{5.17}$$

$$s_H = \begin{bmatrix} 0 & s_{H,12} \\ s_{H,21} & 0 \end{bmatrix} \tag{5.18}$$

$$s_B = \begin{bmatrix} 0 & s_{B,12} \\ s_{B,21} & 0 \end{bmatrix} \tag{5.19}$$

$$s_{BT} = [s_{BT,11}] \tag{5.20}$$

Providing the ideal design of discussed applicator the previous signal flow graph could be simplified to case displayed by following figure, where both full and dashed lines should be taken into account.

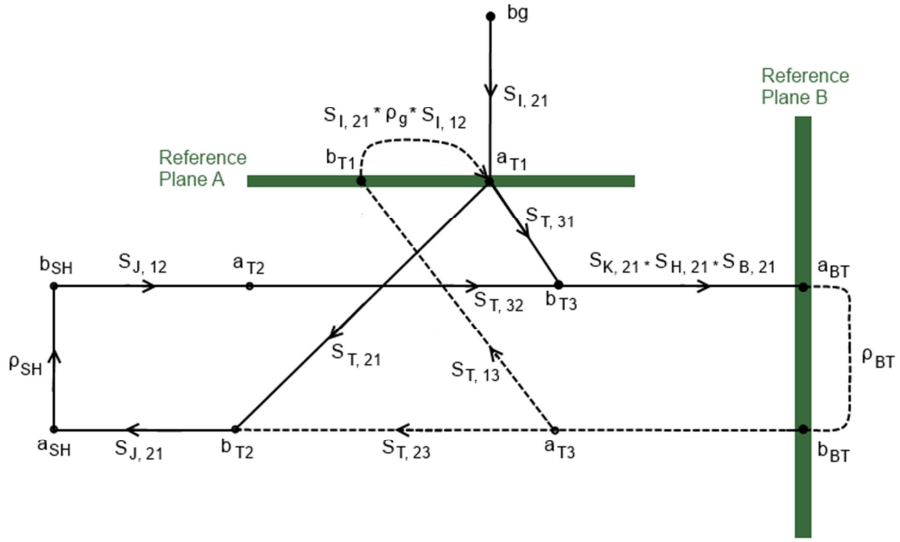

Fig. 5.3 Simplified signal flow graph model of applicator coupled to biological tissue.

In this figure are by dashed lines displayed those branches, which can be consequently eliminated by a perfect impedance matching both at reference plane A of the applicator input (horizontal green line) and at reference plane B where applicator is coupled to BT (vertical green line). Perfect impedance matching at reference plane A can be guaranteed by the perfect impedance matching of the sections G, I and T each to other (e.g. by aid of impedance transformers). Further, perfect impedance matching at reference plane B can be guaranteed by the perfect impedance matching of the sections T, K, H, B and BT each to other (e.g. by aid of impedance transformers plus by filling all those sections by water which has its dielectric parameters very near to those of BT).

In this case the transfer function $T_{BT,G}$ (i.e. transfer function from node b_g to node a_{BT}) can be written by aid of Mason rule:

$$T_{BT,G} = \frac{a_{BT}}{b_G} = s_{I,21}\left(s_{T,31} + s_{T,21}s_{J,21}\rho_{Sh}s_{J,12}\right)s_{K,21}s_{H,21}s_{B,21} \tag{5.21}$$

where all used quantities follow from signal flow graph in Fig. 5.4. From this equation we can see, that for optimal function of studied applicator following conclusions can be derived:

a) All scattering parameters should represent only a phase shift – no attenuation
b) Both parts in parenthesis, i.e. $s_{T,31} and\ s_{T,21}s_{J,21}\rho_{Sh}s_{J,12}$ should be equal each to other (at least approximately).

5.4. Signal flow graphs of several different configurations of biological tissue

Delivery of microwave power does not depend only on microwave applicator itself, it depends very strongly on certain 3D configuration of biological tissue in the treated area as well. In this paragraph we will discuss several possible cases of 1D tissue

configuration and we will show the way how to determine reflection coefficient of the surface plane of the biological tissue in the area to be treated.

In the following picture we can see five basic 1D configurations. Here S designates section of skin, F designates section of fat, M designates section of muscle and C designates section of cancer resp. tumour.

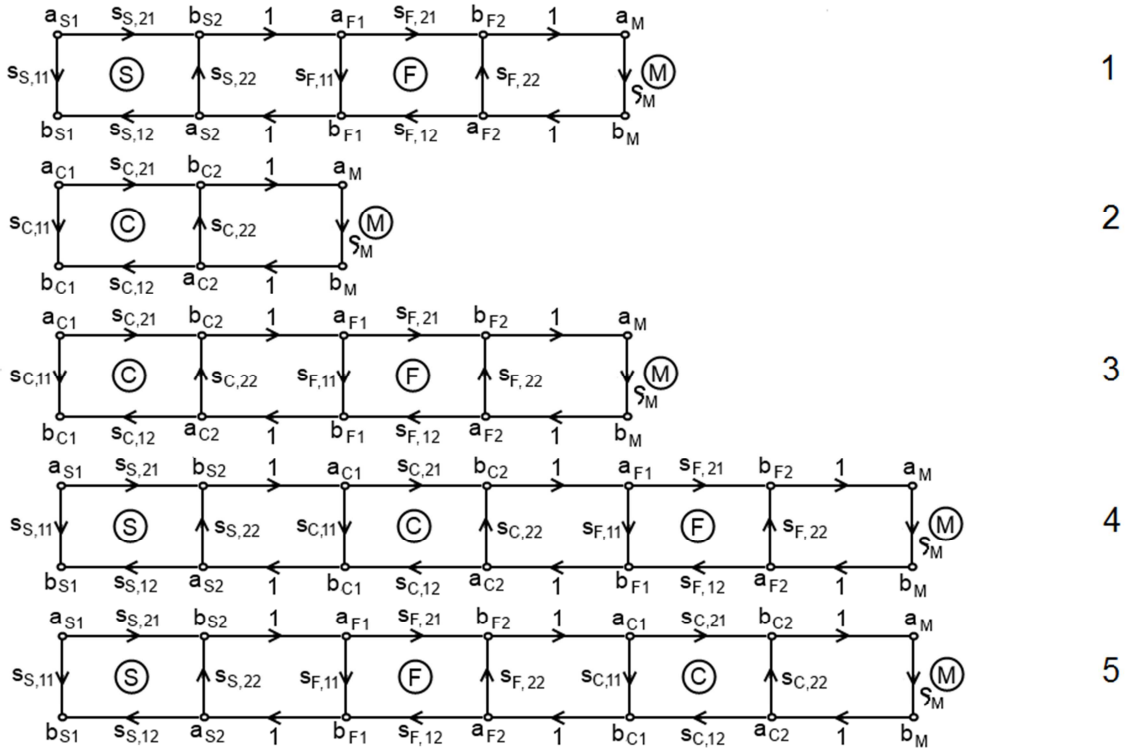

Fig. 5.4 Signal flow graph models of several 1D configurations of biological tissue in the area to be treated.

To be able to determine reflection coefficient of the surface of biological tissue we have to take into account the real anatomical configuration of the biological tissue in the area to be treated. In this paragraph we would like to propose signal flow graphs for several typical cases. In opposite to previous paragraph, where we demonstrated, that by careful design of microwave applicator it is possible to simplify significantly.

First case from Fig. 5.4 describes typical situation in human body, when surface area of the biological tissue has three layers: skin(S), fat (F) and muscle (M). Second case from Fig. 5.4 describes situation when there is a surface tumour (C) and a muscle (M) under it. As we are interested in determination of power P_{L} absorbed in tumour layer then especially in this case approximate following formula can be used:

$$P_L = \frac{1}{2}[(|a_{C1}|^2 - |b_{C2}|^2) + (|a_{C2}|^2 - |b_{C1}|^2)] \tag{5.22}$$

where in the first parenthesis we have power absorbed by forward propagating wave and in the second parenthesis we have power absorbed by reflected wave.

Third case from Fig. 5.4 describes situation when there is a surface tumour (C) and a fat (F) layer and a muscle layer (M) under it. Fourth case from Fig. 5.4 describes situation when there is a skin (S) on the surface, under it then tumour (C) and a fat (F) layer and a

muscle layer (M). Very similar is then case five, where tumour (C) is between fat (F) and muscle (M).

5.5. Design of 434 MHz microwave stripline type applicator with TEM mode

For our research we choose microwave stripline type applicator with TEM mode [23], because it offers the best homogeneity of power density in its aperture.

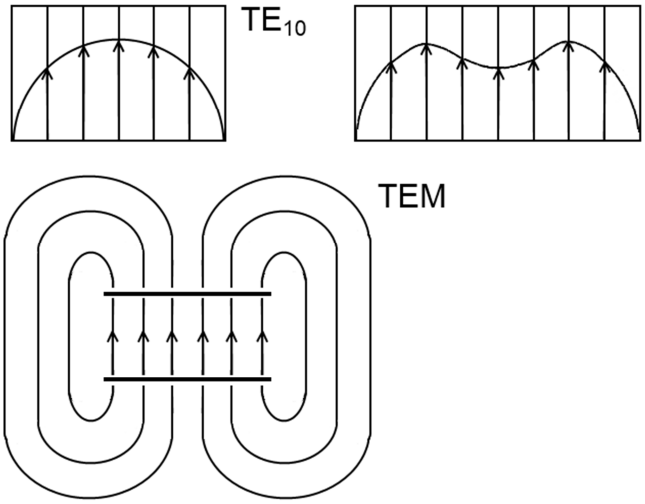

Fig. 5.5 Comparison of homogeneity of microwave power density in aperture of:
a) waveguide applicator with TE_{10} mode, b) waveguide evanescent mode applicator with improved homogeneity c) stripline type TEM applicator.

This is very important for the treatment like in oncology or physiotherapy. We designed two applicators, first applicator works at frequency of 434 MHz and the second one works at 70 MHz. Both applicators were designed by the FDTD simulator [38] (e.g. SEMCAD X EM Field simulator from SPEAG, Schmid & Partner Engineering AG, Switzerland).

Applicator with TEM mode

As it is already known, basic parameters of TEM wave depend mainly on dielectric parameters of media through which it propagates (complex permittivity ε and conductivity σ of that tissue) and on the working frequency, but non on cross section dimensions and type of transmission line. This discussed wave propagates along stripline type transmission line.

Applicator 434 MHz

Applicator is made from a highly conductible material (copper) and lateral sides of applicator are from acrylic glass. TEM wave is being transferred along a section of microwave stripline transmission line with cross-section dimensions 50 x 30 mm and length 80 mm. Horn section of applicator has length 80 mm. The horn aperture has dimensions 120 x 80 mm. Length of applicator equals double wave length, which depends on relative permittivity of biological tissue ($\varepsilon_r = 54$):

$$\lambda_v = \frac{c_0}{f\sqrt{\varepsilon_r}} = \frac{3 \cdot 10^8}{434 \cdot 10^6 \sqrt{54}} = 0,\ 094 \text{ m} \qquad (5.23)$$

The proposal design of applicator consists in solving transition between power supple and applicator, because by filling applicator with dielectric materials are the properties of this applicator similar to biological tissue. In the literature [16], the distance of the excitation probe moves between λ/8 and λ/4 from the shorted end of the waveguide. By calculating the distance we chose the wavelength range from 9.6 mm to 19.2 mm.

Another important feature of the design is the thickness. Although for large thicknesses is secure a good mechanical strength, but poor bending of material. As a rule, the thickness of the material is chosen as five times of the depth of penetration, which is given by:

$$\delta=1/\sqrt{\pi f \mu \sigma} \tag{5.24}$$

where f = 434 MHz , $\sigma_{CU} = 5{,}9.10^7$ S/m. This gives the penetration depth is about 3.14 μm and five times:

$$5\delta = 15{,}73\mu m \tag{5.25}$$

Based on these calculations, was chosen thickness of copper 1.5 mm. Thickness of acrylic glass was chosen 2 mm due to incision of threads.

To avoid reflection of wave back to the generator, applicator is filled with suitable dielectric material. Whereas 70% of human body consists of water, applicator is filled with distilled water. Advantage of the applicator filled by water is at first a better transfer of electromagnetic energy from discussed applicator into human body and at second smaller dimensions of the applicator itself.

Impedance matching of applicators should be simulated by the FDTD simulator to find position and length of the exciting probe (Fig. 5.6).

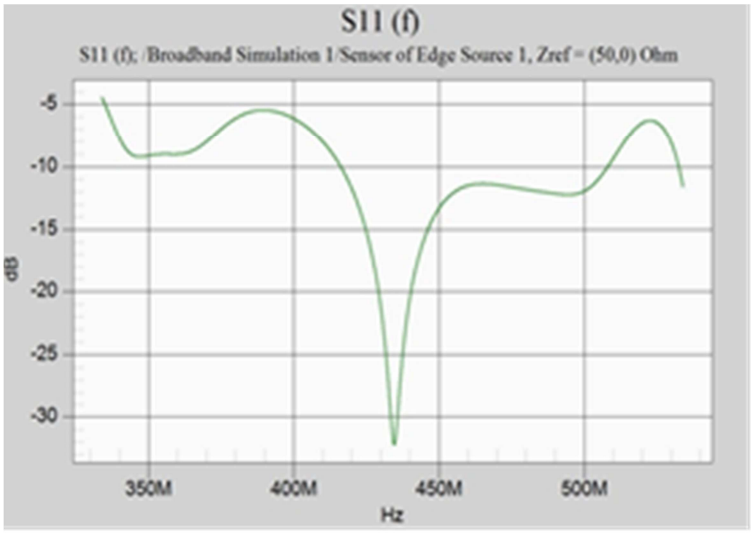

Fig. 5.6 Impedance matching

On this figure it is shown, that at working frequency the reflection parameter *s11* = - 32,3 dB, which represents the value of VSWR = 1,05. The length of the exciting probe equals to 27 mm and the distance from the short-circuited plane is 15 mm. Then we can make measurement of impedance matching of applicator by using ENA series microwave network analyzer Agilent E5062A. By measurement determined impedance matching of

discussed applicator it was found *s11* = - 33,4 dB (i.e. VSWR = 1,04). So, the condition of impedance matching is satisfied.

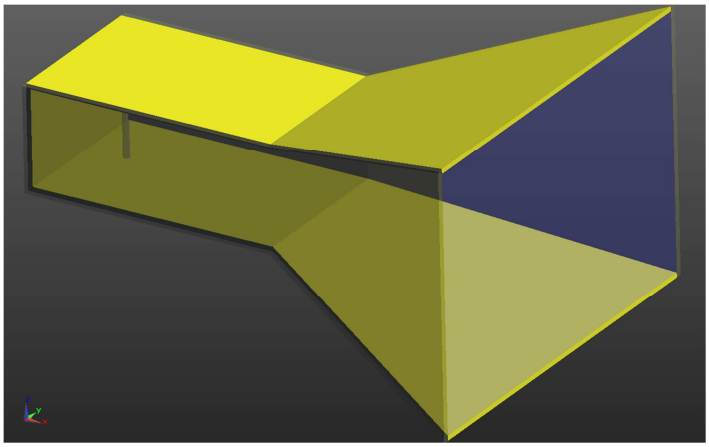

Fig. 5.7 Model of applicator for 434 MHz

5.6. Applicator 70 MHz

Applicator, which works at frequency of 70 MHz, was designed in similar way to the applicator working at 434 MHz. But this applicator is intended to be used for deep or regional treatment due to its lower frequency (depth of penetration of EM energy at 70 MHz into biological tissue is about 8 cm, whereas depth of penetration of EM wave at frequency of 434 MHz is about 4 cm). Of course, in this case of design of applicator dielectric parameters are taken into account, which at frequency ε_r = 70,75 and σ = 0,69 per biological tissue represents muscle [44].

Like applicator for 434 MHz also applicator for 70 MHz was designed like microwave stripline applicator with TEM mode, which its non-divergent part has dimensions 100 x 60 mm. Aperture of this applicator has shape of stripline type horn - its dimensions are 240 x 200 mm and its length equals approximately one quarter of wavelength (λ_v = 0,509 m). Electromagnetic field is in this applicator excited by a capacitive probe, which is located inside the applicator. As applicator for 434 MHz also this applicator is filled with distilled water for better transfer of EM energy into human body.

6. Microwave Thermotherapy in cancer treatment: Evaluation of Homogeneity of SAR Distribution

This chapter is based on:

Vrbova B., Vrba J. - Microwave thermotherapy in cancer treatment: evaluation of homogeneity of SAR distribution. In: *Progress In Electromagnetics Research*, Vol. 129, 181-195, 2012. E-ISSN: 1559-8985

Vrbová, B.(50%), Vrba, J.: Evaluation of Homogeneity of SAR Distribution of Array of TEM Mode Applicators. In Proceedings of the 6th European Conference on Antennas and Propagation (EUCAP 2012). Piscataway: IEEE, 2012, p. 1091-1094. ISBN 978-1-4577-0920-3.

In this chapter we would like to describe our results in area of microwave thermotherapy. It represents a contribution to a theory of phase array applicators for microwave hyperthermia in cancer treatment. As it was mentioned in the "State of the Art" paragraph, hyperthermia is a thermotherapeutical method used for fulguration of cancerous cells by artificially increased temperatures due to electromagnetic field exposure [16, 32, 45]. For real clinical applications of the microwave thermotherapy in general a very high level of homogeneity of a 3D temperature distribution obtained by aid of the discussed phase array applicators is strongly required. It is essentially important for reaching of a high quality assurance of the mentioned treatments. And a basic condition to reach such goal is a very good level of homogeneity of a SAR 3D distribution generated by the discussed phase array applicators [46]. In paper of Gelvich the homogeneity of SAR distribution is defined as the ratio of the area size with SAR > 75 % to the area size with SAR > 25 % of the maximum SAR value and includes information about the existence of 'hot spots' in SAR patterns [47]. This paper therefore deals with a study and with an evaluation of homogeneity of SAR distribution in cylindrical agar phantom for several different values of its radius. Discussed SAR distribution is in our case created by EM field exposure done by aid of four microwave stripline type TEM mode applicators of the same type, which work at frequency 70 MHz. Detailed design of this applicator was described in previous chapter 5.

6.1. Clinical use of microwave thermotherapy

Thanks to the rapid development of technology and especially medical technology in the early eighties we can talk about microwave thermotherapy, which is being used in medicine for the cancer treatment and treatment of some other diseases. Medical applications of microwaves are divided into the three basic groups according to purpose:

- treatment of patient (with the use of thermal or non-thermal effects of microwaves),
- diagnostics of diseases (e.g. by aid of permittivity measurement, microwave tomography),
- part of a treatment or diagnostic system (e.g. linear accelerator).

Microwave thermotherapy, which is mostly used in medical applications of EM fields, is based on thermal effect. Temperatures up to 41^{o}C are used for applications in physiotherapy and this method is called microwave diathermia. Microwave hyperthermia uses the temperature interval between 41^{o}C and 45^{o}C for cancer treatment. Microwave ablation (destruction of cells) occurs, when the temperature is more than 45^{o}C. Such microwave thermo ablation can be used in cardiology (for heart stimulations, treatments of heart arrhythmias, fibrillations, microwave angioplastics), and in urology (for treatment of Benign prostatic Hyperplasia - BPH). Microwave thermotherapy is often used in combination with other medical therapeutical methods, like e.g. immunotherapy, chemotherapy, radiotherapy or chirurgical treatment, for cancer treatment.

6.2. Definition of SAR homogeneity

In this section we describe how to evaluate the homogeneity of SAR distribution in agar phantom. As EM field exposure system we selected a system which consists of four microwave stripline type TEM mode applicators of the same type, described in more details in section 5 of this thesis. The discussed microwave applicators work at frequency of 70 MHz and are designed for deep local or for regional type cancer treatment by microwave power. This exposure system is in our study coupled to a cylindrical homogeneous agar phantom mimicking the biological tissue (muscle tissue in our case). We will present here a sequence of several simulations of SAR distributions with different values of the radius of the cylindrical agar phantom changing in the range from 50 up to 100 mm. To compare quality of homogeneity obtained in different simulations we need to specify a definition of parameter of homogeneity.

In following discussion we would like find out how to describe homogeneity of SAR distribution. We want to specify a special function *H* describing this quantity and to determine, on which parameters will depend the value of this function. As a basic definition of such function describing SAR homogeneity we propose to use following equation:

$$H = SAR_{max}/SAR_{min} \tag{6.1}$$

where SAR_{max} is a maximum value of SAR in the studied volume and SAR_{min} is a minimum SAR value in a studied volume. Such definition enables quantitative evaluation of SAR distribution homogeneity over the heated area. Its efficacy in appreciation of SAR patterns quality is demonstrated on idealized and real SAR distributions. The *H* parameter of a series of applicators widely used in clinics can be calculated easily. *H* could be assumed as a useful parameter additional to the qualified effective field size in characterizing the applicator's properties.

From Eq. 6.1 it follows, that we can specify three basic cases of homogeneity quality (and function *H* value):

1) *Perfect homogeneity of* SAR, when in all studied volume SAR_{min} is almost equal to SAR_{max} (i.e. function *H* is almost equal to 1).
2) *Very good homogeneity*, when in all studied volume $SAR_{min} > SAR_{max}/2$ (i.e. function *H* is in interval between 1 and 2).
3) *Poor homogeneity*, when in studied volume there is region in which $SAR_{min} < SAR_{max}/2$ (i.e. function *H* is bigger than 2).

It is evident, that for such a definition a critical value of SAR homogeneity is a case when $H = 2$. Critical value here means a boundary between acceptable (i.e. at least very good SAR homogeneity) and/or not-acceptable (i.e. very poor SAR homogeneity) distribution of SAR for treatment of selected patient.

We can suppose, that in general the homogeneity *H* of the SAR distribution created by array of the discussed applicators in the homogeneous cylindrical agar phantom is basically a function of frequency *f*, function of complex permittivity ε of the used

cylindrical agar phantom, a function of the phantom radius *R* and a function of the phantom axial dimension (its length) *L*, it can be schematically written as follows:

$$H = H(f,\varepsilon,R,L) \tag{6.2}$$

It can be expected, that up to a certain value of the discussed agar phantom radius there will be created SAR distribution shape with very good level of homogeneity, but with increasing value of the phantom radius the homogeneity of the SAR will decrease very quickly then.

6.3. Description of applicator

For research of above mentioned problem we chose microwave stripline type applicator with TEM mode described in chapter 5.

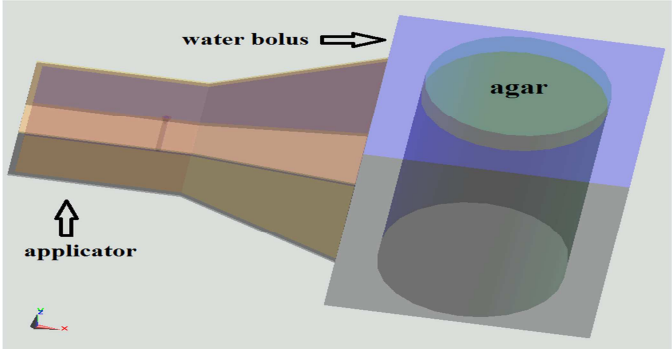

Fig. 6.1 Model of applicator with agar and bolus.

For design and verification of functionality of created applicator is used agar phantom. This is a homogeneous phantom, which represents only one tissue type. In our case an agar phantom represents muscle tissue (ε_r = 70,75 and σ = 0,69). Between applicator and agar phantom is situated water bolus for better transfer energy into tissue, but also for elimination hot spots created on the surface of human body.

6.4. Simulations

By aid of the SEMACD X EM field simulator we simulated array of TEM mode applicators of the discussed type located around cylindrical agar phantom, which in our work we gradually enlarged in several steps and thus we can compare results of single simulations. We selected this particular biological phantom for the following two reasons: Firstly, a cylindrical shape is a very good approximation for the shapes of various parts of human body (e.g., arm, leg, thorax, abdomen, etc.). And secondly the simple homogeneous structure is the best one for the studies of homogeneity of the SAR distribution primarily related to the studied applicators. It should be the first step when new types of the applicators are being studied. In case of the true anatomical phantoms homogeneity of SAR distribution is significantly influenced by selected anatomical part of human body. In our simulations we took into account dielectric properties of muscle tissue. Real cancer cells have somewhat lower values of complex permittivity, but the SAR distribution is influenced by square root of complex permittivity, so the mentioned difference does not play a significant role. Between homogeneous agar phantom and

array of applicators a water bolus is inserted for better transfer of electromagnetic energy into agar phantom, which in our case represents muscle tissue, as can be seen in Fig 6.2.

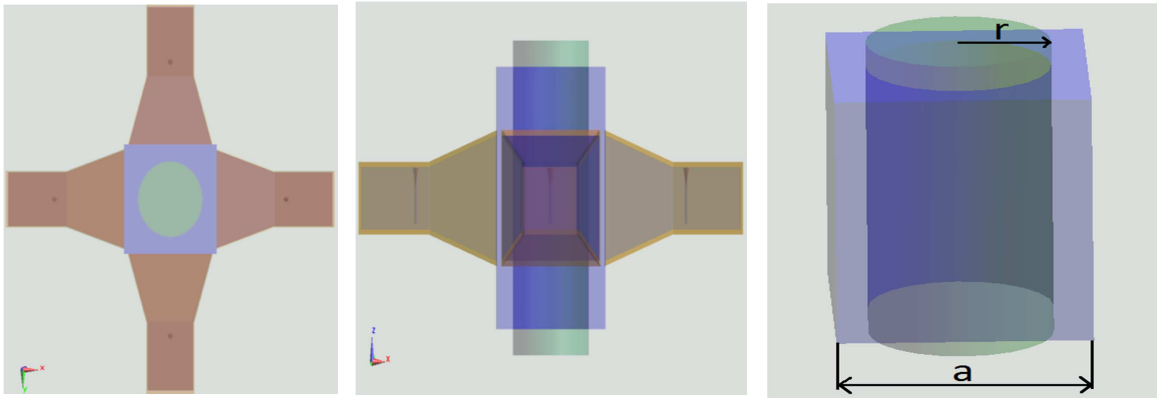

(a) (b) (c)

Fig. 6.2 Definition of phantom cross sections: (a) Transversal plane cross section, (b) sagittal plane cross section and (c) dimensions of cylindrical agar and water bolus.

In discussed case, when we have cylindrical phantom surrounded by four above mentioned applicators, then for the thermotherapy the most important component of EM field will be longitudinal component E_z, which in discussed case can be expressed by equation

$$E_z = K.\, H_0^{(2)}(\gamma r) \tag{6.3}$$

where

$H_0^{(2)}$ is Hankel function of zero order and second kind,

K is a constant,

γ is a constant of propagation.

Hankel function $H_0^{(2)}$ [48], can be calculated as linear combination of Bessel function J_0 and Neumann function N_0:

$$H_0^{(2)}(\gamma r) = J_0(\gamma r) - jN_0(\gamma r) \tag{6.4}$$

As cylindrical agar phantom is mimicking muscle tissue, i.e. lossy medium, then argument of Hankel function is a complex number.

In following picture (Figure 6.3) there are displayed four basic cases of possible SAR distribution. Comparing Figure 6.3 and 6.2 it is evident that diameter $D = 2r$.

a) This curve corresponds to case, when depth of penetration of the studied EM wave is much less than radius of the agar phantom. This typically happens for higher frequencies (i.e. higher attenuation constant) and bigger diameters of the phantom.

b) If frequency is going down (i.e. attenuation constant is decreasing) or diameter of the phantom is decreasing then we can expect to approach to the shape of curve b, where some level of focusing can be seen.

c) If we further continue to go down with the frequency or we continue to decrease diameter of the phantom, then we may have very significant focus of SAR, like e.g. it is shown in the case of curve c.

d) If the frequency is very low and depth of penetration at this frequency is comparable or bigger than radius of the phantom, than shape of SAR distribution may be approaching curve d.

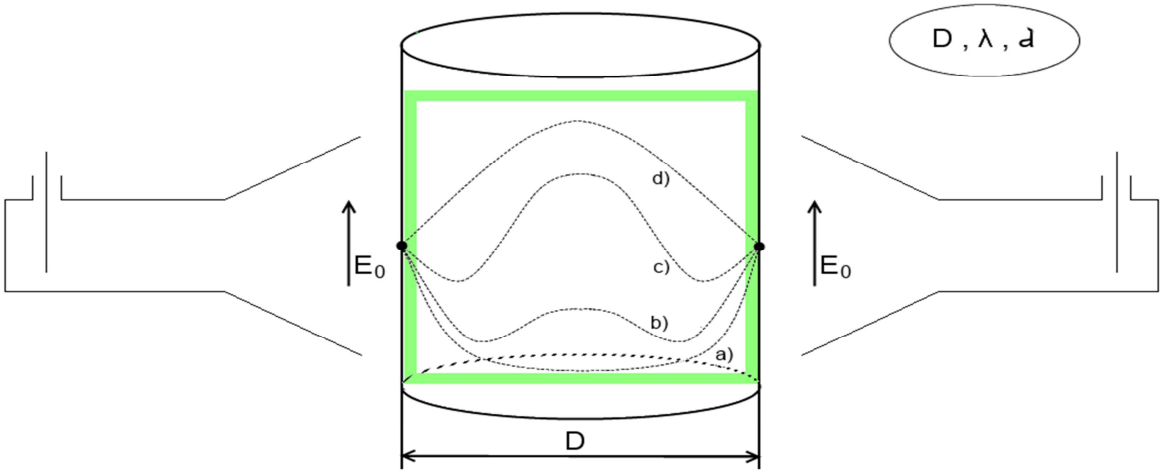

Fig. 6.3 Four different types of SAR distribution in cylindrical agar phantom.

In order to be able to evaluate effect of SAR superposition created by array of four applicators, we did some simulations of the case, when only one of four applicators was active (see Figure 6.4). Here simulations of 3 cases (r = 50mm, r = 75mm and r = 100mm) are displayed.

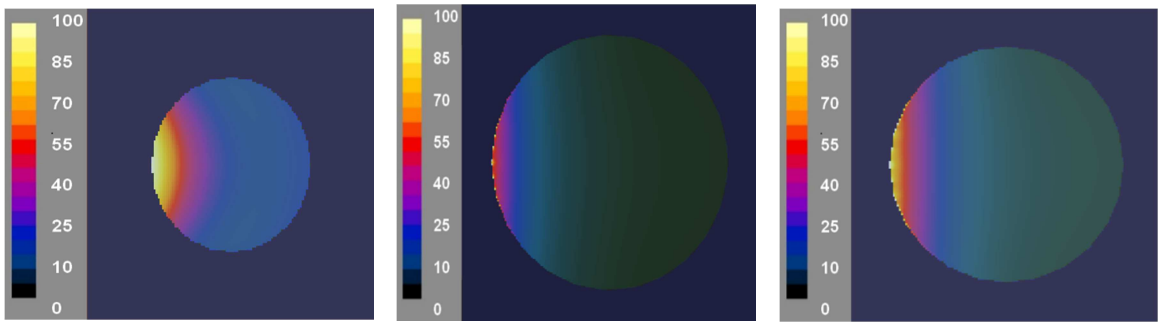

(a) (b) (c)

Fig. 6.4 SAR distribution created by one applicator. (a) r = 50 mm, a = 180 mm, (b) r = 75 mm, a = 25 mm, (c) r = 100 mm, a = 25 mm.

Figures 6.5 to 6.15 display the SAR distribution created in the cylindrical agar phantom by the array of the four applicators located around the cylindrical homogeneous agar phantom, which has radius changing in 11 steps from 50 to 100 mm. The range of radius from 50 to 100mm is very typical to different parts of the human body which we potentially expect to be treated by microwave thermotherapy - e.g., arm, leg, thorax, abdomen, etc. The SAR distribution scale in Figures 6.5 to 6.15 has no units. In all these figures we display normalized value of SAR, i.e., real value in discussed point divided by maximum value in the studied area. And then multiplied by 100, thus we have result in percent with respect to the SAR maximum value. Doing this we can easily find 50% Iso-SAR curve, which is boundary of the area, where we can expect successful treatment.

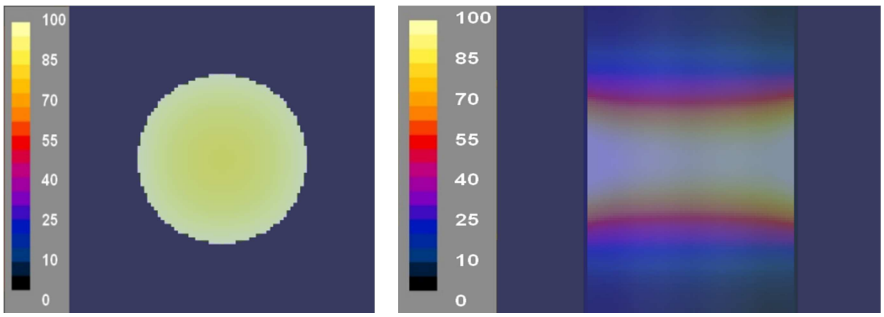

(a) (b)

Fig. 6.5 SAR distribution for case r = 50 mm, a = 180 mm, H = 1.114. (a) in transversal plane cross section and (b) in sagittal plane cross section.

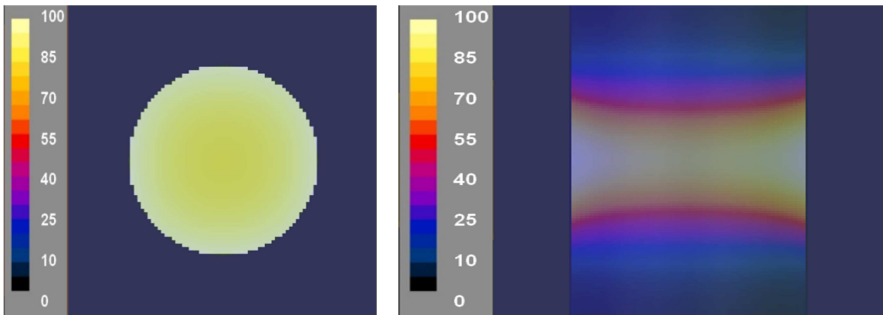

(a) (b)

Fig. 6.6 SAR distribution for case r = 55 mm, a = 180 mm, H = 1.182. (a) in transversal plane cross section and (b) in sagittal plane cross section.

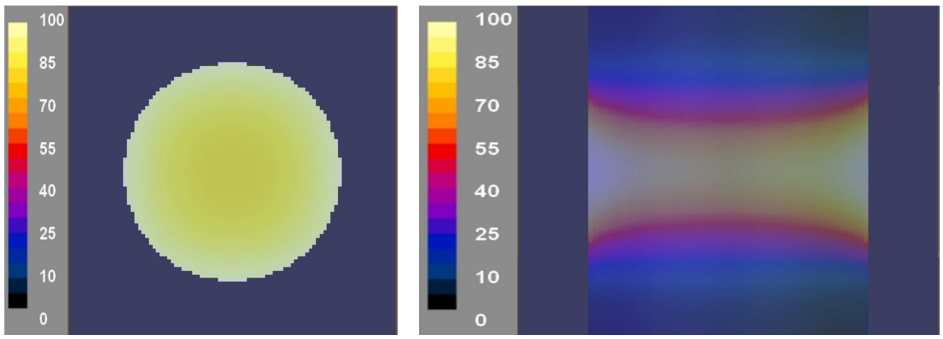

(a) (b)

Fig. 6.7 SAR distribution for case r = 60mm, a = 180 mm, H = 1.258. (a) in transversal plane cross section and (b) in sagittal plane cross section.

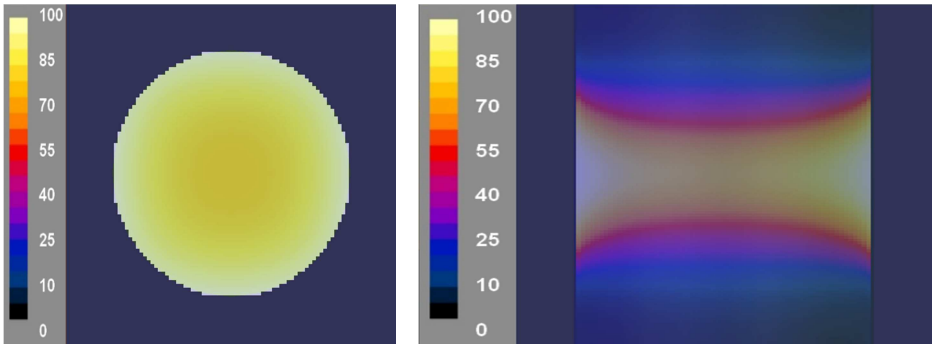

(a) (b)

Fig. 6.8 SAR distribution for case r = 65mm, a = 180 mm, H = 1.3448. (a) in transversal plane cross section and (b) in sagittal plane cross section.

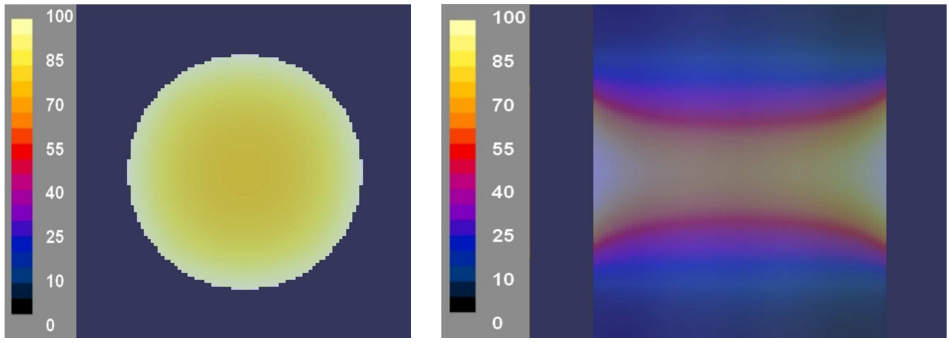

(a) (b)

Fig. 6.9 SAR distribution for case r = 70mm, a = 180 mm, H = 1.3448. (a) in transversal plane cross section and (b) in sagittal plane cross section.

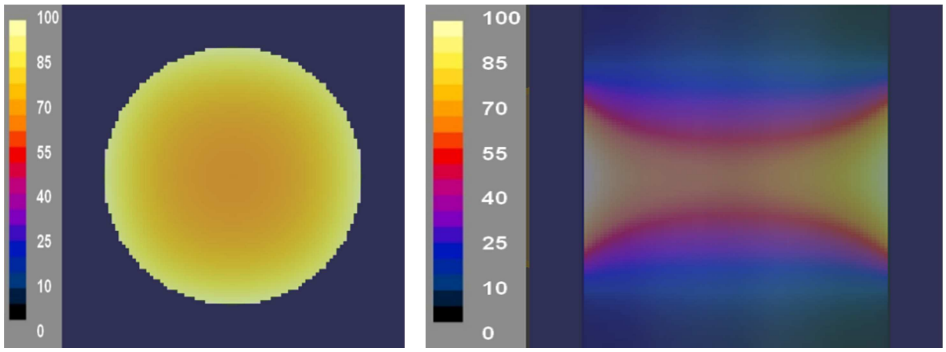

(a) (b)

Fig. 6.10 SAR distribution for case r = 75mm, a = 200 mm, H = 1.444. (a) in transversal plane cross section and (b) in sagittal plane cross section.

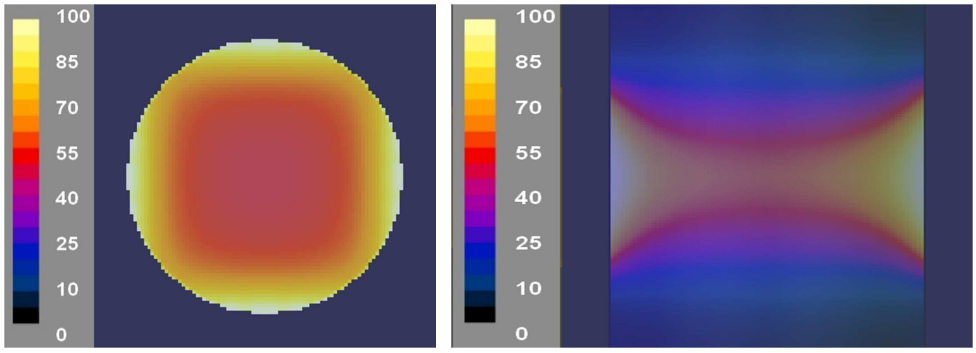

(a) (b)

Fig. 6.11 SAR distribution for case r = 80mm, a = 200 mm, H = 1.857. (a) in transversal plane cross section and (b) in sagittal plane cross section.

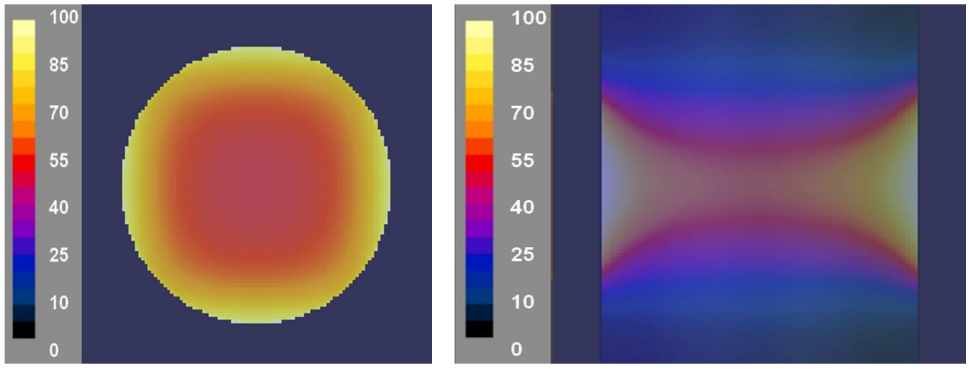

(a) (b)

Fig. 6.12 SAR distribution for case r = 85mm, a = 220 mm, H = 2.05. (a) in transversal plane cross section and (b) in sagittal plane cross section.

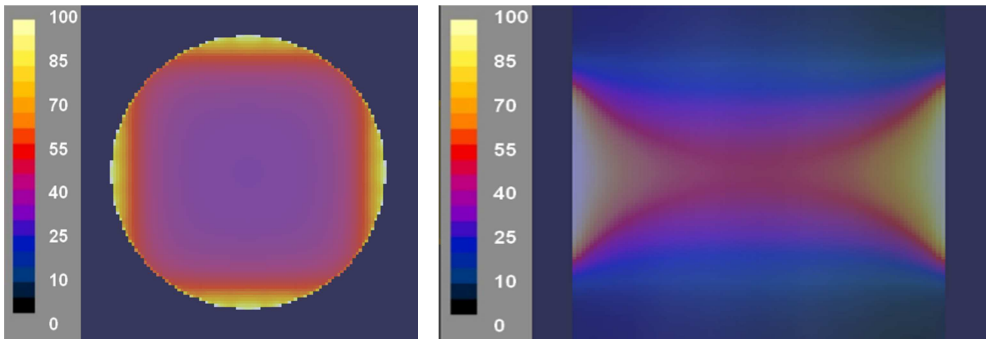

(a) (b)

Fig. 6.13 SAR distribution for case r = 90mm, a = 220 mm, H = 2.599. (a) in transversal plane cross section and (b) in sagittal plane cross section.

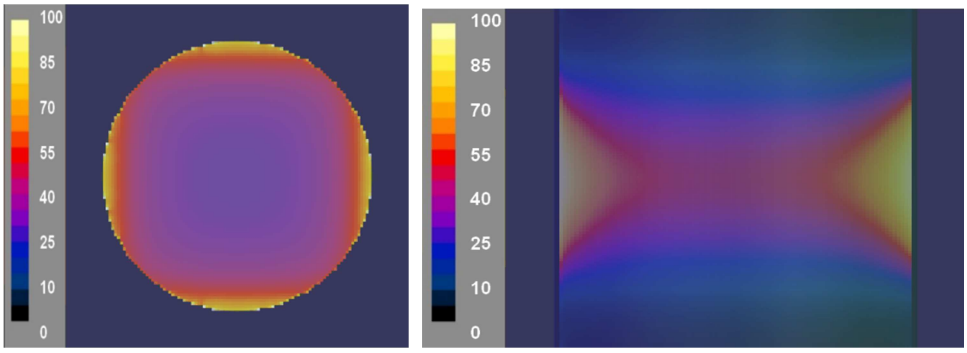

(a) (b)

Fig. 6.14 SAR distribution for case r = 95mm, a = 240 mm, H = 3. (a) in transversal plane cross section and (b) in sagittal plane cross section.

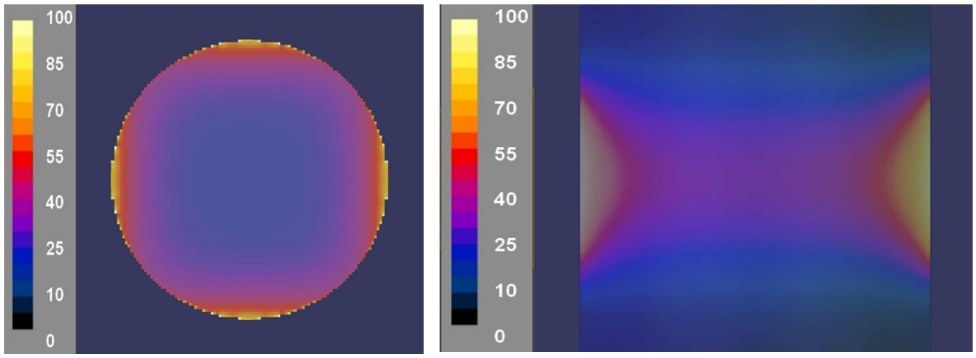

(a) (b)

Fig. 6.15 SAR distribution for case r = 100mm, a = 250 mm, H = 3.552. (a) in transversal plane cross section and (b) in sagittal plane cross section.

6.5. Discussion of presented results

In Fig. 6.5 to 6.15, when comparing the homogeneity of SAR of all the different cases an almost perfect homogeneity of the studied SAR distribution (i.e. SAR almost perfectly constant in all phantom volume) can be observed only for case of the agar phantom radius up to 60 mm. With respect to the SAR maximum (i.e. level of 100%) the SAR value is above the 50% level here in all the agar phantom volume.

When we enlarged in several steps the radius of cylindrical agar phantom up to value of 100 mm (and we will repeat simulations for all these cases, of course) then we can compare homogeneity of SAR created in agar for all these cases, what can be seen very well in all SAR distributions displayed in all cases of Fig. 6.5 till 6.15.

Increasing value of agar phantom radius, we can see that homogeneity of 3D SAR distribution in agar phantoms deteriorates very quickly. Just at radius of 80 mm homogeneity of SAR approaches to its critical value (see please Fig. 6.11 - there is very evident decrease to level of 50% with respect to the *SAR* maximum), i.e. H = 1.857 in this case.

Figures 6.12 to 6.15 show that quality of homogeneity of SAR is deteriorating, i.e., level of SAR is below the level of 50% (with respect to the SAR maximum, which corresponds to 100%) in a substantial part of studied agar phantom volume. Comparing all the studied cases in the Fig. 6.5 to 6.15, we can arrive at the conclusion given by a graph displayed in Figure 6.16.

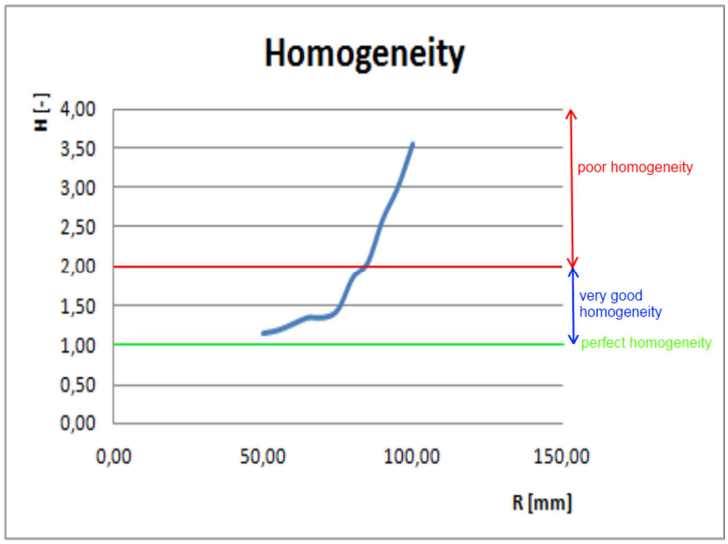

Fig. 6.16 Homogeneity H vs. radius R of cylindrical agar phantom.

6.6. Summary of important results in this chapter

Results of the study of homogeneity of SAR distribution created by the array of TEM stripline type applicators of the same type in homogeneous agar phantom have been described and discussed in this paper. The effect of the phantom dimensions on SAR homogeneity has been demonstrated. In our opinion the techniques selected and tested by us proved to be very accurate and effective. In conclusion it can be stated that up to a certain level radius of agar phantom a very well homogeneous shape of SAR distribution can be created. Here presented results correspond very well to our analytical model of the studied problem. Main conclusion of our work is that from the point of view of real treatments of cancer patients a significant reduction in homogeneity of SAR can be observed for radii more than 85mm.

7. Study of focusing principles for regional treatments by array of applicators in homogeneous phantom

This chapter is based on:

Vrbová B., Vrba J. - Waveguide-based Applicators for Local Microwave Thermotherapy: Feasibility Study of Matrix Array Treatment, In: Conference Proceedings - Progress in Electromagnetics Research Symposium (PIERS 2010 Xi\'an). Cambridge, MA: The Electromagnetics Academy, 2010, p. 1394 – 1397. ISBN 978-1-934142-12-7.

Vrbová B., Vrba J. - Matrix Composition of Microwave Stripline Applicators for Local Thermotherapy, In: Conference proceeding - Proceedings of 15th Conference on Microwave Techniques COMITE 2010. Brno: VUT v Brně, Brno: FEKT, Ústav radioelektroniky, 2010, p. 99 – 101. ISBN 978-1-4244-6351-0.

Vrbová B., Vrba J. – Study of SAR Distribution by Array of Stripline TEM Mode Applicators. In: 26th Annual Meeting of the EUROPEAN SOCIETY for HYPERTHERMIC ONCOLOGY, May 20 – 22, 2010, Rotterdam, The Netherlands.

7.1. Introduction

In this chapter we deal with focusing of EM energy into homogeneous phantom from 2 or 4 applicators of the same type, which could be used to treat malignant tumours located on large area or in extremities of human body. The first and very important step in the process of the design of applicator is impedance matching into homogeneous phantom in order to protect generator against reflected EM power and therefore better transfer of EM energy into homogeneous phantom. In this chapter we study the shape of SAR distribution in homogeneous phantom, through which it would be possible calculate the temperature distribution. This study of focusing of EM energy into homogeneous phantom is very important to verify, whether designed applicator works correctly.

7.2. Methods

For this study we chose microwave stripline applicator, which works at frequency of 434 MHz (see Chapter 5), because this type of applicator uses whole part of its aperture for radiation of EM energy into biological tissue. At first we studied SAR distribution by using two applicator of the same type, which are located immediately next to each other on a planar agar phantom. In this case agar phantom represents areas such as e.g. planar part of human body abdomen.

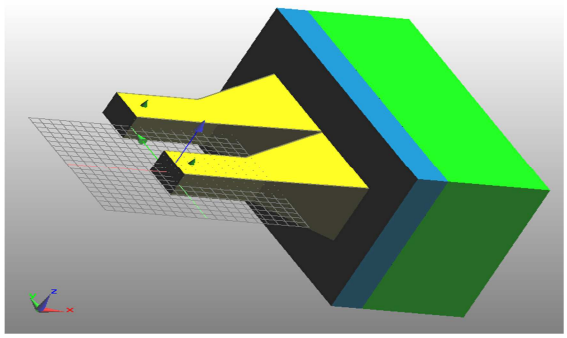

Fig. 7.1 Model of matrix of two applicators.

At second we studied SAR created by a configuration of four applicators each from other turned by 90º angle on cylindrical agar phantom, which has diameter equal to 8 cm to represent e.g. a limb of human body.

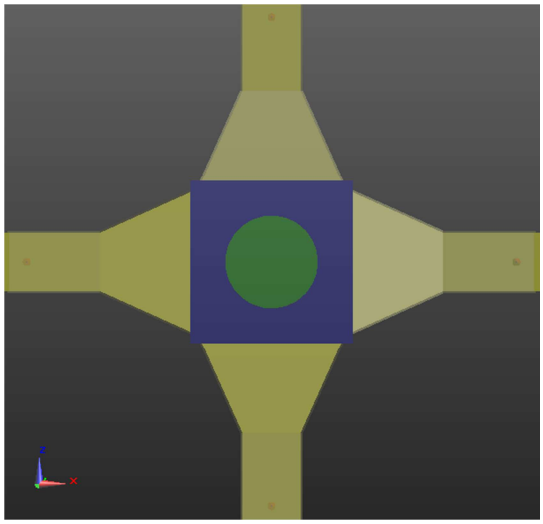

Fig. 7.2 Model of composition of four applicators.

In each studied case discussed were applicators were powered from a single microwave generator with the same amplitude and phase for the entire time. Between applicators and homogeneous agar phantom there is water bolus. Models of applicators, water bolus, homogeneous agar phantom and also the layout of SAR distribution were simulated by EM simulator program called SEMCAD X.

7.3. Results

On the following picture we can observe the shape of SAR distribution created by microwave stripline applicator at a depth of 1 cm under the surface planar agar phantom.

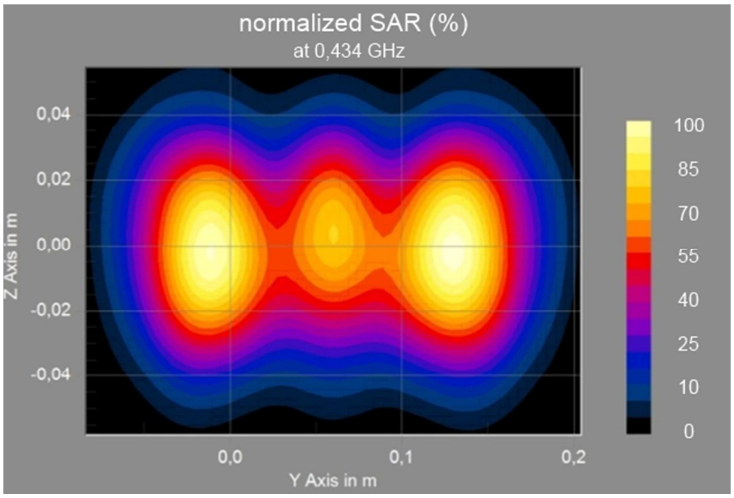

Fig. 7.3 SAR distribution at a depth of 1 cm.

On the Fig. 7.4 it is shown the layout of SAR distribution at level of effective depth. In this case the effective depth is of about 2 cm below the surface of planar agar phantom. The shape of SAR distribution creates three individual maxima in both figures.

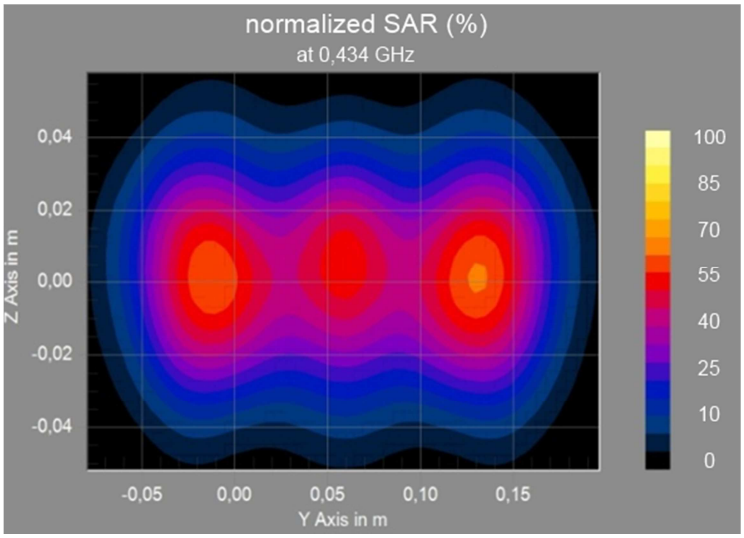

Fig. 7.4 SAR distribution at effective depth.

By using four applicators placed on cylindrical agar phantom with diameter 8 cm is created one maximum of SAR distribution in the middle of homogeneous phantom. This is due to superposition of four applicators of the same type, which work at frequency of 434 MHz. By this frequency is penetration depth in muscle tissue about 4 cm and our agar phantom, which represents muscle tissue, has diameter 8 cm.

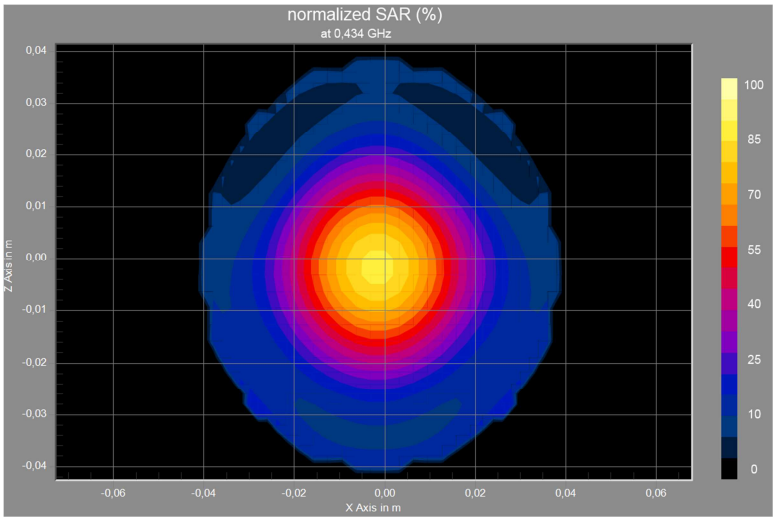

Fig. 7.5 SAR distribution in cylindrical agar phantom.

7.4. Summary of important results in this chapter

The simulations of SAR distribution result in the fact that the microwave stripline applicator can be used to treat tumours located under the surface of tissue and to treat tumors located in the middle of human limbs (like e.g. hand) by using suitable combination of several applicators of the same type.

Composition of several applicators could be used in clinical practice to treat tumours if it is necessary to cover larger area of human body.

8. Study of focusing principles for regional treatments by array of applicators in anatomical model

This chapter is based on:

Vorlíček J., Vrbová B., Vrba J. - Prospective Applications of Microwaves in Medicine. In: Book – Cancer Treatment / Book 3, 2011.p. ISBN: 979-953-307-209-7.

Vrbová B., Víšek L. – Simulation of Hyperthermic Treatment by Using the Matrix of Stripline Applicators. In: Journal - Acta Polytechnica. 2010, vol. 50, no. 4/2010, p. 106 - 110. ISSN: 1210-2709.

Vrbová B.(50%), Víšek L.: Simulation of Hyperthermic Treatment by Using the Matrix of Stripline Applicators. In: Conference proceedings - POSTER 2010 - Proceedings of the 14th International Conference on Electrical Engineering. Praha: ČVUT v Praze, FEL, 2010. ISBN 978-80-01-04544-2.

Vrbová B., Vrba J. – Study of SAR distribution by using two layers of microwave stripline TEM mode applicators. In: ISMOT Proceedings 2011. Praha: ČVUT v Praze, FEL, 2011, p. 325 – 332. ISBN 978-80-01-04887-0.

Vrbová B., Vrba J. - Comparison of SAR Distribution in Homogeneous Phantom and in Anatomical Model by Array of Microwave TEM Mode Applicators. In: 27th Annual Meeting of the EUROPEAN SOCIETY for HYPERTHERMIC ONCOLOGY, May 26 – 28, 2011, Aarhus, Denmark.

8.1. Introduction

To verify basic functionality of created applicator we can use a homogeneous agar phantom. This homogeneous phantom represents only one type of tissue in human body. In reality human body is very inhomogeneous, and therefore it is for hyperthermia treatment planning necessary to use anatomical precise 3D models with all types of biological tissues taken into account. 3D model thus can be created from segmentation of series of several scans from Computer Tomography (CT) or Magnetic Resonance (MR). CT scans are 2 dimensional transversal gray – scale cuts. After then is created 3D model imported to the program, which is used for hyperthermia treatment planning. This program must both cooperate well with a segmentation program and in the same moment to enable calculation of SAR distribution.

8.2. Methods

In this chapter we compare the SAR distribution in a homogeneous agar phantom and in an anatomical based biological model. We made 3D anatomical model of thigh (Fig.8.1) and of woman's calf (Fig.8.2). These models are realized by segmentation program 3D – DOCTOR (vector-based 3d imaging, modeling and measurement software [36]). We should have available DICOM scans from CT [49]. DICOM scans hold the original quality of data. CT provides gray-scale image data as many transverse slices. The gray-scale images first are rescaled to produce appropriate voxels. Each voxel in the images then is identified rigorously as belonging to one type of tissue by assigning each voxel a red-green-blue code that identifies the discrete tissue type of that particular voxel. All identified transverse images then are combined to obtain a three-dimensional numerical model. A fine adjustment generally is required to smoothly connect each slice in the three orthogonal planes (axial, sagittal and coronal).

DICOM CT scans for thigh model were obtained from university hospital Bulovka. This model has the resolution 2mm, meaning voxel size 2 x 2 x 2mm. Each voxel was assigned to one of 3 different tissue types, such as muscle, fat and bone.

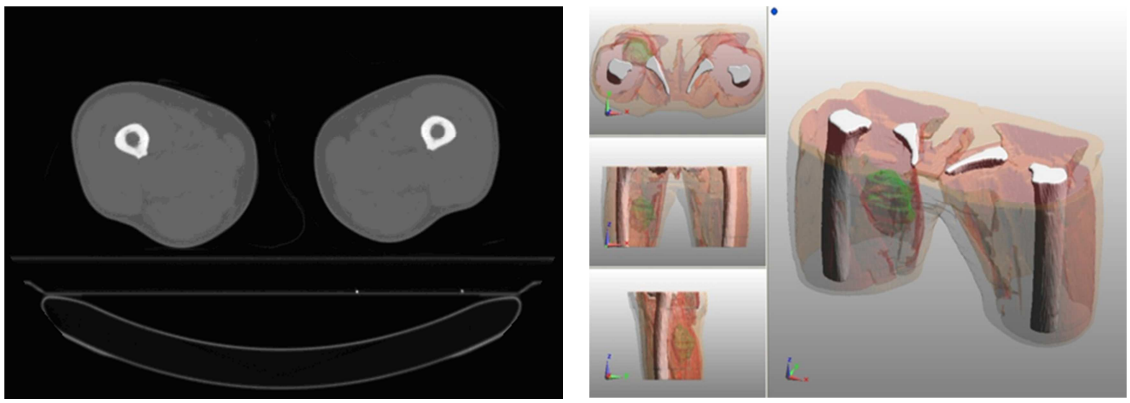

Fig. 8.1 Thigh (a) computed tomography scan [49], (b) 3D anatomical model

Model of woman's calf has resolution of 1 mm and meaning voxel side is 1 x 1 x 1 mm. Like in segmentation of thigh each voxel was assigned also to one of 3 different types of biological tissue (bone, muscle and fat).

Fig. 8.2 3D anatomical model of woman's calf

The dielectric properties at the frequency of 434 MHz of both anatomical models are shown in the next table:

Name	Conductivity [S/m]	Relative permittivity
Agar	0,8	54
Bone Cortical	0,09	13,07
Muscle	0,8	56,86
Fat	0,04	5,56

Tab. 8.1 Dielectric properties at frequency 434 MHz [44]

In this chapter we used microwave stripline applicator with TEM mode works at frequency of 434 MHz and for simulations of SAR distribution we used homogeneous agar phantom, which dielectric parameter are stored in table (Tab.8.1). All of compositions like applicators, agar phantom,3D model of thigh and of calf were simulated by FTDT program SEMCAD X.

This chapter consists from three parts. In the first part we chose the matrix composition of two applicators of the same type. In the first case of this part we put two applicators on cylindrical agar phantom next to each other (Fig.8.3a). This homogeneous agar phantom represents thigh of human body. The radius of cylindrical agar phantom is 8 cm. In the second case we put matrix of two applicators on anatomically based biological model (Fig.8.3b).

In the second part of this chapter we studied composition of 2 and 4 applicators located on homogeneous cylindrical agar phantom and consequently on 3D anatomical model of woman's calf. Cylindrical agar phantom represents muscle tissue of human limb. In our case we simulated muscle tissue of woman's calf with diameter of 8 cm.

The last part of this chapter is to address the influence of two layers on the shape of SAR distribution in homogeneous agar phantom and in anatomic model of woman calf as well. In each layer there is always the same number of applicators. The distance between two layers is gradually enlarged about 5, 10, 15 and 20 mm.

8.3. Results

- **The results of simulations of SAR distribution of the first part**

On the following figure are two same applicators put on cylindrical agar phantom and then on 3D model of human thigh (Fig.8.3)

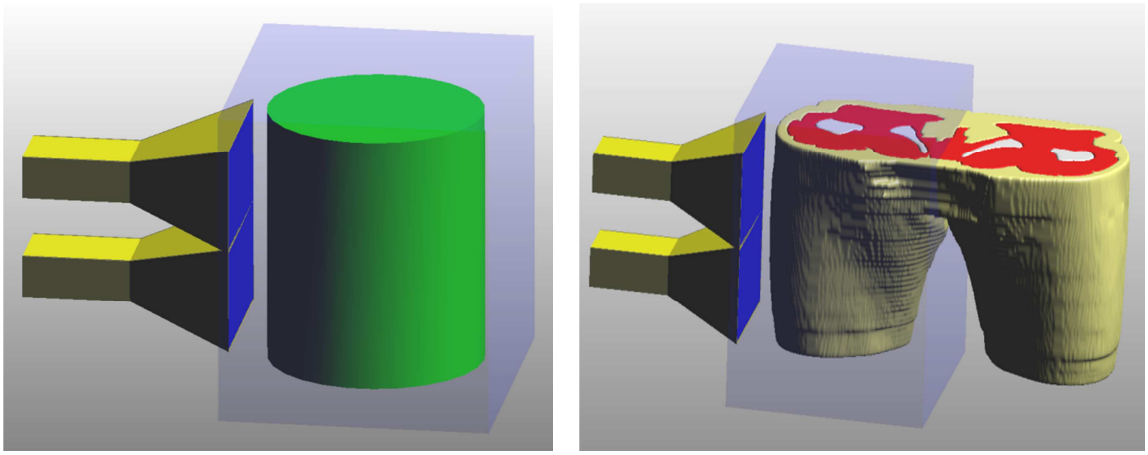

Fig. 8.3 Matrix of two applicators (a) on cylindrical agar phantom, (b) on anatomically based biological model

Maximum of SAR distribution is situated in the middle of two applicators in homogeneous agar phantom (Fig.8.4a).

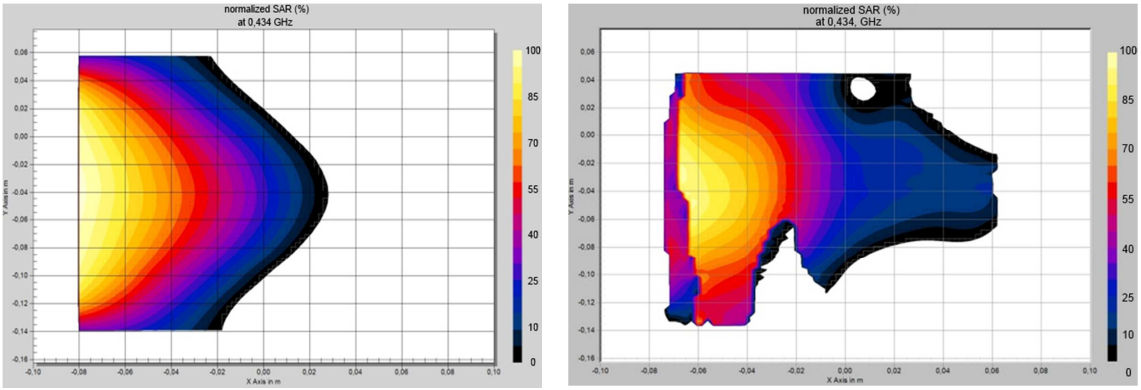

Fig. 8.4 SAR distribution (a) in agar phantom in longitudinal layer, (b) in anatomic model in longitudinal layer

By comparison of SAR distribution in agar phantom and in anatomic model is shown, that the SAR distributions acquire maximum at the same locations, but the shape of SAR distribution in anatomic phantom is influenced by fat and bone (Fig.8.4b).

Fat has a lower value of permittivity as a muscle and therefore low part of energy is absorbed in it and the most of energy goes into another layer, into muscle. Muscle

behaves as lossy environment, therefore is energy in it absorbed. Also bone affects the shape of SAR distribution as seen in transversal section of femur (Fig.8.5a).

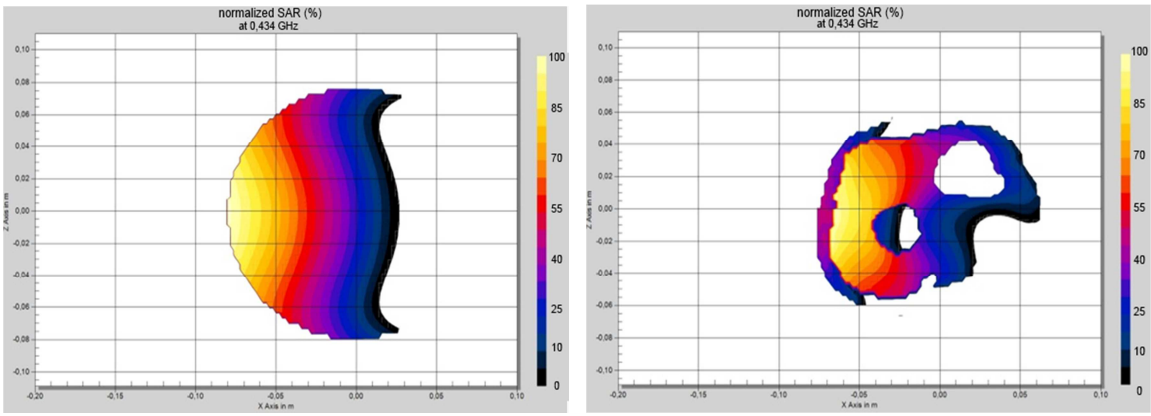

Fig. 8.5 SAR distribution in transversal layer (a) of agar phantom, (b) of anatomic model

Bone analogous to fat has a low value of permittivity (contains a small amount of water), but value of SAR is in this place zero, because bone behaves like a lossless environment and energy goes through bone.

- **The results of simulations of SAR distribution of the second part**

One of possibilities of composition of applicators is case of 2 applicators on cylindrical agar phantom and on 3D anatomical model of woman's calf shown on pictures (Fig.8.6).

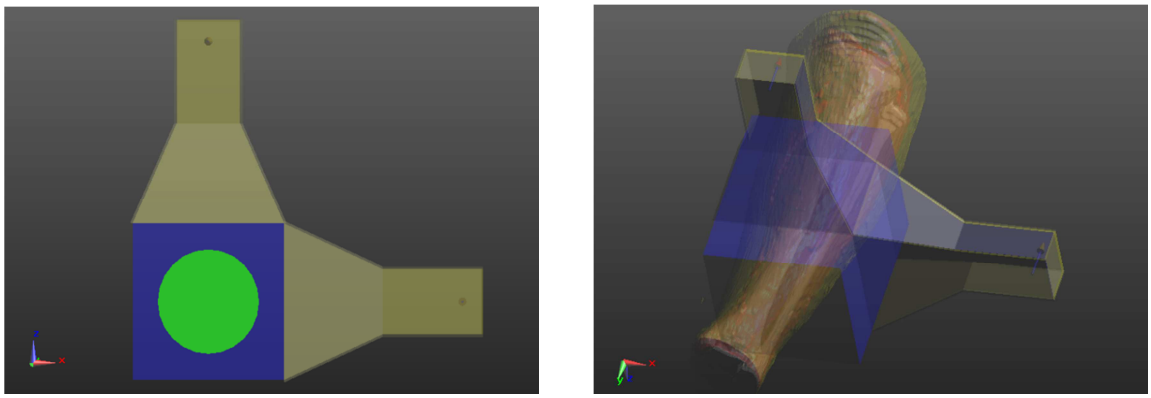

Fig. 8.6 Composition of 2 applicators (a) on cylindrical agar phantom, (b*) on anatomical model*

From both normalized SAR distributions (Fig.8.7) flow that this composition of 2 applicators is suitable for treatment of tumor, which cover larger area near to surface of human limb.

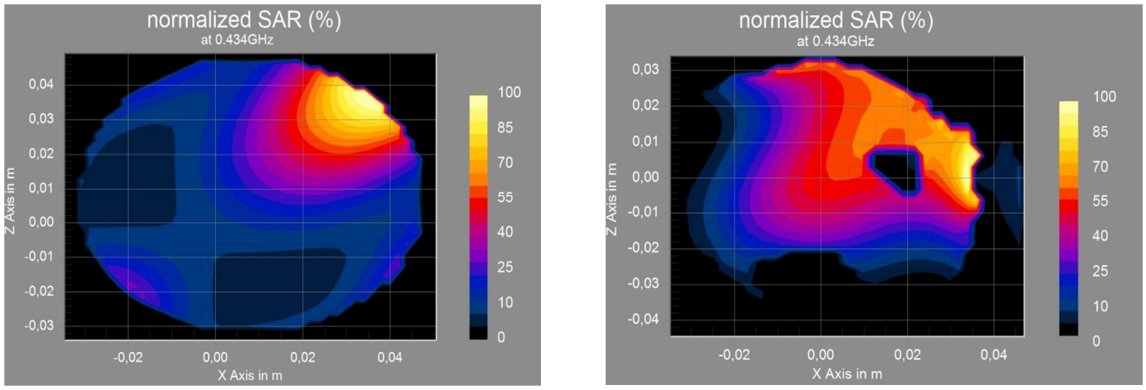

Fig. 8.7 Normalized SAR (a) in agar phantom, (b) normalized SAR in anatomical model

By using 4 applicators we can see on picture (Fig.8.8) that in both cases is a good focusing of SAR distribution near to the cylindrical axis.

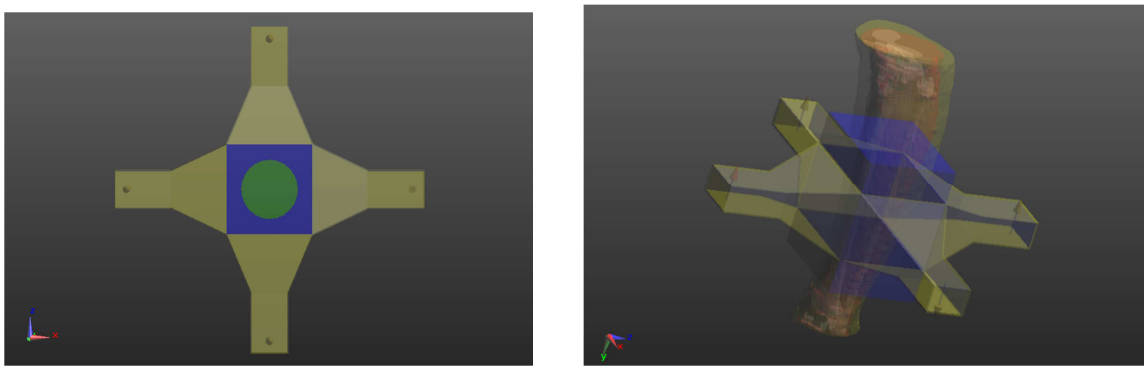

Fig. 8.8 Composition of 4 applicators (a) on cylindrical agar phantom, (b) on anatomical model

By alternation of phases of several applicators we achieved better focusing in the middle of both homogeneous agar phantom and 3D anatomical model. This composition of 4 applicators could be used for treatment tumors located in the middle of human limb.

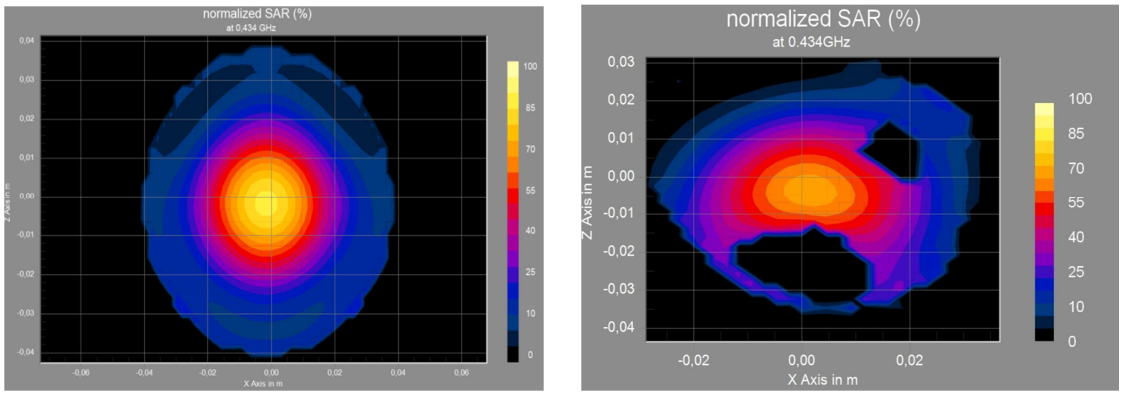

Fig. 8.9 Normalized SAR (a) in agar phantom, (b) normalized SAR in anatomical model

- **The results of simulations of SAR distribution of the second part**

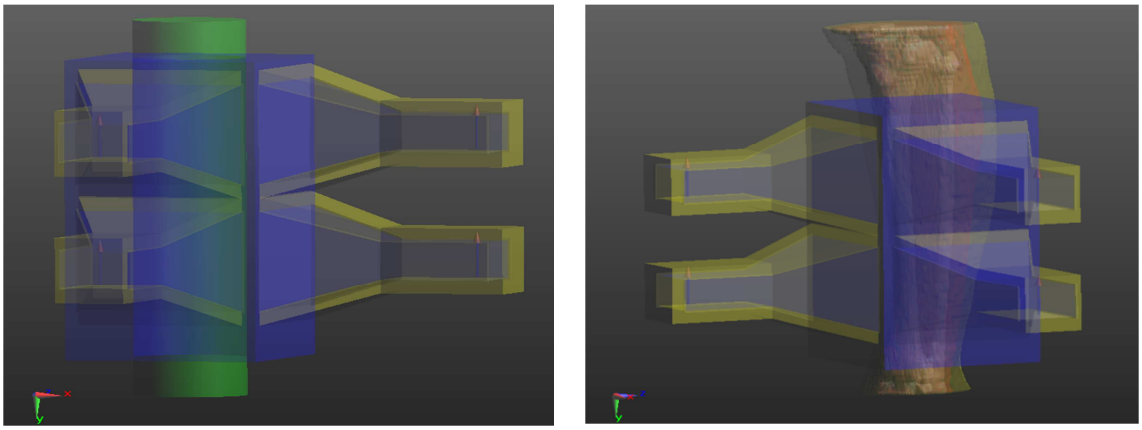

Fig. 8.10 Model of two layers with two applicators in each layer coupled (a) to cylindrical agar phantom,

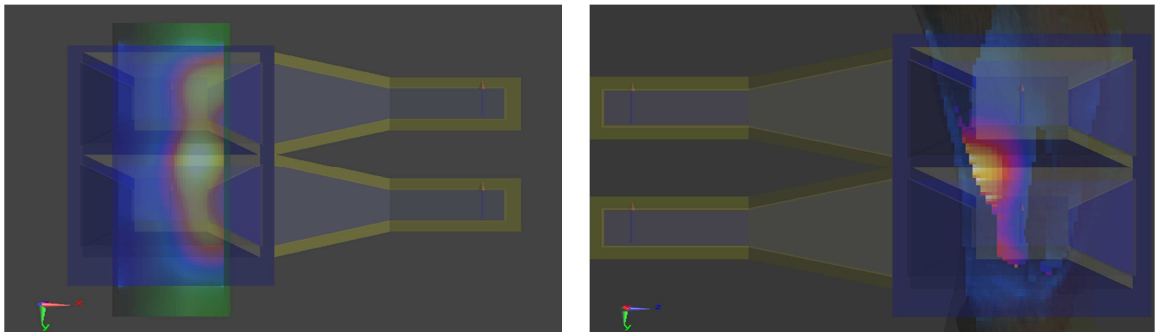

Fig. 8.11 Two layers with two applicators in each layer coupled (a) to cylindrical agar phantom, (b) to anatomical model

On the previous picture (Fig.8.11) we can see maximum of SAR distribution in the plane of symmetry of both layers. The shape of SAR distribution in anatomical model are created in the middle of both layers too, but the shape is distinct from the previous picture.

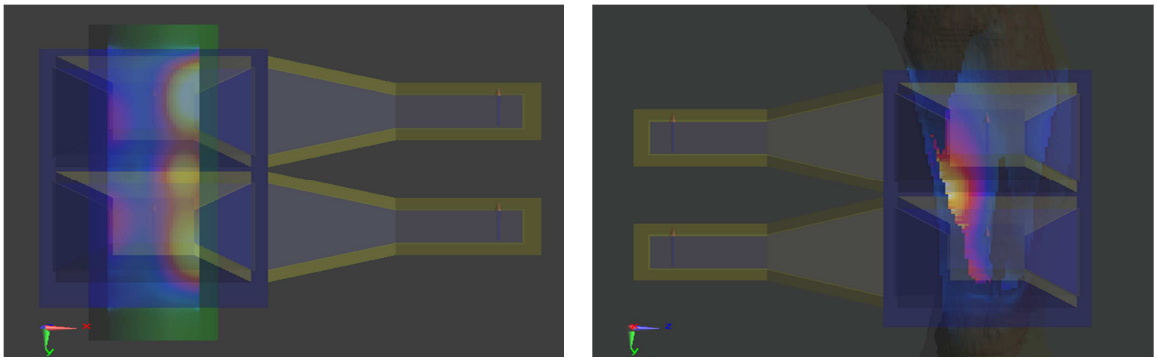

Fig. 8.12 Two layers with two applicators in each layer (a) to agar phantom, (b) to anatomical model

If we enlarge the distance between two layers with applicators about 5 mm (Fig.8.12), shapes of SAR distribution are very similar to simulations, when two layers are situated on agar phantom and on anatomical model side by side.

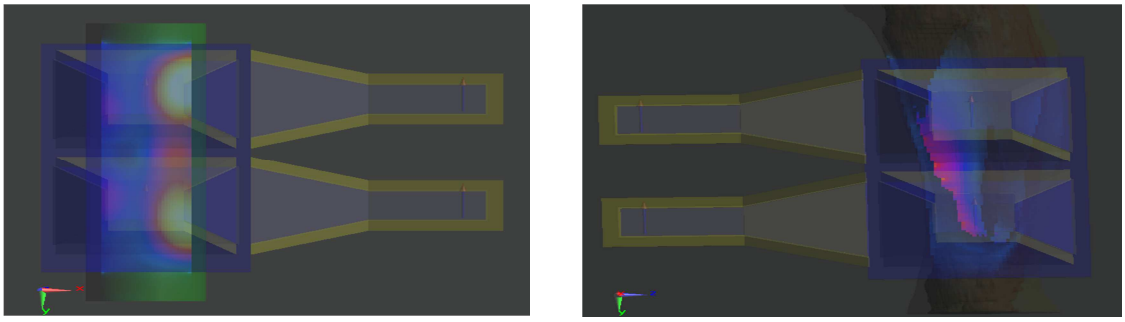

Fig. 8.13 Two layers with two applicators in each layer, distance 10 mm between both layers, coupled (a) to agar phantom, (b) to anatomical model

When the distance between layers is enlarged about 10mm, in agar phantom (Fig.8.13a) are created 2 local maxima of SAR distribution, but in anatomical model (Fig.8.13b) of calf is created reduced shape of SAR distribution.

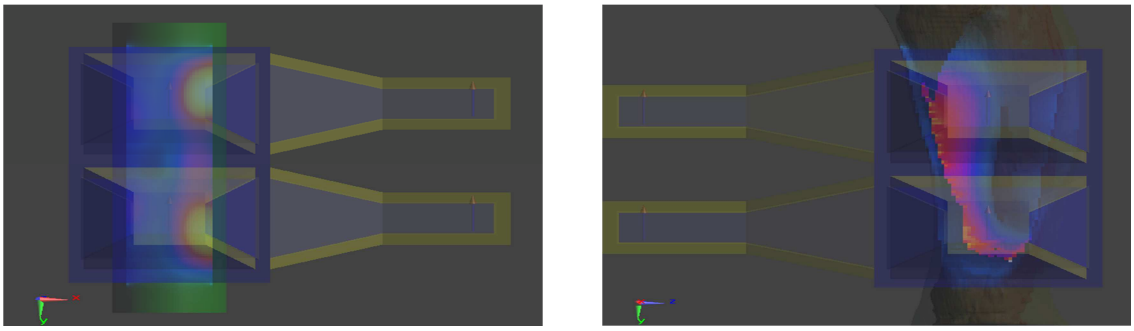

Fig. 8.14 Two layers with two applicators in each layer, distance 15 mm between both layers, coupled (a) to agar phantom, (b) to anatomical model

If the distance between layers is 15 mm, we can see two local maxima of SAR distribution in homogeneous agar phantom (Fig.8.14a) and in anatomical model is created two connected maxima of SAR distribution (Fig.8.14b).

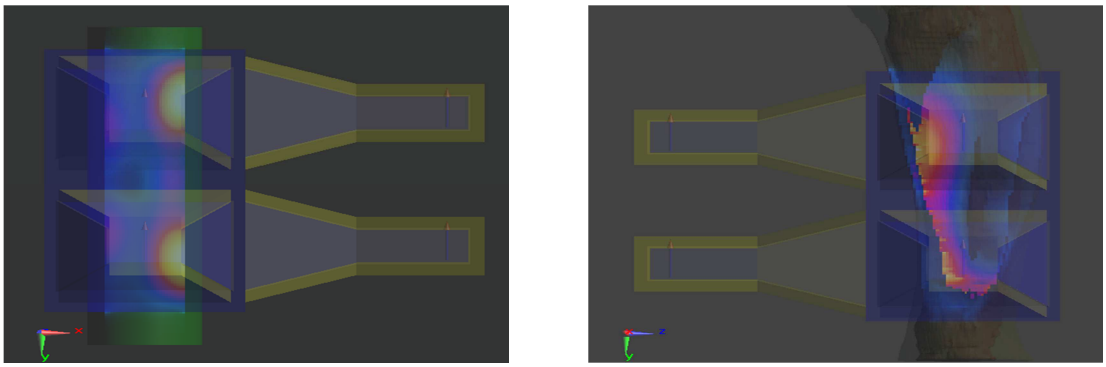

Fig. 8.15 Two layers with two applicators in each layer, distance 20 mm between both layers, coupled a) to agar phantom, b) to anatomical model

On the pictures (Fig.8.15) we can see, that shapes of SAR distribution in homogeneous agar phantom and in anatomical model are similar like on previous picture, where the distance between two layers of applicators are 15 mm.

By using eight applicators we used the same procedure and thus we gradually enlarge distance between layers (Fig.8.16).

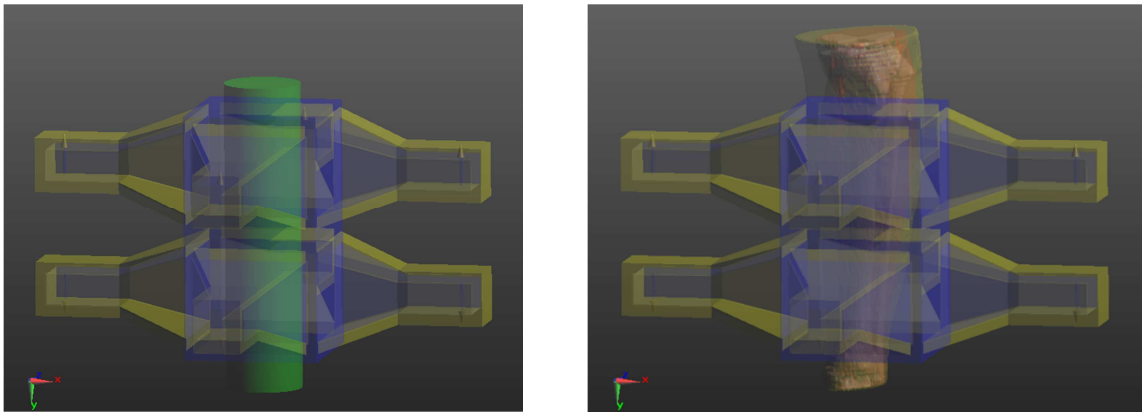

Fig. 8.16 Model of two layers with four applicators in each layer (a) to agar phantom, (b) to anatomical model

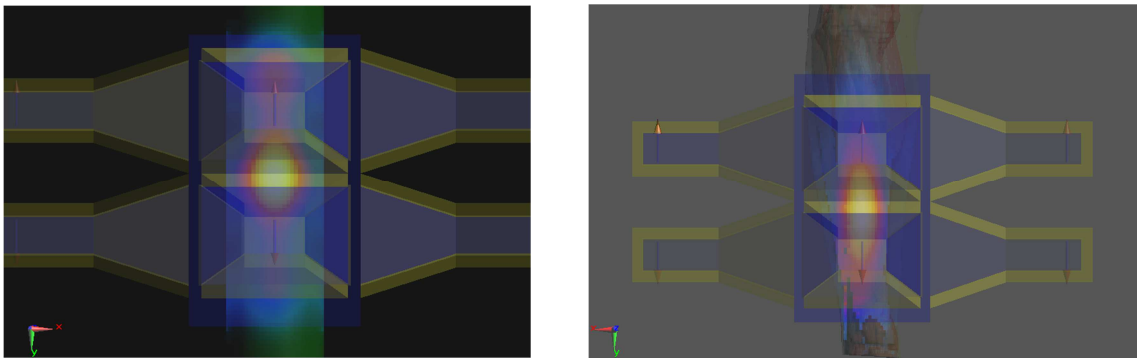

Fig. 8.17 Two layers with four applicators in each layer, distance 0 mm between both layers, coupled (a) to agar phantom, (b) to anatomical model

If two layers are situated side by side, then are in agar phantom and in anatomical model created shape of SAR distribution in the center of these layers.

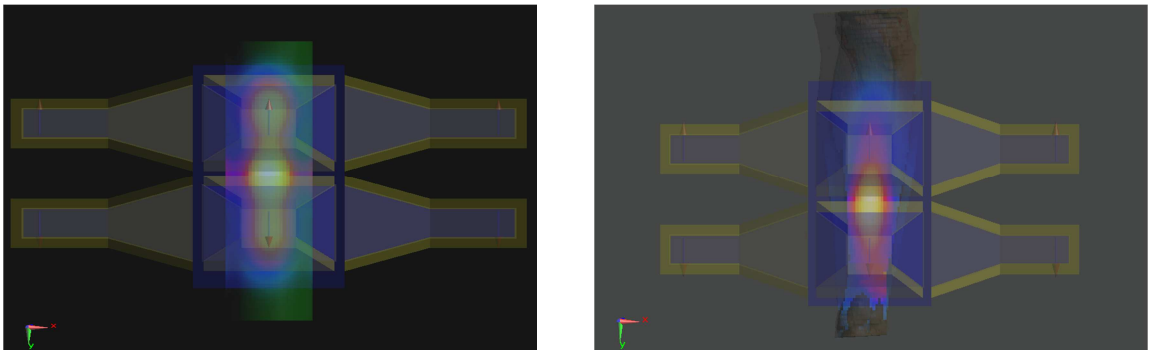

Fig. 8.18 Two layers with four applicators in each layer, distance 5 mm between both layers, coupled (a) to agar phantom, (b) to anatomical model

The SAR distribution in homogeneous agar phantom has elongated shape, if the distance between two layers of applicators is 5 mm (Fig.8.19a). When two layers of applicators situated on anatomical model are distant about 5 mm asunder (Fig.8.19b), then the shape of SAR distribution in anatomical model is similar like in anatomical model, where two layers are located side by side.

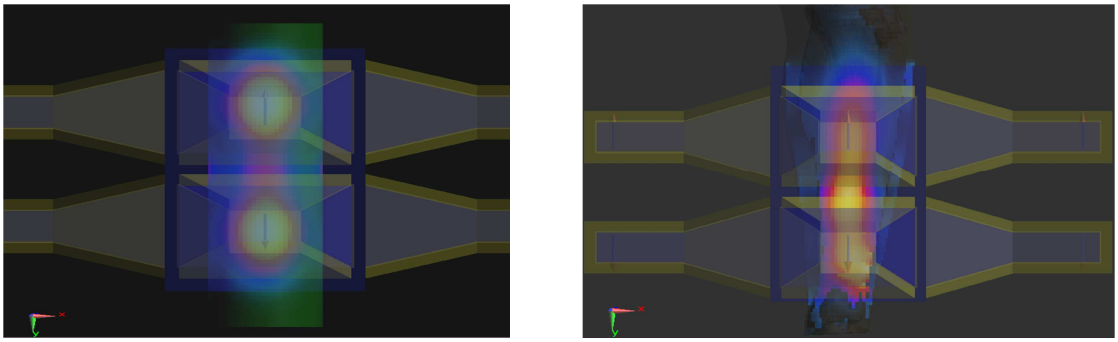

Fig. 8.19 Two layers with four applicators in each layer, distance 5 mm between both layers, coupled (a) to agar phantom, (b) to anatomical model

By distance 15mm or 20 mm from both layers we can observe 2 local maxima of SAR distribution in cylindrical agar phantom and one elongated maximum of SAR distribution in anatomical model of calf.

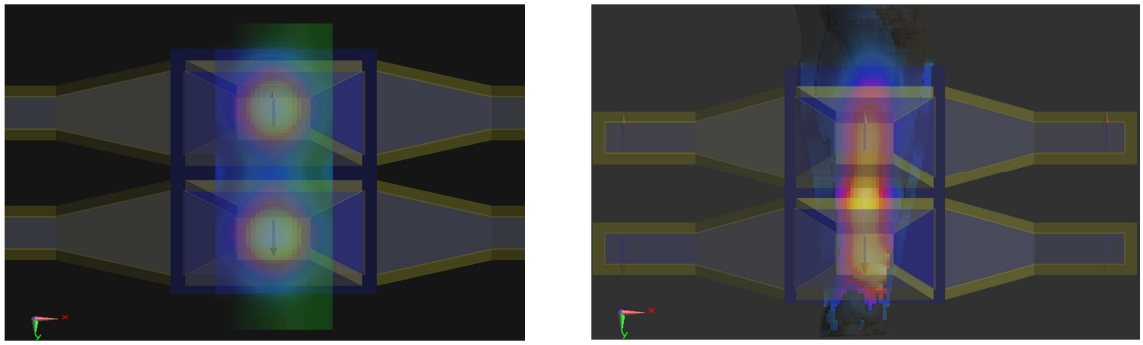

Fig. 8.20 Two layers with four applicators in each layer, distance15 mm between both layers, coupled (a) to agar phantom, (b) to anatomical model

If two layers of applicators are 20 mm away from each other, 2 local maxima of SAR distribution are created in both cases: in agar phantom and in anatomical model of woman's calf.

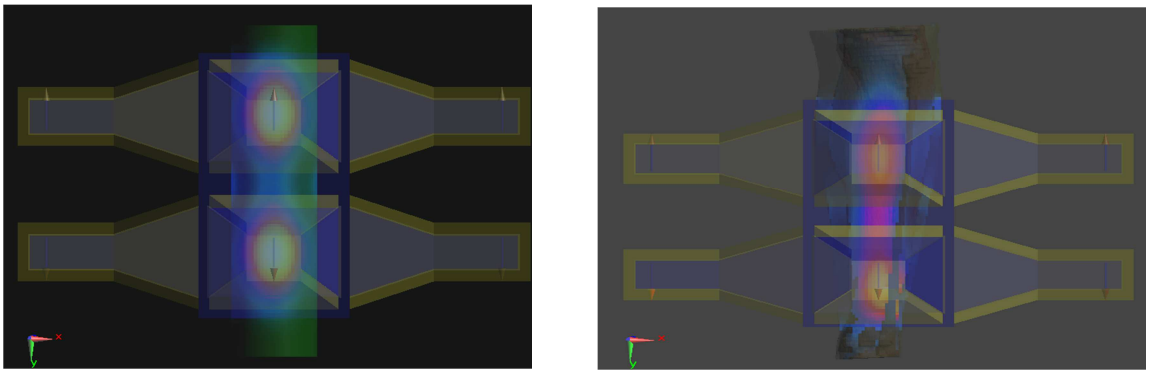

Fig. 8.21 Two layers with four applicators in each layer, distance 20 mm between both layers, coupled (a) to agar phantom, (b) to anatomical model

8.4. Summary of important results in this chapter

For basic evaluation of microwave stripline applicator simulations of SAR distributions in homogeneous agar phantom are used. Whereas human body is very inhomogeneous, for hyperthermia treatment planning is very useful to create a 3D anatomical model of the patient. We studied the shape of SAR distribution in homogeneous agar phantom and in

anatomical based biological model and the basic results of discussed SAR distribution flows, that these compositions of applicators of the same type could be used for treatment tumors located in various areas of human extremities. For better results we changed phases and amplitudes of several applicators. The SAR distributions are influenced by bone and fat tissue in both 3D anatomical models of thigh and calf.

In last part of this chapter we studied change of SAR distribution with gradually increasing distance of two layers of applicators of the same type located either on homogeneous cylindrical agar phantom or on anatomical model of woman's calf. If two layers are situated side by side on agar phantom or on anatomical model, the shape of SAR distribution is created in the middle of agar phantom / anatomical model. By gradually enlarged distance between two layers of applicators working at the frequency of 434 MHz two local maxima in agar phantom as well as in anatomical model are arising. Shapes of SAR distribution often differ from shapes of SAR distribution created in anatomical model of calf.

9. Study of Hot-Spots Induced by Electromagnetic Surface Waves

This chapter based on:

Vrba, J., Vrbová, B., Vrba, J., Vrba, D.: Microwave Thermotherapy: Study of Hot-Spots Induced by Electromagnetic Surface Waves. In Proceedings of the 7th European Conference on Antennas and Propagation (EUCAP 2013). Piscataway: IEEE, 2013, p. 3017-3018. ISBN 978-88-907018-1-8.

Vrbová B., Vrba J.: Study of Hot-Spots Generated by Electromagnetic Surface in Microwave Thermotherapy. In: 28th Annual Meeting of the EUROPEAN SOCIETY for HYPERTHERMIC ONCOLOGY, June 19 – 22, 2013, Munich, Germany.

9.1. Introduction

From hyperthermia cancer treatment clinical experiences it is known, that so called hot-spots (i.e. local overheating – burning) can sometimes be observed after the treatment. Mostly it may happen in front of the aperture of the applicator (see Fig.9.1), but sometimes surprisingly far from its aperture, typically right on the other side with respect to the applicator aperture. Such effect can be explained e.g. by aid of surface waves excited from applicator aperture (see Fig.9.2).

According to theory of electromagnetic field and waves, either interface between two different dielectric media or interface between dielectric media and conductor can support propagation of the so called surface waves. We can often have such situations in microwave hyperthermia treatment, please see description of discussed case in Fig.9.1.

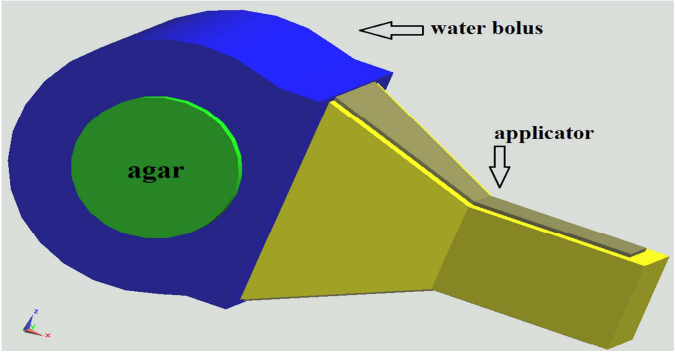

Fig. 9.1 Model of TEM wave stripline type applicator radiating to agar phantom trough water bolus.

Except of the EM wave going directly into area of agar phantom surface waves will travel around agar phantom either inside water bolus or even outside of it, i.e. surface wave propagates along the interface between agar phantom and water bolus [16,17].

9.2. Methods

For our study and discussion we have chosen microwave stripline type applicator with TEM mode, which can be used for treatment of cancer patients at frequency 434 MHz (see Chapter 5). To understand well the discussed problem we studied it both analytically and by aid of numerical solutions.

9.3. Analytical solution

Our basic approach to develop analytical solution of the discussed problem comes from idea of resonances in water bolus. If the central circle of the water bolus is approximately equal to any of whole number multiple wavelength, then under certain conditions surface waves can create hot spots on the surface of the treated area or on the surface of agar phantom, mostly right on the opposite side with respect to position of the TEM mode applicator in agar phantom (Fig.9.2).

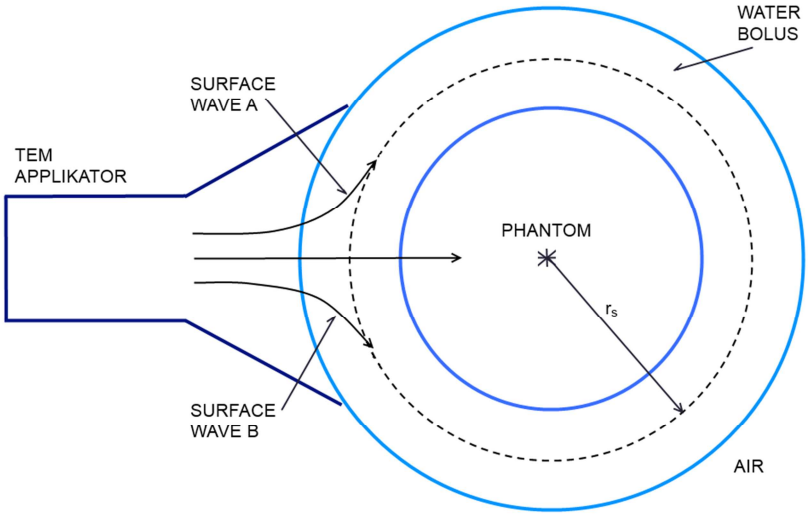

Fig. 9.2 Analytical model of hot-spots created by surface waves.

From this figure it follows that there is an EM wave going into the biological tissue and is used for treatment. Contemporaneously there will be excited two surface waves – one (wave A) travelling on clockwise and the other one (wave B) anti-clokwise direction. These two waves can (due to their superposition) create a hot spot right on the other side of applicator aperture. Under certain conditions these two waves can resonate along central circle of water bolus. It will happen when wavelength (or their n-multiples) of the discussed waves will be approximately equal to circle with a radius r_s and length l_s), i.e. when:

$$l_s = 2\pi r_s = n\frac{\lambda_0}{\sqrt{\varepsilon_r}} \tag{9.1}$$

9.4. Numerical simulations

Our approach to numerical simulations and its first results are displayed in figures 9.3 to 9.8. In these cases cylindrical agar phantom has its diameter equal to 4 cm.

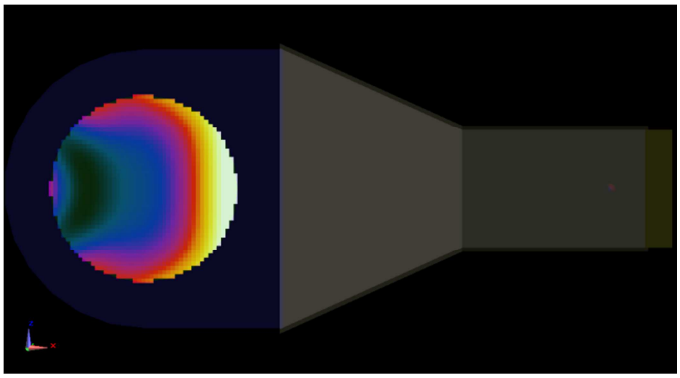

Fig. 9.3 SAR distribution in transversal plane cross section, hot spot can be observed in this case.

In Fig.9.3 there is a result of numerical simulation of SAR distribution displayed in transversal plane cross section. We can see here the hot spot on the other side with respect to position of applicator.

On the next picture we can observe the same case, i.e. hotspot created by surface wave in cylindrical agar phantom but this time displayed in sagittal plane cross section (Fig.9.4). Thickness of water bolus, which is situated around agar phantom, is 2 cm.

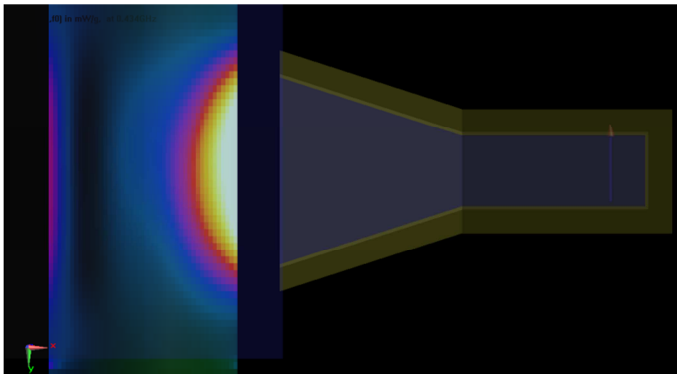

Fig. 9.4 SAR distribution in sagittal plane cross section, hot spot can be observed in this case.

If we increase wavelength then this leads to suppression of surface wave resonance in water bolus around cylindrical agar phantom (Fig.9.5). In this case is thickness of water bolus equal to 3 cm.

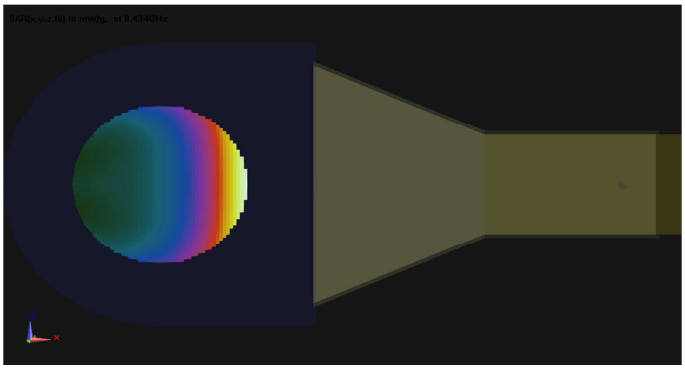

Fig. 9.5 SAR distribution in transversal plane cross section, in this case hot spot cannot be observed.

On the following picture there is located simulation, where we can see SAR distribution in agar phantom seen in sagittal plane cross section (Fig.9.6).

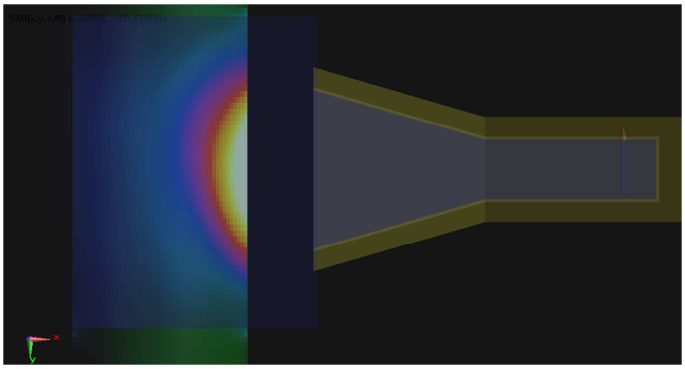

Fig. 9.6 SAR distribution in sagittal plane cross section, hot spot can't be observed in this case.

The same case of creating of hot spots is, when water bolus between cylindrical agar phantom and ring of four applicator is approximately equal to any of whole number multiple wavelength, such case is shown on the next picture.

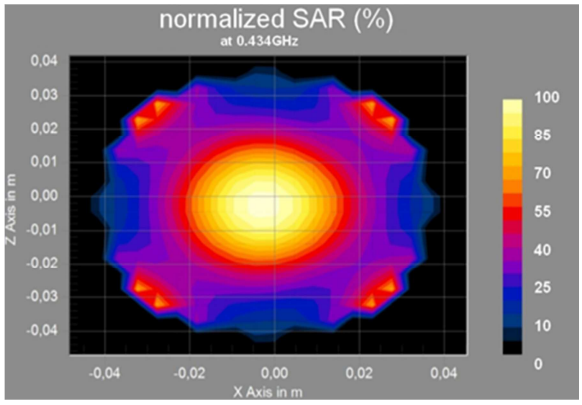

Fig. 9.7 SAR distribution with hot spots

When we increase thickness of this water bolus by about 1 cm (from 2 to 3 cm), hot spots are suppressed (Fig.9.8) and we obtained clear focusation of SAR distribution in the middle of agar phantom.

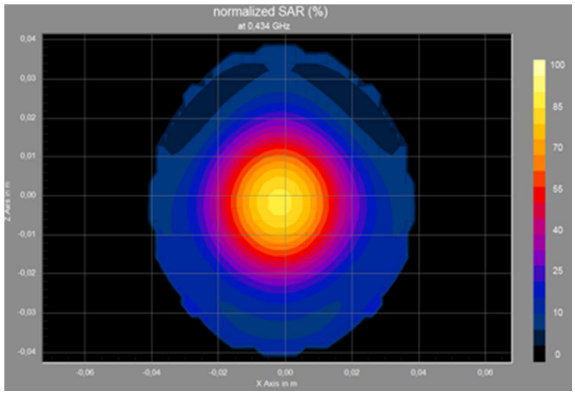

Fig. 9.8 SAR distribution without hot spots

9.5. Summary of important results in this chapter

This research contains first results of analytical and numerical simulations to eliminate excitations of surface waves. In this case we eliminate surface waves by optimization of dimensions of water bolus, which is demonstrated on the few pictures including in this chapter.

10. Intracavitary Helix Applicator to be used for BPH and for Prostate Cancer Treatment

This chapter is based on:

Vrba, J. - Vrbová, B. - Lungariello, B. - Franconi, C.: Intracavitary Helix Applicator to Be Used for BPH and for Prostate Cancer Treatments. In Proceedings of the 6th European Conference on Antennas and Propagation (EUCAP 2012). Piscataway: IEEE, 2012, p. 3655-3658. ISBN 978-1-4577-0920-3.

Vrbová B.(50%), Vrba J.: Intracavitary Hyperthermia Applicator Research for Cancer Treatments. In: ISMOT Proceedings 2011. Praha: ČVUT v Praze, FEL, 2011, p. 337 - 341. ISBN 978-80-01-04887-0.

10.1. Introduction

This chapter deals with EM simulations of intracavitary coaxial applicator with helix structure used for BPH and prostate cancer treatment (described in [50]), especially with simulations of its SAR distribution. Comparison of these simulations with SAR distribution measurements is discussed.

10.2. Methods

Picture (Fig.10.1) shows the 27.12 MHz prototypal structure of the RF radiator developed in the investigation given by paper [50]. The radiating circuit is constructed over the surface of the insulating cable mandrels the lengths of which establish the active lengths of the radiators.

Fig. 10.1 Model of helix applicator [50]

Helix radiator is part of a resonant circuit connected to the RF power source through a match-and-tune (M&T) external box that includes a manually controlled tuning capacitor and matching air-transformer [50]. The helix winding of the H-radiator is made of thin and narrow (2 x 0.1mm) phosphor bronze ribbon strip spiralled over the mandrel [51]. This intracavitary helix applicator was developed using the coaxial cable RG - 58 and same technology and a similar length as the existing U10 helix prototype [51,52]. The outer diameter of mandrel is 4.7 mm. Length of helix is 55 mm and its outer diameter is 4.9 mm

Prior to insertion into the 8-mm inner diameter (ID) hole in the agar phantom cavity, radiator was covered with a bottom-tapped thin plastic cannula in order to create inner and outer cylindrical interstices after insertion in the cavity. These interstices were filled with a selected combination of dielectric media to constitute a bi-layer structure as a tissue interface

Non-conductive water and air were the only dielectric media used. Non-conductive water (W) was selected because it has a very high dielectric constant, minimal losses, and it is readily available, and can be easily set into any shape and thickness. Air (A) is an unavoidable part of the gap and its layer can also be easily sized and shaped. The very thin plastic cannula of fixed OD is physically compatible with all active structures [50].

The phantom of biological tissue is simulated with dimensions 700 x 800 x 1400 mm. In solid region of simulator SEMCAD X is electrical conductivity set on 0.2 S/m a relative permittivity on 85. This phantom is created from a poly-methyl-ethacrylate material.

10.3. Results

In the FDTD simulator SEMCAD X EM Field simulator we designed a model of helix antenna which consists of coaxial cable, helix coil and high conductive spike (Fig.10.2).

Helix coil is connected with outer conductor of coaxial cable and spike. Dielectric media and inner conductor of coaxial cable are prolonged to conductive spike, with which they are connected. There is a long coaxial line section connected to the helix coil. Discrete port is placed between outer and inner conductor of coaxial cable.

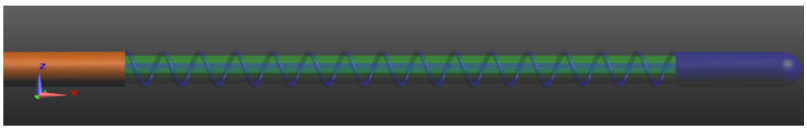

Fig. 10.2 SEMCAD X model of helix antenna

On the next picture (Fig.10.3) is intracavitary helix applicator put in a cannula and subsequently they both are inserted into the cavity inside the phantom of biological tissue.

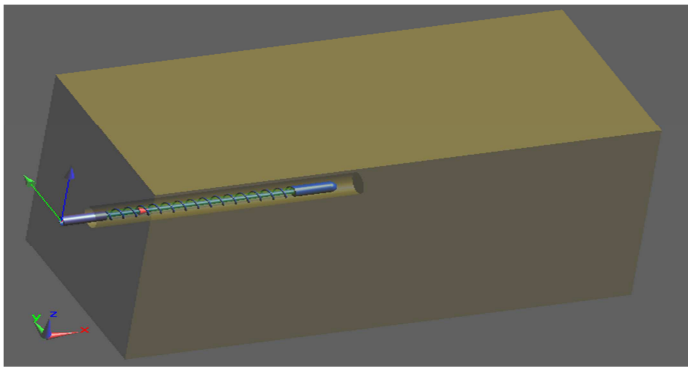

Fig. 10.3 Helix antenna put into phantom

In the following pictures (Fig.4, Fig.6 and Fig.8) there are displayed measured SAR data which are obtained experimentally by a matrix of number of thermocouple multi-channel interface used for measuring temperature increase after EM exposure of phantom [50]. Appropriate results of EM simulations are then given in Fig. 5, 7 and 9.

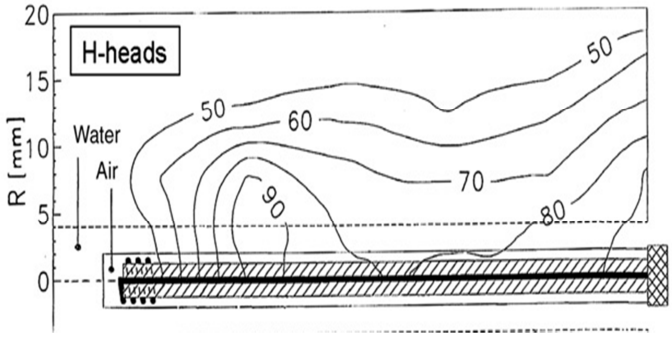

Fig. 10.4 Measured SAR created in bi – layer [50]

In previous picture (Fig.10.4) and in following picture (Fig.10.5), there we can see that shape of SAR distribution created by measurement and by simulation is very similar.

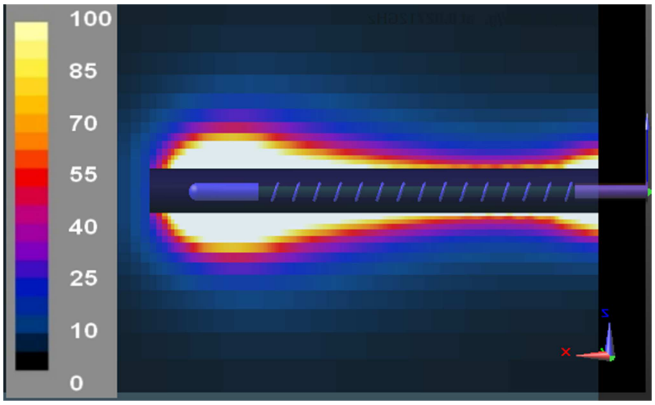

Fig. 10.5 Simulated SAR created in bi - layer

If the intracavitary helix applicator is placed into cavity of the phantom (where is air only), then the result of measured SAR distribution is given in Fig.10.6.

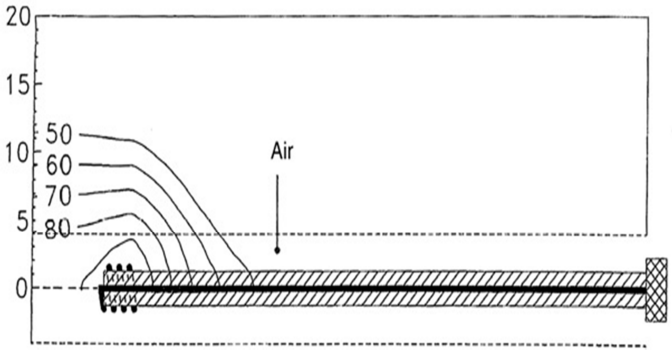

Fig. 10.6 Measured SAR created in air layer [50]

Similar shape of SAR distribution was obtained by simulation of this case (Fig.10.7). On the following picture of simulated shape of SAR distribution created by applicator in air layer we can see somewhat prolonged shape of SAR.

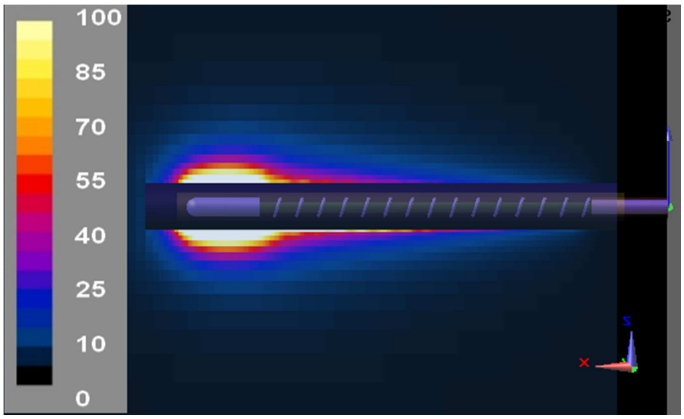

Fig. 10.7 Simulated SAR created in air layer

Very similar shapes of SAR distribution were obtained both by measurement (Fig.10.8) and by EM simulation (Fig.10.9), when H radiator was situated in the cavity phantom, where hole in phantom is filled by water.

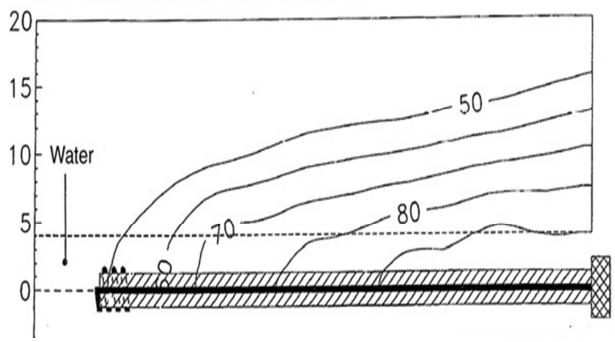

Fig. 10.8 Measurement of SAR created in case of water layer [50]

Also, similar value of SAR distribution is shown in next picture, when H radiator is inserted in the cavity of phantom, which is filled by water too.

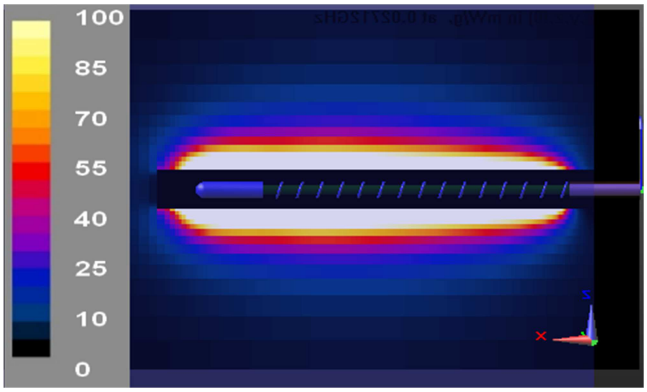

Fig. 10.9 Simulated SAR created in water layer

Comparing in paper [50] given experimental SAR evaluations and related calculated results of FDTD SAR simulations (i.e. Fig.10.4 with Fig.10.5, Fig.10.6 with Fig.10.7 and Fig.10.8 with Fig.10.9) we can arrive to conclusion that they are quite similar.

10.4. Summary of important results in this chapter

In the paper [50] the intracavitary helix applicator was designed, created and experimentally evaluated. In the first part of this paper we made EM simulations of 3D SAR distribution of this applicator and thus we could make a comparison between experimental evaluations of SAR distribution with EM simulations of 3D SAR distribution of designed intracavitary helix applicator. Results of SAR simulations in all three cases (i.e. when the helix antenna is firstly inserted in the bi-layers (air - water) media, secondly in air and thirdly in cavity of phantom filled by water) are very similar to theirs appropriate measurements.

Simulations of SAR distributions confirms, that EM field simulator SEMCAD X is a very useful tool to design and optimize thermotherapy microwave applicators, because it enable us to study real properties of these applicators.

11. Feasibility of Treatment Based on Combination of External and Intracavitary Applicators

This chapter is based on manuscript of the paper: “Feasibility of Treatment Based on Combination of External and Intracavitary Applicators”. To be published.

11.1. Introduction

In hyperthermia cancer patients treatment a combination of applicators of the same type (most frequently e.g. dipole or waveguide or applicator with evanescent mode is used quite often. Such applicators set externally on the surface of a patient's body. For treatment of tumours situated near the tubes and/or cavities in the patient body so called intracavitary applicators are used. And for destruction of malignant tumour inside organs, like e.g. liver, so called interstitial applicators can be applied. But sometimes tumours are situated in areas, where it's very difficult or even impossible to deliver microwave energy to these areas in human body either by local external applicators or by intracavitary resp. interstitial applicators. In such cases, sometimes, it could be used combination of external and either intracavitary or interstitial applicator.

11.2. Materials

One of the main aims of this doctoral thesis was to do a feasibility study of above mentioned combination of local external applicator with intracavitary resp. interstitial applicator. For this preliminary study we decided to use as local external applicator the microwave stripline applicator with TEM mode (chapter 5). And then microwave monopole, which is used like interstitial applicator. Both applicators work at the same frequency of 434 MHz.

11.3. Design of microwave monopole

Monopole is the simplest type of interstitial or intracavitary applicator. Coaxial cable in this case has at some reference plane terminated the outer conductor and inner conductor is continuing behind this reference plane roughly a quarter wavelength out. For design of interstitial applicator was used 50 Ohm's coaxial cable RG 178 which has small dimensions of inner and outer conductor.

Fig. 11.1 Coaxial cable RG 178 [53]

In the following table parameters of this coaxial cable are described:

ITEM	MATERIAL	DIMENSIONS
Jacket	FEP	1,8 ± 0,1 mm
Shield	95% silver-plated copper braid	1,3 ± 0,08 mm
Dielectric	PTFE	0,84 ± 0,05 mm
Inner conductor	silver-plated copper clad steel	7/0.1 ± 0,02 mm

Tab. 11.1 Parameters of coaxial cable [54]

Inner conductor of coaxial cable is created with seven grains from silver-plated cooper. Dielectric is from PTFE, teflon, characterized by exceptional resistance to chemicals and heat and is harmless. Outer conductor is like inner conductor also created from silver-plated cooper. Jacket of this cable is from FEP. It's kind of teflon, which has similar chemical and heat characteristics like PTFE.

There aren't specific theories to implement this type of antenna, therefore was necessary to assume some simplifying hypothesis to get the dimensions of microwave monopole. The wavelength at working frequency is found by following equation:

$$f_r = \frac{c_\circ}{\lambda_\circ \sqrt{\varepsilon_r}} \tag{10.1}$$

where the working frequency fr = 434 MHz, speed of light c_0 = 3x10^8 m/s and relative permittivity of air ε_r = 1. From equation 10.1 we obtain λ_0 = 0,69 mm. For the calculation of wavelength along monopole effective electric permittivity ε_{ef} should be used, which in first approximation can be considered as a function of relative permittivity of cable ε_{cable} = 2,1 and relative permittivity of agar phantom ε_{agar} = 54:

$$\varepsilon_{ef} = \frac{\varepsilon_{cable} + \varepsilon_{agar}}{2} \tag{10.2}$$

$$\lambda = \frac{\lambda_0}{\sqrt{\varepsilon_{ef}}} \tag{10.3}$$

From previous equations we can determine that the wavelength of EM wave along a monopole is 130 mm. Under these assumptions, was in simulation program SEMCAD X designed a first quarter-wave monopole, whose inner conductor has length 130mm and outer conductor 97,5 mm.

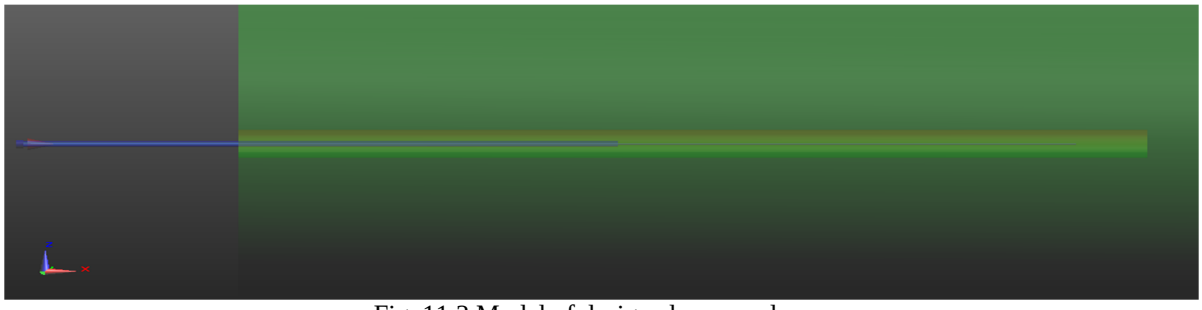

Fig. 11.2 Model of designed monopole

Very important part of the design of the discussed applicator is finding the best value of impedance matching. This is a very important to prevent reflections of electromagnetic energy back to the generator. After some modification of length inner and outer conductor was find the reflection parameter s_{11} = -14,3 dB. The length of inner conductor changed to value 147 mm and the length of outer conductor is 53 mm. By measurement impedance matching of discussed and realized applicator was found the value of the reflection parameter s_{11} = - 22,6 dB, which is much better value of s_{11} than the simulation by SEMCAD X.

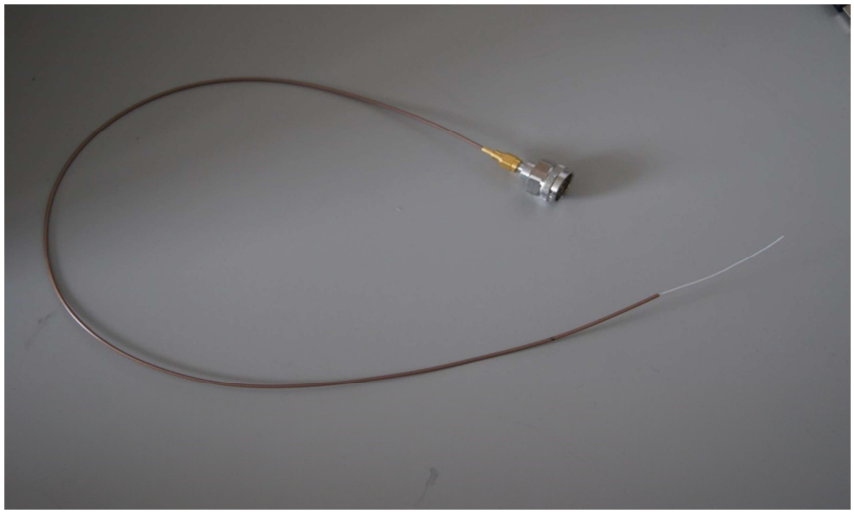

Fig. 11.3 Created microwave monopole

11.4. Methods

At first we made simulations of SAR distribution of both applicators separately, and then the shape of SAR distribution by simulation of radiated EM energy into the agar phantom from both applicators simultaneously was obtained. In all three cases was used homogeneous agar phantom representing muscle tissue (ε_r = 54, σ = 0.8 S/m) with dimensions 140 x 140 x 74 mm. Microwave stripline applicator was located on the surface of this agar phantom and monopole was situated 4 cm under the surface of phantom. Both applicators were powered coherently. Coherent waves allow their mutual interference.

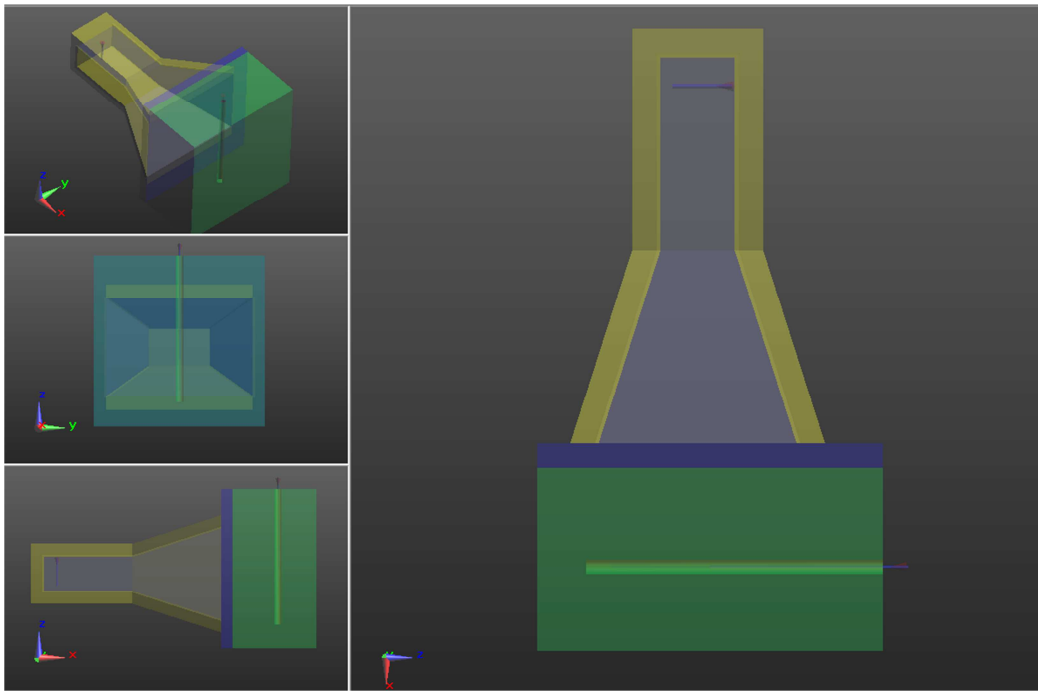

Fig. 11.4 Model of two applicators

Then agar phantom from distilled water, salt and agar's powder with dimensions 140 x 200 x 80 mm with similar dielectric parameters like muscle tissue was created. Both

applicators were powered by generator UHF-POWER-GENERATOR PG 70.150.2 at the frequency 434 MHz with 100 W. On the first day was measured temperature distribution, which was created by EM power radiated from microwave stripline applicator. On the same day was made measurement of temperature distribution created by above described microwave monopole. On the second day measurement of temperature distribution for the case of EM power radiated from both applicators simultaneously. As a power divider we used coaxial T coupling element. Temperature was measured by IR camera FLIR P25.

Fig. 11.5 Measurement system

11.5. Results

On the following figure there is the shape of SAR distribution of monopole obtained by EM Field simulator SEMCAD X.

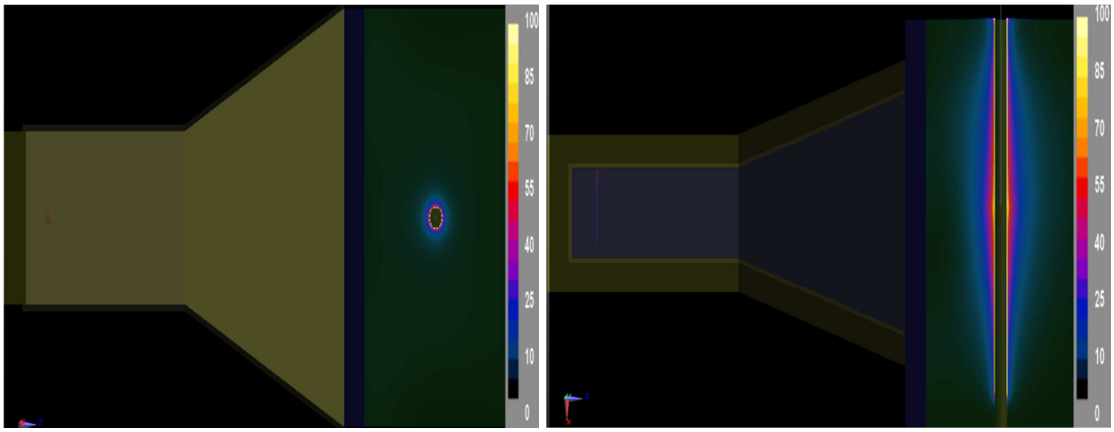

Fig. 11.6 normalized SAR distribution of monopole (a) in transversal plane cross section, (b) in sagittal plane cross section

After 5 minutes exposition of agar phantom, which has diameter 4 cm, thermogram of realized monopole was obtained. Simulated SAR distribution of designed monopole has similar shape like thermogram of realized applicator.

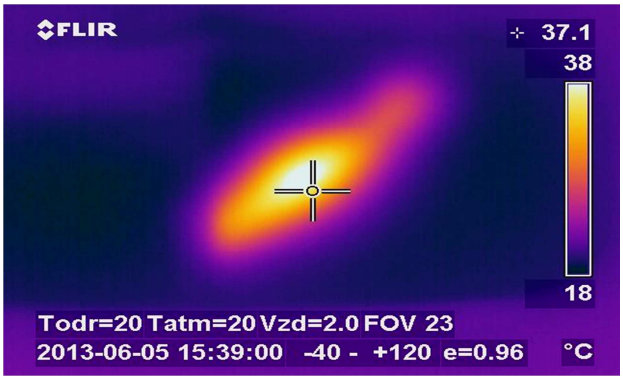

Fig. 11.7 Thermogram of monopole

In the case of microwave stripline applicator with TEM mode is the shape of simulated SAR distribution quite the same like the shape displayed on the thermogram. Decrease to 50% of SAR (with respect to its maximum) is 3 cm under the surface of agar phantom.

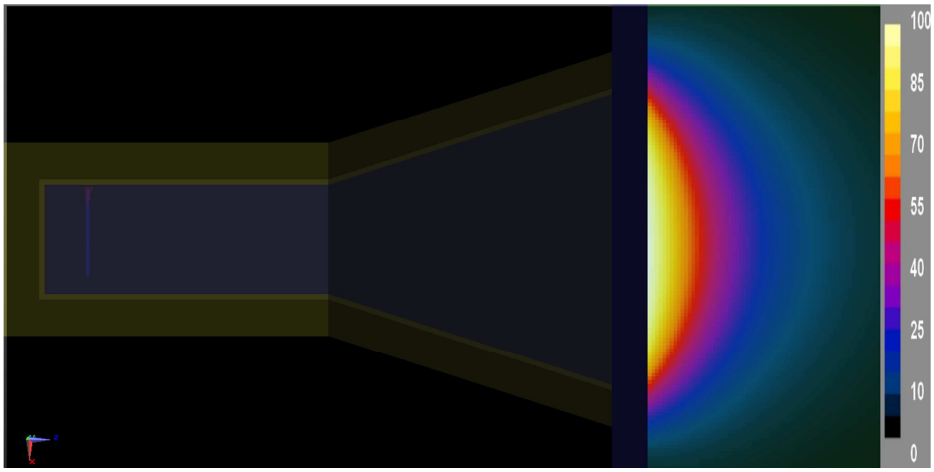

Fig. 11.8 Normalized SAR distribution of stripline applicator with TEM mode

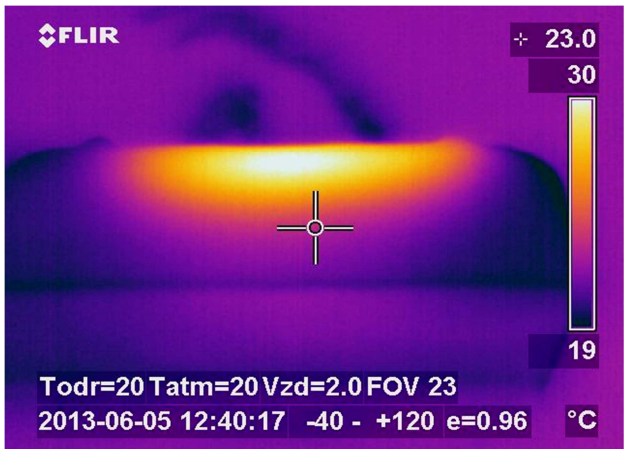

Fig. 11.9 Thermogram of stripline applicator

On the following figures are shown superposition of both applicators that means SAR distribution created by radiation of both applicators simultaneously powered from one generator.

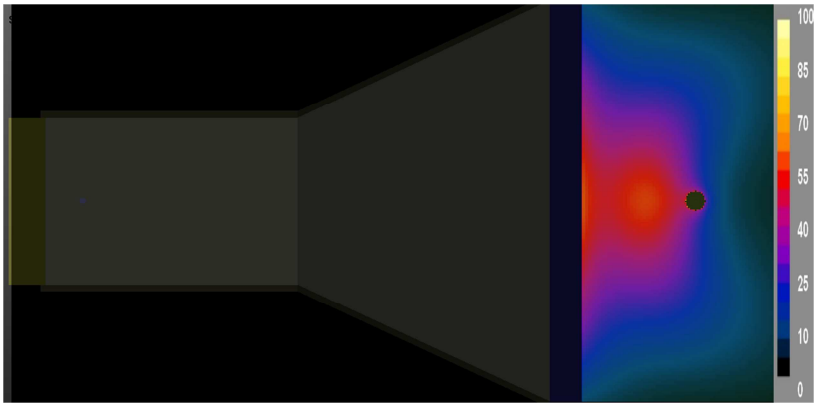

Fig. 11.10 Normalized SAR distribution in transversal plane cross section

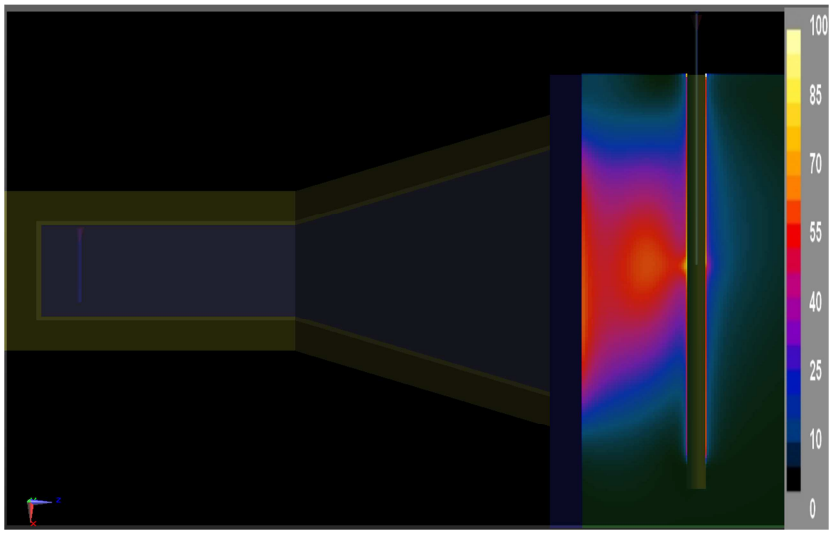

Fig. 11.11 Normalized SAR distribution in sagittal plane cross section

On the next two figures there is shown the shape of temperature distribution obtained from composition of external and interstitial applicator after 5 minutes exposition of agar phantom. On the first picture there is seen surface distribution of temperature and on the last thermogram we can observe temperature distribution in agar phantom cross-section.

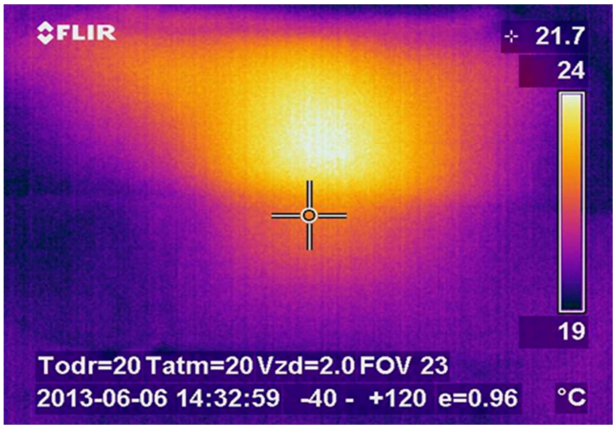

Fig. 11.2 Temperature distribution in agar phantom cross-section.

Comparing result of EM numerical simulation and experimental results it can be told, that there is a very good agreement between both results.

11.6. Summary of important results in this chapter

In this chapter we studied combination of local external applicator with interstitial applicator at first by simulations and then by measurement. Comparing result of EM numerical simulation and experimental results it can be told, that there is a very good agreement between both results.

12. Conclusions

In this chapter I would like to make a summary of the original results obtained in the frame of this doctoral thesis. The main goal of my doctoral thesis was to bring some new scientific contributions to the topics of medical applications of EM field, especially then to microwave thermotherapy.

In previous chapters I have described main topics (problems) I have solved in my DT including description of working methods and presentation of many significant results. In this chapter I would like to make an overview of the original results obtained in the frame of my doctoral thesis:

a) New model of microwave hyperthermia applicator coupled to patient body.

New model of microwave hyperthermia applicator coupled to patient body has been proposed in this doctoral thesis. This new model is based on theory of signal flow graph and is in details described in Chapter 5 of the doctoral thesis. Firstly a general version of this model has been created and after it an ideal case was derived from the general version. Both from the general model and from its ideal case as well we can determine basic important requirements for optimal design of microwave applicators for hyperthermia cancer treatment.

b) New definition for evaluation of the SAR homogeneity during the treatment.

New definition for evaluation of the SAR homogeneity during the treatment has been proposed in the doctoral thesis (see Chapter 6, please). Results of the study of homogeneity of the SAR distribution created by the array of TEM stripline type applicators of the same type in the homogeneous agar phantom have been described and discussed in the doctoral thesis. The effect of the phantom dimensions on the SAR homogeneity has been demonstrated. In my opinion the techniques selected and tested by me proved to be very accurate and effective. In conclusion it can be stated that up to a certain level radius of agar phantom a very well homogeneous shape of SAR distribution can be created. Here presented results correspond very well to our analytical model of the studied problem.

c) Study of focusing possibilities for deep heating and for case of regional treatment,

Doctoral thesis brings new results based on studies of the shape of the SAR distribution in the homogeneous agar phantom and in the anatomical based biological model (see Chapters 7 and 8, please). Basic results of discussed SAR distribution show that optimized compositions of applicators of the same type could be used for treatment of tumours located in various areas of human extremities. In some cases in order to obtain better results we changed phases and amplitudes of selected applicators. The SAR distributions are influenced by bone and fat tissue in both 3D anatomical models of thigh and calf.

Here used anatomical model were created by me myself. In this thesis I have described basic points of methodology how to create them from CT or MRI scans.

Studies of 3D SAR simulations were done firstly for the case of homogeneous planar resp. cylindrical phantom irradiated by EM wave from by us proposed applicators. Our work was focused on a study of superposition effects by using a matrix of hyperthermia applicators.

Logical continuation then was to study of 3D SAR distribution in true anatomical model of human body, again focusing on the study of superposition effects by using a matrix of hyperthermia applicators. On the other hand array applicators can be used for treatment of diseases on bigger areas for clinical purposes.

In the last part of these studies we followed influence of change of the SAR distribution with gradually increased distance of two layers of applicators of the same type located either on homogeneous cylindrical agar phantom or on anatomical model of woman's calf. If two layers of applicators are situated side by side on agar phantom or on anatomical model, the shape of SAR distribution is created in the middle of agar phantom / anatomical model. By gradually enlarged distance between two layers of applicators working at the frequency of 434 MHz two local maxima in agar phantom as well as in anatomical model are arising. Shapes of SAR distribution often differ from shapes of SAR distribution created in anatomical model of calf.

d) Analytical and numerical study of excitations of surface waves.

Doctoral thesis brings new ideas about mechanisms which in therapy can cause so called hot-spots (see Chapter 9, please). We have verified the hypothesis that in some cases these hotspots can be created by surface waves and resonances of these surface waves excited in the water bolus. Doctoral thesis contains first results of analytical and numerical simulations which can be used to eliminate excitations of surface waves. We propose to eliminate surface waves by optimization of dimensions of water bolus (this possibility was demonstrated in doctoral thesis by aid of a few pictures included in the mentioned chapter).

e) Study of EM field irradiated both from external and from intracavitary applicators.

Another important topic of this doctoral thesis is an initial study and optimization of applicators for intracavitary treatment based on helix structure. As a very original contribution of this doctoral thesis we consider a feasibility study of contemporaneous treatment by external applicator for local treatment in combination with interstitial applicator (see Chapter 10 and 11, please).

Based on these results this doctoral thesis brings a proposal of applicators suitable for medical applications and for biological experiments (including numerical simulations of their SAR distribution and impedance matching and measurements of temperature distribution in agar phantom).

Results obtained by research in the frame of my doctoral thesis were presented in several international scientific conferences (e.g. Annual Meeting of European Society for Hyperthemic Oncology - ESHO 2010 in Rotterdam (NL), ESHO 2011 in Aarhus (DN), ESHO 2013 in Munich (D), Progress In EM Research Symposium - PIERS 2011 in

Morocco, ISMOT 2011 in Prague (CZ) and EDALC 2011 in Prague (CZ), PIERS 2012 in Moscow, PIERS 2013 in Stockholm). Some of my results were published in international journal PIER (Progress in EM Research, IF=5,39).

13. List of literature

[1] De Gannes, F. P. et al., *Effects of head-only exposure of rats to GSM-900 on blood-brain barrier permeability and neuronal degeneration*. Radiation research. 172(3), p. 359-367, 2009.

[2] Sonmez, O. F., Odaci, E., Bas, O., Kaplan, S., *Purkinje cell number decreases in the adult female ratcerebellum following exposure to 900MHz electromagnetic field.* Brain research. 1356, p. 95-101, 2010.

[3] Volkow, N. D. et al., *Effects of cell phone radiofrequency signal exposure on brain glucose metabolism.* JAMA: the journal of the American Medical Association. 305(8), p. 808-813, 2011.

[4] Kirschvink, J. L., Kobayashi-Kirschvink, A., Woodford, B. J., *Magnetite biomineralization in the human brain*. Proceedings of the National Academy of Sciences. 89(16), p. 7683-7687, 1992.

[5] Adey, W. R., *Biological effects of electromagnetic fields. Journal of cellular biochemistry*, 51, p. 410-410, 1993.

[6] Kortekaas, R. et al., A Novel Magnetic Stimulator Increases Experimental Pain *Tolerance in Healthy Volunteers-A Double- Blind Sham-Controlled Crossover Study*. PloS one, 8(4), e61926, 2013.

[7] Assiotis, A., Sachinis, N. P., & Chalidis, B. E., *Pulsed electromagnetic fields for the treatment of tibial delayed unions and nonunions. A prospective clinical study and review of the literature*. Journal of orthopaedic surgery and research, 7(1), p. 1-6, 2012.

[8] Lehrer, S., Green, S., & Stock, R. G., *Association between number of cell phone contracts and brain tumor incidence in nineteen US States*. Journal of neuro-oncology, 101(3), p. 505-507, 2011.

[9] Aydin, D. et al., *Mobile phone use and brain tumors in children and adolescents: a multicenter case–control study*. Journal of the National Cancer Institute, 103(16), p. 1264-1276, 2011.

[10] Berg, H. et al., *Bioelectromagnetic field effects on cancer cells and mice tumors*. Electromagnetic Biology and Medicine, 29(4), p. 132-143, 2010.

[11] Gobba, F., Bargellini, A., Scaringi, M., Bravo, G., Borella, P., *Extremely low frequency-magnetic fields (ELF-EMF) occupational exposure and natural killer activity in peripheral blood lymphocytes*. Science of the Total Environment, 407(3), p. 1218-1223, 2009.

[12] Srivastava, P. K., Callahan, M. K., and Mauri, M. M., *Treating human cancers with heat shock proteinpeptide complexes: the road ahead*. 2009.

[13] Caubet R, Pedarros-Caubet F, Chu M, et al., *A radio frequency electric current enhances antibiotic efficacy against bacterial biofilms*. Antimicrob Agents Chemother. Vol.48, p.4662–4664, 2004.

[14] Ruediger, H. W., *Genotoxic effects of radiofrequency electromagnetic fields*. Pathophysiology. 16(2), p. 89- 102, 2009.

[15] Torgomyan, H., and Trchounian, A., *Escherichia coli membrane-associated energy-dependent processes and sensitivity toward antibiotics changes as responses to low-intensity electromagnetic irradiation of 70.6 and 73 GHz frequencies*. Cell biochemistry and biophysics. 62(3), p. 451-461, 2012.

[16] Vrba, J., Introduction to microwave technology.Nakladatelství ČVUT. 2007, ISBN 978-80-01-03670-9, (in Czech).

[17] Vrba, J., Medical Applications of Microwaves. Nakladatelství ČVUT. 2007, ISBN 978-80-01-02705-9, (in Czech).

[18] Corry P. M., Dewhirst M. W., *Thermal medicine, heat shock proteins and cancer*. Int. J. Hyperthermia. Vol. 21, No. 8, p. 675 – 677, December 2005.

[19] Falk M. H., Issels R.D., *Hyperthermia in oncology*. Int J. Hyperthermia. Vol. 17, No. 1, p. 1 - 18, 2001.

[20] Wust P. Et al., *Hyperthermia in cancer treatment: Hyperthermia in combined treatment of cancer*. THE LANCET Oncology. Vol. 3, p. 487 – 497, 2002.

[21] Dřížďal T., *New types of applicators for local hyperthermia*. Doctoral thesis, Prague, 2010, (in Czech).

[22] van Rhoon G.C., Rietveld P.J., van der Zee J., *A 433 MHz Lucite cone waveguide applicator for superficial hyperthermia*. Int. J. Hyperthermia. Vol. 14, No. 1, p. 13-27, 1998.

[23] Vrbová B., *Microwave stripline applicator for local thermotherapy*. Diploma thesis, Prague, 2009, (in Slovak).

[24] Franconi C., Vrba J., Montecchia F., *27 MHz hybrid evanescent-mode applicators (HEMA) with flexible heating field for deep and safe subcutaneous hyperthermia*. Int. J. Hyperthermia. Vol. 9, No. 5, p. 655-673, 1993.

[25] CAMART J. C. et al., *New 434 MHz interstitial hyperthermia system monitored by microwave radiometry: theoretical and experimental results*. Int. J. Hyperthermia. Vol. 16, No. 2, p. 95 – 111, 2000.

[26] Vrba J., *Microwave Applicator for Medical Aplications: Imaging and Thermotherapy Treatment*. Mikrotalasna revija, p. 43 – 46, 2005.

[27] Vrba, J., Franconi, C., Lapeš, M., *Theoretical Limits for the Penetration Depth of Intracavitary Applicators*. Int. J. of Hyperthermia,Vol.12, No.6, p.737-42 , 1996.

[28] Franconi C., Vrba J. et al, *Prospects for radiofrequency hyperthermia applicator research. I – Pre-optimised prototypes of endocavitary applicators with matching interfaces for prostate hyperplasia and cancer treatments*. Int. J. Hyperthermia. Vol. 27, No. 2, p. 187 – 198, 2011.

[29] Kröger T. et al., *Numerical Simulation of Radio Frequency Ablation with State Dependent Material Parameters in Three Space Dimensions*. Sporring (Eds.): MICCAI 2006, LNCS 4191, p. 380–388, 2006.

[30] Kok H. P. et al., *The impact of the waveguide aperture size of the 3D 70 MHz AMC-8 locoregional hyperthermia system on tumour coverage*. Phys. Med. Biol. Vol. 55, p. 4899–4916, 2010.

[31] Greef M. De et al., *3D versus 2D steering in patient anatomy: A comparison using hyperthermia treatment planning*. Int. J. Hyperthermia. Vol. 27, No. 1, p. 74 -85, 2011.

[32] Margarethus M. et al., *A head and neck hyperthermia applicator: Theoretical antenna array design*. Int. J. Hyperthermia. Vol. 23, No. 1, p. 59 – 67, 2007.

[33] Gellermann J. et al., *Simulation of different applicator positions for treatment of a presacral tumour*. Int. J. Hyperthermia. Vol. 23, No. 1, p. 37 – 47, 2007.

[34] European society for hyperthermic oncology http://www.esho.info/professionals/hyperthermia/applications.html .

[35] Christ A. et al., *The Virtual Family—development of surface-based anatomical models of two adults and two children for dosimetric simulations*. Phys. Med. Biol., Vol. 55, p. 23 – 38, 2010.

[36] 3D-DOCTOR, 3D Imaging, Modelling, Rendering and Measurement Software. (http://www.ablesw.com/3d-doctor/tutor.html).

[37] Computational Life Sciences. iSEG. , SPEAG Zurich Med Tech AG. (http://www.zurichmedtech.com/products/cls/components/iseg/).

[38] SEMCAD: the Simulation platform for EMC, Antenna Design and Dosimetry. Schmid & Partner Engineering AG (http://www.semcad.com).

[39] van Rhoon G. C. et al., *Development of a clinical head and neck hyperthermic applicator: Local SAR distortion by major anatomical structures*. Book, p. 27 – 46, ISBN: 978 -90-8891-009-8, 2007.

[40] Liu J., *Uncertainty analysis for temperature prediction of biological bodies subject to randomly spatial heating*. J Biomech. No. 34, p. 1637–42, 2001.

[41] Deng ZS, Liu J., *Mathematical modeling of temperature mapping over skin surface and its implementation in thermal disease diagnostics*. Comput Biol Med. No. 34, p. 495–521. 2004.

[42] Shih TC et al., *Analytical analysis of the Pennes bioheat transfer equation with sinusoidal heat flux condition on skin surface*. Medical Engineering & Physics Vol. 29, p. 946–953, 2007.

[43] Pennes HH. *Analysis of tissue and arterial blood temperature in the resting forearm*. J Appl Physiol. Vol. 1, p. 93–12, 1948.

[44] Dieletric Properties of Body Tissue: in the frequency range 10 Hz – 100 GHz. (http://niremf.ifac.cnr.it/tissprop/)

[45] Iero, D. A. M. et al., *Optimal constrained field focusing for hyperthermia cancer therapy: A feasibility assessment on realistic phantoms*. Progress In Electromagnetics Research. Vol. 102, p. 125-141, 2010.

[46] IEEE Standard for Safety Levels with Respect to Human Exposure to Radio Frequency Electromagnetic Fields, 3kHz to 300GHz, IEEE C95.1-2005, 2005.

[47] Gelvich, E. A. et al., *An attempt at quantitative specification of SAR distribution homogenity*. Int. J. Hyperthermia. Vol. 12, No. 3, p. 431 - 436, 1996.

[48] Korenev B. G., *Cylindrical functions of the third kind.* In book: Introduction to the theory of Bessel functions. SNTL. p. 26, 1977, (in Czech).

[49] Visible Human CT Datasets https://mri.radiology.uiowa.edu//VHDicom/

[50] Franconi C., Vrba J., Micali F., Pesce P.,: *Prospects for radiofrequency hyperthermia applicator research. I–Preoptimised prototypes of endocavitary applicators with matching interfaces for prostate hyperplasia and cancer treatments*. Int. J. Hyperthermia, Vol. 27, No. 2, p. 187–198, 2011.

[51] Franconi C, Holowacsz J, Vrba J, Micali F, Bonacina R, Pesce F.: *27MHz flexible heating field for interstitial and endocavitary applicators.* In: Gerner EW and Cetas TC, editors. Hyperthermic Oncology. Vol. I. Tucson: Arizona University Press. p 270, 1992.

[52] Ellinger D. C., Chute F. S., Vermeulen F. E.: *Evaluation of a semicylindrical solenoid as an applicator for radiofrequency hyperthermia*. IEEE Trans Biomed. Vo.16, p. 967–994, 1989.

[53] Wellshow Technology. RG178 Coaxial Cable. http://www.wellshow.com/ products/rf-coaxial-cables/rg-coaxial-cable/rg178-coaxial-cable/

[54] Farnell element 14. BELDEN - MRG178.0125 - CABLE, COAX, RG178, BROWN, 25M. http://uk.farnell.com/belden/mrg178-0125/cable-coax-rg178-brown- 25m/dp/1423308

14. List of candidate's works relating to the doctoral thesis

Publications in impacted journals:

[L1] Vrbová, B.(50%), Vrba, J.: Microwave Thermotherapy in Cancer Treatment: Evaluation of Homogeneity of SAR Distribution. Progress in Electromagnetics Research (IF 2012: 5.298). 2012, vol. 129, p. 181-195. ISSN 1559-8985.

Cited:

- Xia, Z. X.; Cheng, Y. J.; Fan, Y.: Frequency-reconfigurable TM010-mode reentrant cylindrical cavity for microwave material processing. In: Journal of Electromagnetic Waves and Applications. ISSN 1569-3937.
- Husni, Nur A.; Islam, Mohammad T.; Faruque, Mohammad R. I.; et al.: Effects of Electromagnetic Absorption towards Human Head Due To Variation of Its Dielectric Properties At 900, 1800 And 1900 Mhz With Different Antenna Substrates. In: Progress in Electromagnetics Research.. ISSN 1559-8985.
- Basar, Md R.; Malek, Fareq; Saleh, Mohd I. M.; et al.: A NOVEL, HIGH-SPEED IMAGE TRANSMITTER FOR WIRELESS CAPSULE ENDOSCOPY. In: Progress in Electromagnetics Research. ISSN 1559-8985.
- Basar, M. R.; Malek, F.; Juni, K. M.; et al.: The Use of a Human Body Model to Determine the Variation of Path Losses in the Human Body Channel in Wireless Capsule Endoscopy. In: Progress in Electromagnetics Research. ISSN 1559-8985.

Publications in reviewed journals:

[L2] Vrbová B.(50%), Víšek L.: Simulation of Hyperthermic Treatment by Using the Matrix of Stripline Applicators. In: Journal - Acta Polytechnica. 2010, vol. 50, no. 4/2010, s. 106 - 110. ISSN: 1210-2709.

Chapter in book:

[L3] Vorlíček J., Vrbová B.(33%), Vrba J.: Prospective Applications of Microwaves in Medicine. In ADVANCES IN CANCER THERAPY. Rijeka: InTech, 2011, p. 507-532. ISBN 978-953-307-703-1.

Patent:

No patent

Membership in conference organizing committee, session co-chair-woman:

- Member of organizing committee of ISMOT 2011 (13th International Symposium on Microwave and Optical Technology, June 20 – 23, 2011, Prague, Czech Republic).
- Chairperson of ISMOT 2011 session: Biological Effects and Medical Applications of EM Fields.
- Member of organizing committee of EDALC 2011 (Electrodynamic Symposium of Living Cells, July 1 – 3, 2011, Prague, Czech Republic).

Project participation:

- **MSM6840770012**: “Transdisciplinary Research in the Area of Biomedical Engineering II” of the CTU in Prague, sponsored by the Ministry of Education, Youth and Sports of the Czech Republic.
- **GD102/08/H081**: "Non Standard Applications of Physical Fields", supported by the Czech Science Foundation (Grant Agency of the Czech Republic).
- **SGS10/175/OHK4/2T/13**: “Development of Microwave Applicators”, supported by the Czech Technical University in Prague.
- **SGS12/070/OHK4/1T/13**: “Optimalilzation of hyperthermia treatment planning by using microwave diagnostisc and new types of thermotherapeutic superposition applicators”, supported by the Czech Technical University in Prague.
- **SGS13/077/OHK3/1T/13**: “Study of Electromagnetic Processes in biomolecules, cells and tissue”, supported by the Czech Technical University in Prague.

Web of Science excerpted publications:

[L4] Vrbová B.(50%), Vrba J.: Waveguide-based Applicators for Local Microwave Thermotherapy: Feasibility Study of Matrix Array Treatment, In: Conference Proceedings - Progress in Electromagnetics Research Symposium (PIERS 2010 Xi\'an). Cambridge, MA: The Electromagnetics Academy, 2010, p. 1394 – 1397. ISBN 978-1-934142-12-7.

[L5] Vrba, J., Vrbová, B.(25%), Lungariello, B., Franconi, C.: Intracavitary Helix Applicator to Be Used for BPH and for Prostate Cancer Treatments. In Proceedings of the 6th European Conference on Antennas and Propagation (EUCAP 2012). Piscataway: IEEE, 2012, p. 3655-3658. ISBN 978-1-4577-0920-3.

[L6] Vrbová, B.(50%), Vrba, J.: Evaluation of Homogeneity of SAR Distribution of Array of TEM Mode Applicators. In Proceedings of the 6th European Conference on Antennas and Propagation (EUCAP 2012). Piscataway: IEEE, 2012, p. 1091-1094. ISBN 978-1-4577-0920-3.

[L7] Vrba, J., Vrbová, B.(50%): EM Field based Microwave Technologies in Medicine. In Proceedings of the 7th European Conference on Antennas and Propagation (EUCAP 2013). Piscataway: IEEE, 2013, p. 3013-3015. ISBN 978-88-907018-1-8.

[L8] Vrba, J., Vrbová, B.(25%), Vrba, J., Vrba, D.: Microwave Thermotherapy: Study of Hot-Spots Induced by Electromagnetic Surface Waves. In Proceedings of the 7th European Conference on Antennas and Propagation (EUCAP 2013). Piscataway: IEEE, 2013, p. 3017-3018. ISBN 978-88-907018-1-8.

Other publications:

[L9] Vrbová B.(50%), Vrba J.: Matrix Composition of Microwave Stripline Applicators for Local Thermotherapy, In: Conference proceeding - Proceedings of 15th Conference on Microwave Techniques COMITE 2010. Brno: VUT v Brně, Brno: FEKT, Ústav radioelektroniky, 2010, p. 99 – 101. ISBN 978-1-4244-6351-0.

[L10] Vrbová B.(50%), Víšek L.: Simulation of Hyperthermic Treatment by Using the Matrix of Stripline Applicators. In: Conference proceedings - POSTER 2010 - Proceedings of the 14th International Conference on Electrical Engineering. Praha: ČVUT v Praze, FEL, 2010. ISBN 978-80-01-04544-2.

[L11] Vrbová B.(50%), Vrba J.: Study of SAR distribution by using two layers of microwave stripline TEM mode applicators. In: ISMOT Proceedings 2011. Praha: ČVUT v Praze, FEL, 2011, p. 325 – 332. ISBN 978-80-01-04887-0.

[L12] Vrbová B.(50%), Vrba J.: Intracavitary Hyperthermia Applicator Research for Cancer Treatments. In: ISMOT Proceedings 2011. Praha: ČVUT v Praze, FEL, 2011, p. 337 - 341. ISBN 978-80-01-04887-0.

[L13] Vrba J., Vrbová B.(14%) et al.: EM Field Based Microwave Technologies in Medicine. ISMOT Proceedings 2011. Praha: ČVUT v Praze, FEL, 2011, p. 319 - 323. ISBN 978-80-01-04887-0.

[L14] Vrba J., Vrbová B.(50%) et al.: Microwave Exposure Systems for research of Biological Effects of EM Field. In: ISMOT Proceedings 2011. Praha: ČVUT v Praze, FEL, 2011, p. 343 - 345. ISBN: 978-80-01-04887-0.

[L15] Vrba, J., Oppl, L., Vrba, D., Vorlíček, J., Vrbová, B.(16%) et al.: Prospective Applications of EM Fields in Medicine. In: PIERS 2011 Marrakesh Proceedings. Cambridge, MA: The Electromagnetics Academy, 2011, p. 1816-1821. ISBN 978-1-934142-16-5.

[L16] Vrbová B.(50%), Vrba J.: Study of SAR Distribution by Array of Stripline TEM Mode Applicators. In: 26th Annual Meeting of the EUROPEAN SOCIETY for HYPERTHERMIC ONCOLOGY, May 20 – 22, 2010, Rotterdam, Netherlands.

[L17] Vrbová B.(50%), Vrba J.: Comparison of SAR Distribution in Homogeneous Phantom and in Anatomical Model by Array of Microwave TEM Mode Applicators. In: 27th Annual Meeting of the EUROPEAN SOCIETY for HYPERTHERMIC ONCOLOGY, May 26 – 28, 2011, Aarhus, Denmark.

[L18] Vrbová B.(50%), Vrba J.: Study of Hot-Spots Generated by Electromagnetic Surface in Microwave Thermotherapy. In: 28th Annual Meeting of the EUROPEAN SOCIETY for HYPERTHERMIC ONCOLOGY, June 19 – 22, 2013, Munich, Germany.

List of candidate's other publications

Publications in impacted journals:

No other publications

Publications in reviewed journals:

No other publications

Patent:

No patent

Project participation:

- **TA02010854**: "The development of high-performance broad-spectrum light sources for use in medicine".
- **P102/11/0649:** "Research and Measurements of Signals Generated by Nanostructures", supported by the Grant Agency of the Czech Republic.

Web of Science excerpted publications:

No other publications

Other publications:

No other publications